The Dependence of the Electrical Properties of Oxide Coated Cathodes on their Surface and Bulk Characteristics.

A Thesis Presented for the Degree of Doctor of Philosophy at the University of Birmingham.

by

R. Dowsberry B.A., Grad.Inst.P.

Physics Department.

U.C.N.S.

August 1961.

Synopsis

'Probe' tubes, 'Retarding Potential' tubes and a tube in which the oxide was 'sandwiched' between two nickel electrodes have been used to investigate the conductivity and thermionic emission of barium oxide coated cathodes. The results obtained, for various states of cathode 'activity' and cathode temperatures, indicated that the 'Probe' tubes were the most satisfactory for this type of investigation. Values of the apparent Richardson work function have been obtained from these measurements, together with values of the apparent surface and internal work functions, while values of the apparent contact potential difference and the apparent anode work function have been obtained from the emission measurements.

It was found that large values of Richardson work function were associated with positive values of intercept on the Richardson plot, in accordance with a simple model involving adsorbed layers of an electronegative substance The smaller values of Richardson work function were associated with negative values of the intercept. It has been shown that a linear relationship sometimes exists between the slope and the intercept of Richardson lines and that this is to be expected when these lines intersect in a common point.

The apparent internal and surface work functions were both found to decrease as activation of the cathode occurred. Changes in the apparent surface work function

were found to ~~increase~~ occur more rapidly than the internal work function when the pressure in the experimental tube was altered.

Conductivity measurements have indicated a small rectification effect which is probably due to the metal/oxide interface. Measurements of the Seebeck e.m.f. have indicated that the oxide usually behaves as an n-type semiconductor, but at higher internal gas pressures, a transition from n-type to p-type semiconductivity was observed as the temperature of the cathode was decreased. The conductivity measurements at high temperatures were consistent with the Loosjes-Vink pore-conduction hypothesis. Measurements at higher temperatures indicated a saturation of both the conductivity and the emission current which were attributed to a space charge effect in the pores of the oxide. Other experimental results indicated that the emitting surfaces were within the pores of the oxide and this was confirmed by an experiment in which the oxide was removed from the base metal. Measurements of the conductivity at lower temperatures indicated the possibility of either a surface conduction mechanism or donor depletion.

The values of the apparent anode work function indicated the presence of an active film of barium and/or barium oxide, on the nickel anode, which was further modified by the presence of an electronegative layer and which could be removed by electron bombardment and heating. Some results have indicated that gettering by means of an evaporated film of barium may not be as effective as might have been hoped.

CONTENTS.

List of Figures.

CHAPTER 1.

General Properties and Preparation of Oxide Coated Cathodes

1. Introduction

A cathode, as used in vacuum tubes, may be defined as a device used for the production of electrons. Electron emission can be obtained by a number of methods but the most used and most tractable method is that known as thermionic emission. In this process, electrons are emitted from a hot body. It is important, from an economic point of view, that the energy expended to obtain each electron should be the minimum possible, that is, the work function (or the energy required to remove an electron from the cathode in vacuo) should have the smallest possible value. The first practicable cathodes consisted of a metal wire heated by the passage of an electric current, but in 1903 Wehnelt[1,2,3] noticed an increase of emission when the wire was contaminated by metallic oxides. He consolidated this discovery by investigating the electron emitting properties of many metallic oxides and concluded that alkaline earth oxides were the best emitters. He and his collaborator Jentzch, found that the Richardson equation for the thermionic emission of electrons from metals was also obeyed by the oxides and determined the work function of various oxides.

Cathodes involving the alkaline earth oxides are now almost exclusively used in thermionic vacuum tubes, but while many of these devices have been produced and used, their mode of operation presents many basic problems in physics which

have not been completely solved.

2. Description

An oxide cathode consists of a quantity of an alkaline earth oxide, or a mixture of such oxides, supported upon a metallic base which is capable of being heated either in vacuo or in a suitable atmosphere.

3. The Base Metal

The base metal must satisfy a number of demands which vary according to the prospective useage.

A number of generally required properties may be listed.

(1) A favourable influence on the electron emission.

(2) Chemical inertness with respect to the cathode material and any gases or vapours existing in the tube.

(3) General stability during operation and processing, in particular, a low rate of evaporation, a high melting point, high tensile strength, and a low rate of recrystallisation.

(4) The ability to be readily 'out-gassed' during manufacture.

(5) Low thermal conductivity and emissivity.

Few metals satisfy these requirements, but the most suitable ones are listed below:-

(a) Tungsten. This metal is used exclusively for directly heated cathodes where the oxide is deposited on the heating filament. It has a disadvantage in that chemical reactions with the oxides produce tungstates which have a high resistance. This disadvantage is negated by coating the wire with a suitable chemically inert metal.

(b) Platinum. Platinum is chemically inert and does not react with the oxides. Barium is said to dissolve in the metal (Metson[4]) and thus may increase the effective life of the cathode. The main disadvantages are the high cost and difficulty in 'activation'. The term 'activation' will be defined in section 6.

(c) Nickel and Nickel Alloys. These are the most commonly used base metals. Liebold[5] states that, of all the metals, Nickel has the best influence on the emission. It is also chemically inert and does not react with the oxides. Nickel is seldom used as the pure metal. Alloys, containing reducing agents, are used to help reduce the oxide and liberate free barium. Aluminum, magnesium and titanium are commonly used. Other additions, for example silicon and manganese, give increased tensile strength.

One of the most widely used commercial alloys is '0 Nickel' and this alloy has been almost exclusively used as the basemetal by workers in this laboratory. The additions are as follows:-

Co	0.5%	Si	0.10%	Mn	0.15%	Cu	0.10%
Fe	0.20%	C	0.06%	Mg	0.10%	S	0.005%

The advantages which the additions confer are offset by the formation of high resistance silicon and manganese compounds which reduce emission[6,7,8]. These compounds are situated between the oxide and the base metal and constitute the 'interface layer'. Additions of copper reduce the radiant

emissivity, thus cutting radiation losses to the minimum possible level.

Nickel and nickel alloys are almost exclusively used for indirectly heated cathodes. Generally speaking there are two types. The first is in the form of a hollow cylinder for tubes of cylindrical geometry, while the second type is in the form of a cup and is used in tubes with plane parallel geometry. Both types are heated by an electric current passed through a wire or coil insulated from the base by a ceramic body. The heater should make good thermal contact with the base metal so that heating is due to conduction rather than radiation.

Indirectly heated cathodes are used more frequently than directly heated cathodes. They have the advantage that the cathode is at a uniform potential, whereas the directly heated cathode has a potential gradient due to the heating current. Indirectly heated cathodes have been used for all the work carried out in this laboratory.

4. The Alkaline Earth Oxide Layer.

The alkaline earth oxides are not stable in air. Chemical reactions occur with carbon dioxide, water, and the sulphur compounds present in industrial atmospheres, to give the carbonates, hydroxides, sulphides and sulphates.

The cathodes are therefore prepared almost exclusively by applying the cathode material as the carbonates. The carbonates are then converted to the oxides by heating while

the tube is continuously evacuated. The carbonates can be deposited onto the base metal by the following methods:- 1. Dipping, 2. Painting, 3. Electrophoresis, 4. Spraying. The mixtures which are deposited upon the base are prepared in the following general manner.

The carbonates are precipitated by passing carbon dioxide into a solution of the nitrates or hydroxides. These are then finely ground in a mill, and suspended in a volatile organic liquid which acts as a solvent for an organic binder such as nitrocellulose. After application, the organic solvent evaporates leaving the carbonates attached to the base metal by means of the organic binder. This binder is eventually removed during the heating process, when the carbonates are simultaneously converted to oxides.

The first two methods give a very similar cathode of fairly low porosity. Electrophoresis gives the minimum volume of pore space, while spraying gives the highest proportion of pore space together with a much rougher surface. All methods result in a pore volume of greater than 50% and usually as much as 80%[9]. These pores have a considerable influence on the operation of the cathode. The spraying method is the one most generally employed by manufacturers, and this method has also been employed for the construction of cathodes in this laboratory.

The behaviour of the oxide coating is also dependent upon the method of production of the carbonate, which influences

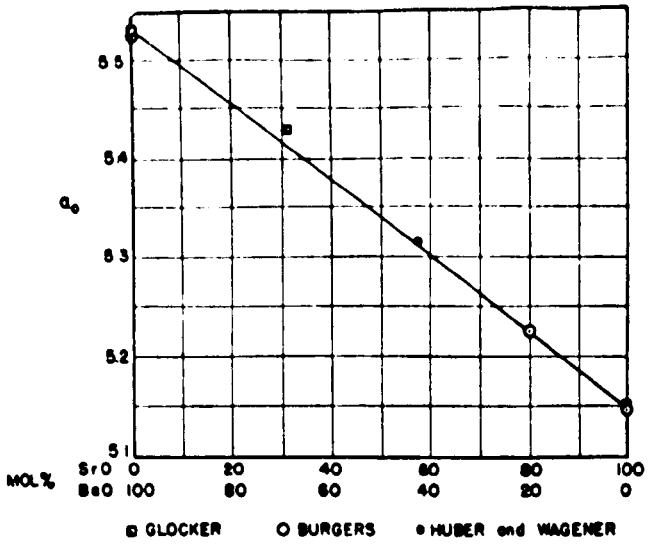

FIG. 1.4.1. —Variation of lattice constant with composition for solid solutions of (BaSr)O.

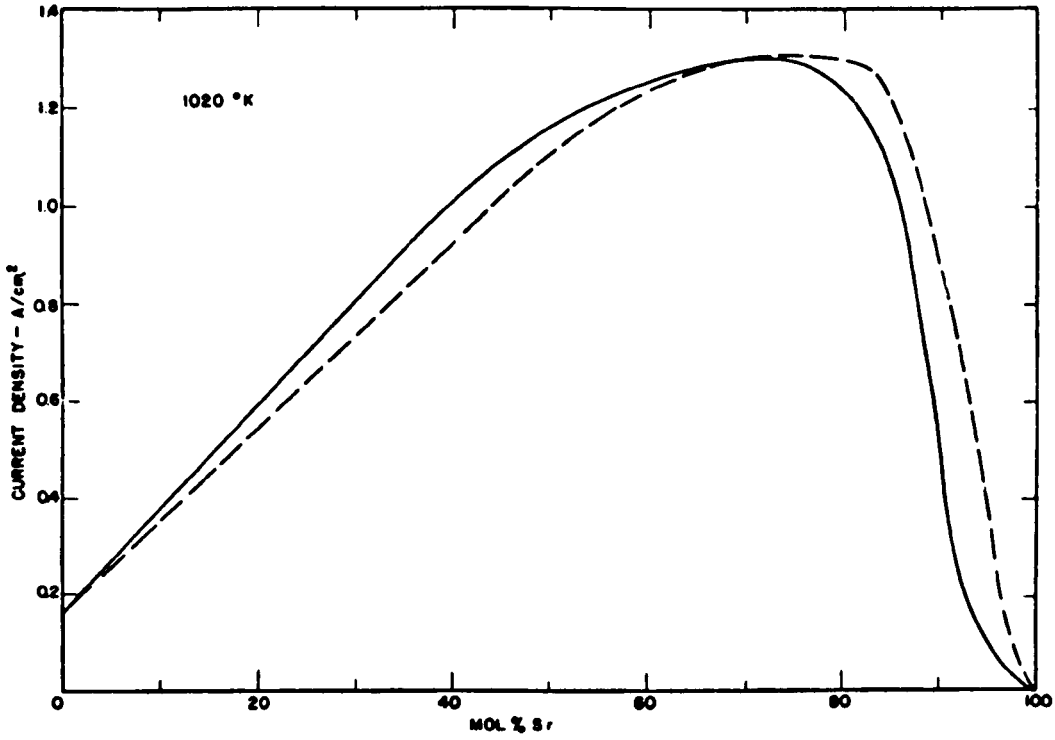

FIG. 1.4.2. --Dependence of d.-c. emission on mol per cent Sr content of (BaSr)O cathode. Solid line, carbonate content before heat treatment; broken line, oxide content after activation.

the particle size and purity. The volatility of the solvent, together with the humidity and temperature of the air during spraying, has a considerable influence on the porosity. All these factors must be rigidly controlled if cathodes of consistent behaviour are to be obtained.

Soon after the introduction of the oxide cathode into commerical use, it was noted that barium oxide was the best single oxide, whilst a mixture of two or more alkaline earth oxides gave cathodes which were more successful than those containing only one oxide. The investigations indicated that the mixed oxides gave a better bond to the base metal and, more important, gave greater electron emission at the optimum operating temperature. These facts were first recognised by Spanner[10] and Simon[11]. Later work by Benjamin and Rooksby[12]; Burgers[13], Huber and Wagener[14], and Eisenstien[15], confirmed these facts and indicated that there was a definite relationship between emission and crystallographic structure (Figs. 1.4.1 and 1.4.2.) It was found that barium and strontium oxides formed a continuous series of mixed crystals and that these resulted in enhanced emission. The addition of about 10% calcium oxide was also found to increase emission by a method which is still not understood, (Violet and Ruthmuller[16]).

Work in this laboratory is performed on cathodes of the single oxides, which results in a simpler system, more conducive to the investigation of cathode behaviour.

5. Cathode Processing

The cathode coated with the appropriate carbonate mixture, is mounted with the other electrodes and sealed inside the envelope of the tube. The tube is next sealed onto a vacuum system and the pressure reduced to at least 10^{-5}mm.Hg. The temperature of the cathode is now slowly increased to convert the carbonates to the oxides and the carbon dioxide evolved is pumped away. When the 'break-down' is complete all metal parts are out-gassed by heating with a radio frequency eddy current heater. The non-metallic parts are out-gassed by baking in an oven to a temperature just below the softening point of the glass. In this way the maximum possible quantity of gas is removed from the tube. Breakdown is generally recognised as being complete when the pressure is less than 10^{-6}mm.Hg, with the cathode at a temperature of 1200° K.

6. Activation

At this stage, electron emission from the cathode is extremely small and before such a tube can be used it is necessary to carry out the process known as 'activation'. A number of methods are available, all of which are thought to produce the same effect. It is thought that activation results from the production of a stoichiometric excess of metal atoms. A stoichiometric excess of barium is thought to be mainly responsible for the activation of all oxide cathodes which contain barium oxide, but it is likely that

Strontium and calcium will also be responsible to a more limited extent. Moore, Wooten and Morrison[17] have shown that the quantity of excess barium is not greater than one atom in 10^6 for the case of a practicable barium oxide cathode.

The methods available for activation are:-

a. Drawing Emission Current at the Operating Temperature.

When emission current is drawn (at constant temperature) it increases slowly to a maximum value. It is thought that barium and oxygen are liberated electrolytically. The oxygen escapes from the coating but the barium is left as free metal.

b. Heating or 'Flashing' the Cathode to High Temperatures.

In this case, any reducing components of the base metal are thought to react with oxygen present in the oxide, thus liberating barium. The organic binder also behaves as a reducing agent, (Benjamin, Cosgrove and Warren[18]).

c. Exposure of the Hot Cathode to Reducing Gases.

Methane, ethane and carbon monoxide have all been shown to activate the cathode (Prescott and Morrison[19], Eisenstein[20], and Forman[21]). This process has also been studied by Huber[22] who found that cathodes prepared from barium peroxide were not as active as those prepared from the carbonate.

d. Activation by the Addition of excess Barium.

When barium from an external source is evaporated onto the cathode, an immediate increase of emission is noted. At high cathode temperatures the emission decreases and it is thought that barium diffuses into the body of the cathode.

The final steady level of emission is found to be higher than before evaporation. At low cathode temperatures the emission falls rapidly and it is thought that the barium evaporates off the cathode. (Kawamura[23], Nergaard[24], Wright[25]). See also with reference to thin film cathodes on an MgO base

e. Activation by electron Bombardment.

This method has been investigated by Becker[26]. It has been found to be feasible but is not often used.

It may be noted that Metson[27] has suggested that neither the theory of chemical reduction nor the theory of electrolysis are sufficient to explain the very considerable increase in emission produced by activation.

Throughout the life of an oxide cathode there is continual evaporation of the alkaline earth oxides, together with a certain quantity of the corresponding metals. Thus, the fully activated oxide cathode will reach a state of dynamic equilibrium which is characteristic of the cathode temperature.

When the desired state of cathode activity has been attained the tube may be sealed off and the getters fired. The tube is then ready for use.

7. The life of an Oxide Cathode

A decrease in emission is normally observed as an oxide cathode is operated over a period of time. If maximum life is required it is necessary to operate the cathode within the temperature range 900°K to 1200°K. As the operating temperature is reduced there is an increasing tendency for the

emission to decrease due to 'poisoning'. Poisoning is thought to be the reverse of the activation process in so much as the stoichiometric excess of barium is thought to be removed by reactions with gases and vapours present in the experimental tube. The poisoning effects of different gases and vapours have been studied by Herrmann and Krieg[28], and their work indicates that most gases involved in the manufacture of the valve produce some sort of poisoning effect. The only gases involved which do not give a poisoning effect are hydrogen and the inert gases. It is interesting to note that gases which produce activation at low pressures give the opposite effect at high pressures. Oxygen, in particular, produces a marked poisoning effect which has been investigated by Metson[29] and Higginson[30]. Higginson has also studied the effects of sulphur poisoning.

Herrmann[31] has shown that solids can also produce poisoning effects. This is due to chemical reactions with the oxide to produce complex compounds. Liebold[32] has shown that the core metal can cause poisoning if reactions occuring during manufacture produce similar compounds. Chromium, iron, and molybdenum are particularly prone to this kind of behaviour.

At temperatures above 900^{o}K poisoning effects produced by gases are reduced to a minimum. Electron emission is quite high at these temperatures, but unfortunately the increased temperature of the cathode increases the rate of

evaporation of the cathode material. Barium oxide is preferentially evaporated because the vapour pressure of this oxide is higher than that of strontium oxide, and calcium oxide but the vapour pressures of the metals are lower than those of the oxides, with barium having the lowest vapour pressure of the three. Thus, the composition of the cathode will change with time. This change has been detected and measured by Eisenstein[33] who also found that the changes were not affected by drawing current. It was also found that the proportion of barium oxide declined more rapidly when the base metal contained reducing agents. This might be attributed to the more rapid production of the metals from the oxides by chemical reduction. The metals have a much higher vapour pressure than the oxides so that the rate of evaporation will be increased. At 1200°K evaporation effects limit the life of an oxide cathode to about 1000 hours.

8. The Function of the Stoichiometric Excess of Barium.

It has been stated that barium metal is produced in the oxide cathode and that this has been held responsible for the activation of the cathode. Some of the evidence concerning the amount of free barium produced will now be discussed.

One proof of the presence of excess barium has been noted above when it was stated that Wooten and Morrison showed barium to be present in the proportion of one atom in 10^6. These workers determined this figure by chemical analysis. Other workers have provided proof of the existence

of excess barium and some have indicated where it is located.

Qualitative proof was first given by Becker[34] who used an experimental tube with a BaO/SrO cathode arranged close to a carefully cleaned tungsten ribbon. The temperature of the cathode was increased to 1260°K and increased emission was obtained from the tungsten ribbon, which corresponded to the emission obtained from a tungsten/barium cathode as barium was evaporated onto the surface. Becker concluded that barium was evaporated from the cathode onto the ribbon and that free barium must exist in, or on, the cathode coating. Further proof was given by Gehrts[35], who observed a green glow, spectroscopically characteristic of barium, when the grid and anode of his experimental tube were bombarded.

The first chemical analysis of excess barium in the cathode was performed by Berdennikowa[36] who used a BaO/SrO/CaO cathode on a platinum/iridium base. The method utilised the reaction:

$$Ba + H_2O = BaO + H_2 .$$

Water vapour was introduced into the experimental tube and the pressure of the hydrogen produced was measured by means of a MacLeod gauge. The results indicated that the coating contained 5 micrograms of barium. Clausing[37] used the same technique and also a method based on the oxidation of the barium by oxygen to barium oxide. Both methods indicated 0.5 mole per cent of barium.

More recent determinations by Jenkins and Newton[38] using the method first described, indicated 0.01 mole per cent

barium. Other methods have been used and the most reliable of these indicate a similar quantity. These more recent determinations have distinguished between barium actually present in the coating and that evaporated onto the electrodes and the envelope.

Production of excess barium is accompanied by the liberation of an equivalent quantity of oxygen. This should also provide a method for the estimation of the excess barium. Qualitative proof was first given by Barton[39] who found the O_2^- ion by means of a mass spectrometer. However, this ion was not found by Shepherd[40] who, more recently, has carried out a similar study. Direct chemical analysis of the liberated oxygen has been performed by Isensee[41], who found that 0.2 mole per cent of oxygen was liberated from a BaO/SrO/CaO cathode.

The analyses described so far do not indicate the location of the metal. This knowledge is essential if a physical picture of the emission process is required. It was originally suggested that the barium was located either at the surface of the base metal or the surface of the oxide. It was also suggested that it could only be effective at the cathode surface. The quantities of barium found by analysis indicated that any surface film must be about 100 atoms thick. If however, the metal is also to be found at grain boundaries, the layer would be several atoms thick. It would seem that this explanation could not explain the behaviour of the cathode. Layers of this order of magnitude should behave

like the bulk metal, and this is certainly not the case for actual cathodes. Quite apart from this, the vapour pressure of barium is such, (3×10^{-2}mm. Hg. at 1000° K.), that layers of this thickness could not exist on the cathode surface. In addition, experiments by Becker and Sears[42], in which the excess barium was produced at the surface of the cathode, indicated an increase in emission with time when, it was supposed, the excess barium diffused into the body of the cathode.

It seems likely that most of the barium must be actually incorporated in the crystals, although this does not, of course, prohibit the formation of an adsorbed layer. Calculations of the ionic radii and the dimensions of the crystal lattice indicate that the excess barium is probably effectively produced by the formation of oxygen vacancies rather than by the production of interstitial metal atoms, (Schottky[43], Host and Nehlep[44], and Shriel[45]).

Measurements of the Hall coefficient by Wright[46] have indicated that the oxide cathode is an excess or n-type semiconductor. This behaviour is consistent with the hypothesis which invokes the presence of oxygen vacancies.

9. Summary.

The oxide cathode has been described as a porous structure of an alkaline earth oxide, or a mixture of these oxides, bonded to a metallic core. Excess barium has been shown to exist in the cathode and is probably mainly produced by the

formation of oxygen vacancies. While it is likely that such a system should behave as an n-type semiconductor, the possible existence of adsorbed layers of barium and other atoms should not be overlooked. An intermediate high resistance layer (interface layer) is also often present between the oxide and the base metal and may considerably modify the behaviour of the cathode. The behaviour of the cathode, in the light of these facts, will be discussed in the next chapter.

The Mechanism of Emission from the Oxide Coated Cathode.

(1) Early Theories.

The previous chapter has presented evidence which suggests that emission from the oxide coated cathode is in some way due to the presence of excess barium in the cathode. Early theories of emission from the oxide coated cathode invoked the presence of thin films of barium on the surfaces of the crystals. These theories were probably suggested by the fact that cathodes involving thin films of metal adsorbed on tungsten had been used successfully for many years. The adsorbed layers gave a pronounced reduction of the work function. The most successful of these cathodes involved films of thorium or caesium which were thought to be present as adsorbed layers only one or two atomic layers thick. Langmuir[47] attributed the reduction of the work function to the adsorption of the metal on the surface as a positive ion, the ion being bound to the surface by the image force. The positive charge on the ion and its image force constituted a dipole, which reduced the work function by an amount $\Delta \phi$ given by

$$\Delta\phi = 4\pi\theta\sigma_0\mu \qquad 2.1.1.$$

Where μ is the dipole moment, σ_0 is the number of sites available per square cm. and θ is the fraction of the surface covered.

A change of work function would also be produced by any adsorbed atom which possesses a dipole moment and is orientated in a characteristic manner at the surface.

Negative ions would, of course, produce an increase in the work function. Hence, in general, elements more electropositive than the metal onto which they are adsorbed would give a reduction in work function. Conversely, elements more electronegative than the base metal would increase the work function. For example, the strongly electronegative element oxygen adsorbed onto tungsten produces a particularly marked increase in work function, (Johnson and Vick[48]).

Lowry[49] extended these theories to explain the emission of electrons from the oxide cathode. He proposed that the excess barium was either occluded or alloyed with the surface of the base metal, which thus behaved as a thin film emitter. Lowry based this proposition on his experimental work, which indicated that barium was produced at the base metal both by electrolysis and the reduction of the oxide by agents present in the base metal. On his theory, electrons were liberated from the barium layer on the base metal and then diffused through the pores of the oxide. He regarded the oxide as a poor conductor.

Riemann and Murgoci[50] also regarded the base metal as the main source of electrons, but suggested that the electrons emitted from the base were captured and then emitted by the oxide several times, to be finally emitted at the surface of the oxide. On the other hand, Becker hold that emission originated from a barium layer at the surface of the oxide. This theory was supported by his experiments[52] in which a

cathode was found to be activated by the evaporation of barium onto its surface from an external source, and by experiments in which barium was found to be evaporated from the cathode. Additional evidence was provided by experiments in which the oxide layer was partially removed from the base metal without altering the electron emission, thus indicating that the core metal was not the source of electrons. Independent work by other investigators[53,54] also seemed to show that the emission came from a metallic layer at the surface. On the other hand, in addition to Becker's experiments, Jones[55] has described an experiment in which the emission was reduced by three orders of magnitude when the outer surface of the coating was removed. In this case the emission was restored by re-activating the cathode.

Electron diffraction techniques have been employed to examine the surface of the oxide. Work by Darbyshire[56] was interpreted as indicating a surface layer, but more recent work by Huber and Wagner provided no conclusive evidence for the existence of a monolayer.

The influence of adsorbed layers on the oxide surface is now often neglected by modern writers. The modern theory of semi-conductors has indicated that excess barium in the cathode may be located in the crystals to give an excess or n-type semiconductor. This has suggested that emission may be obtained from the surfaces of all the individual semi-conductor crystals, rather than a "special surface" located either at the base metal or the outside of the cathode.

It may be noted, however, that some modern workers, particularly Metson[57], consider that a "special semiconductor" exists at the base of the cathode and that this is responsible for the emission. The modern theory does not rule out the presence of adsorbed layers of barium and these may well play a significant part in the emission process.

2. Modern Theories of Emission.

In 1931, Wilson[58] extended the band theory of solids to explain the electrical properties of semiconductors. This theory has been used to explain the emission of electrons from the oxide cathode. It must be stressed that the theory outlined in this chapter and used by most modern workers in the field, assumes a clean surface free from adsorbed layers. If these are present the work function of the semiconductor will be modified by a mechanism similar to that described in section one.

The band theory was originally developed to explain the electrical properties of metals. Isolated atoms of any element contain a definite number of electrons which exactly neutralise the positive charge of the nucleus. These electrons exist in a configuration of discrete energy levels characteristic of the element. If the atoms are brought together to form a solid, a periodic field is produced in which quantum mechanical leakage of electrons occurs between the potential wells associated with each nucleus. The electrons are therefore no longer bound to a particular nucleus

but are shared by all the nuclei which make up the crystal. In consequence, the energy levels of the individual atoms can no longer be considered and instead a series of discrete energy bands, existing throughout the solid, and made up of closely packed energy levels must be considered. One or more of the higher energy bands may not contain the maximum number of electrons so that electrons may be readily caused to move to a higher energy level under the influence of an applied field or the addition of energy in a suitable form. A band of this type is called the 'conduction band', while the other bands are said to be 'filled'. Solids which contain electrons in an unfilled band behave as metals, but if the band is completely empty they behave as insulators until enough energy is supplied to promote an electron from a filled band across the forbidden band and into the conduction band. The bottom of the conduction band is usually considerably 'higher' than the top of the filled band (a typical value for this energy gap in an insulator would be 10eV) and thus conduction is not possible unless either extemely high fields are applied, the temperature is suitably increased, or the body is bombarded with sufficiently energetic particles. There is another class of solids known as intrinsic semi-conductors, in which the energy gap or 'forbidden zone' between the filled band and the conduction band is much smaller (~1eV). In this case, sufficient electrons can exist in the conduction band at room temperature for the solid to exhibit

Energy Levels for Sodium

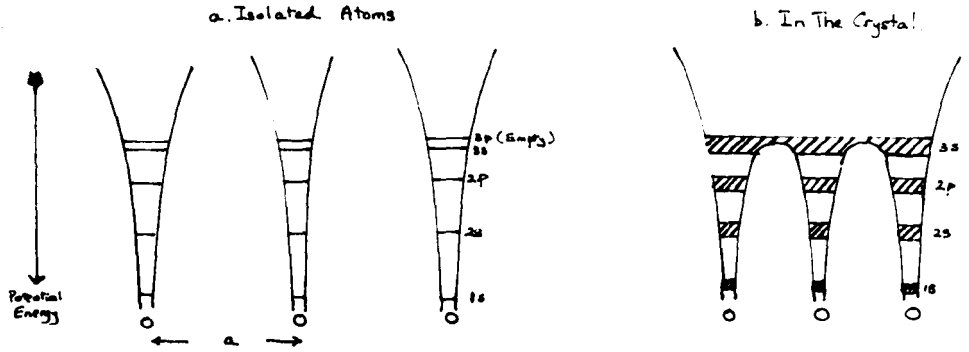

BAND STRUCTURES :-

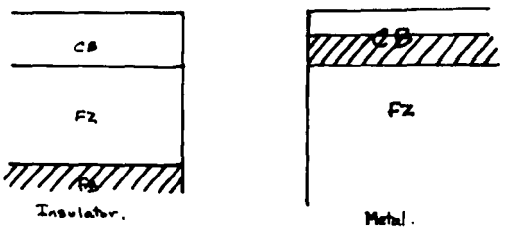

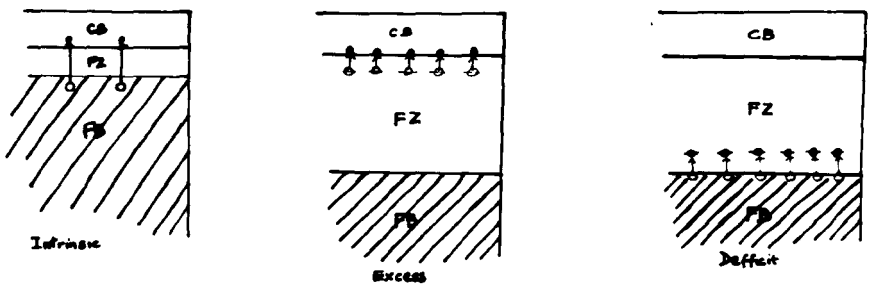

Semiconductors

(Not to Scale)

FIG. 2.2.1.

low electrical conductivity.

Two other types of semiconductor exist and are known respectively as excess or n-type and deficit or p-type semiconductors. Basically their band structures are identically similar to those of insulators but there are also additional levels in the forbidden zone which are produced by vacant lattice sites or impurity atoms. The n-type semiconductor contains energy levels situated below the conduction band (fig. 2.2.1) and electrons may be excited from these levels into the conduction band. The number of electrons which may be excited from these levels into the conduction band is controlled by a Boltzmann factor.

The p-type semiconductor has levels which are energetically situated just above the filled band in the forbidden zone. These may be occupied by electrons promoted from the filled band. This process produces unoccupied levels in the filled band and conduction may take place by the excitation of these 'positive holes'.

The evidence available indicates that the oxide cathode may be classified as an n-type semiconductor. The work of Wright and Forman, already mentioned, gave a value of the Hall coefficient consistent with an n-type semiconductor. Other work by Wright seemed to indicate a 'p' to 'n' transition at 800°K, but this has been shown to be anomalous.

Fowler[59] has formulated equations for an impurity semiconductor, based on the following assumptions:-

(1) The conduction band is completely empty at $0^{\circ}K$.

(2) The impurity levels are completely filled at $0^{\circ}K$.

(3) The density of the impurity levels is n_b per cc.

(4) The energy gap, ΔE, between the conduction band and the impurity levels, is larger than kT, (0.025 eV at room temperature).

(5) The energy gap between the filled band and the conduction band, is so large that the contribution of carriers from this band is negligible.

Taking the energy zero to be at the impurity levels, the value of the chemical potential (or the depth of the Fermi level) is:-

$$\mu = \frac{\Delta E}{2} - \frac{kT \log n_b^{-\frac{1}{2}}}{\log (2\pi m' kT/h^2)^{\frac{3}{4}}} \qquad 2.2.1$$

Where m' is the effective mass of the electron in the conduction band, and the other symbols have the usual meaning.

The value of kT at room temperature is $\sim 1/40$ eV so that, for normal values of n_b, the ratio:-

$$\frac{n_b}{(2\pi m' kT/h^2)^{\frac{3}{4}}}$$

is approximately equal to unity. Hence, at low temperatures:-

$$\mu \simeq \frac{\Delta E}{2} \qquad 2.2.2$$

or in other words, the Fermi level is half way between the impurity level and the conduction band.

The density of electrons in the conduction band is given by:-

$$n_f = \frac{(g)^{\frac{1}{2}} (2\pi m^* kT)^{\frac{3}{4}} n_b^{\frac{1}{2}}}{h^{3/2}} \exp - \frac{e\Delta E}{2kT} \qquad 2.2.3$$

Here g is a weighting factor $1 \leqslant g \leqslant 2$ to account for levels occupied by electrons of opposite spin. It must again be stressed that the above equations apply to a very simple model. ($g=2$ except when overlapping of energy bands occurs).

Quite apart from the possible effect of adsorbed layers, it is likely that the metal oxide boundary will profoundly influence the properties of the cathode. Other factors which should be considered include diffusion and ionic conduction. It is also extremely unlikely that the cathode will be of uniform composition, so that the electrical properties of the individual crystals may vary considerably.

3. The Hall Effect.

It has already been stated that the determination of the Hall coefficient provides a method for distinguishing between n-type and p-type semiconductors. An outline of the relevant theory will now be given.

If a magnetic field H is applied between opposite faces of a cube of a semiconductor, and a current I is flowing in a direction perpendicular to the magnetic field, an emf E is produced between the two remaining faces of the cube such that:-

$$E = RIH \qquad 2.3.1.$$

E is the Hall emf., and R is the Hall coefficient for the material. For a semiconductor:-

$$R = \frac{3\pi}{8n_f ec} \text{ e.s.u.} \qquad 2.3.2.$$

Where n_f is the number of free electrons or positive holes available for conduction, c is the velocity of light, and e is the unit of charge with the sign indicated so that R will be negative for electrons and positive for positive holes. The sign of the Hall coefficient thus provides a method of distinguishing between n-type and p-type materials while n_f can be readily calculated by the use of equation 2.3.2. The specific conductivity of the material is given by:-

$$\sigma = n_f ev \qquad 2.3.3.$$

Where v is the mobility. If R and σ are determined, the mobility can be obtained from the equation:-

$$V = \frac{8\sigma_o R}{3\pi} \qquad 2.3.4.$$

which is obtained by combining equations 2.3.2. and 2.3.3. From this value the mean free path l_o can be calculated from the equation:-

$$V = \frac{4l_o e}{3(2\pi m' kT)^{\frac{1}{2}}} \qquad 2.3.5.$$

The above treatment indicates that determinations of the Hall coefficient and conductivity should provide a powerful method for investigating the properties of a semiconductor.

Unfortunately the porous multicrystalline structure of the oxide cathode makes the determination of the Hall coefficient extremely difficult. Consequently, very few determinations have been made and simultaneous measurements of conductivity have rarely been attempted. Foreman[21] has performed experiments of this type over the temperature range 500°K to 1,000°K, which indicated that the cathode was an n-type semiconductor and that the electron mobility was very large above 700°K.

Ishikawa, Sato, Okumara and Sasakai[60] have reported similar experiments, which also indicated that the oxide cathode exhibited n-type conductivity in vacuo. They concluded furthermore, that the oxide exhibited p-type conductivity in an atmosphere of oxygen. This was previously shown by Wright[46].

4. The Thermo Electric Effect.

An electron passing from the Fermi level to the conduction band of a semiconductor undergoes a change in energy μ. The change in potential $\frac{\mu}{e}$ is known as the Peltier coefficient and the thermo electric power is given by:-

$$\frac{dE_s}{dT} = \frac{\mu}{eT} \qquad 2.4.1.$$

where E_s is the Seebeck emf. Seitz[61] has derived an equation for the Seebeck emf. in terms of the density of free electrons n_f and the density of impurity levels n_b:-

$$E_s = \frac{-\Delta T}{e}\left[\frac{\Delta E}{T} + k \log \frac{n_f}{n_b}\right] \qquad 2.4.2.$$

where ΔT is the temperature difference and ΔE the depth of the impurity levels below the conduction band. Measurements of this e.m.f. provide a method for determing ΔE. Blewett[62] has measured the Seebeck e.m.f. for two identical probes embedded in a barium oxide cathode. The observed negative e.m.f. corresponded to an n-type semiconductor. Results obtained by Nishibori and Kawamura[63] also indicated this, while, more recently Young[64] has published results which can be interpreted in terms of the Loosjes-Vink hypothesis.

5. The Conductivity of the Oxide Coating.

When considering the conductivity of the cathode as a whole, it is important to remember that a metal to semiconductor junction can give rise to rectification effects. If a semiconductor is brought into contact with (or in close proximity to) a metal, there is a 'levelling' of the Fermi levels. This causes the formation of a potential barrier. In the case of an n-type semiconductor, this barrier ensures that the transfer of electrons from metal to semiconductor is only possible when a high field is applied (Schottky[65] and Mott and Gurney[66]). The 'height' of the barrier is given by:-

$$\phi_m - (\chi + \frac{\Delta E}{2}) \qquad 2.5.1.$$

ϕ_m is the work function of the metal χ is the surface work function of the semiconductor and $\frac{\Delta E}{2}$ is the depth of the Fermi level below the conductior band (fig. 2.5.1.).

Experimental determinations of the conductivities of the

RECTIFICATION.

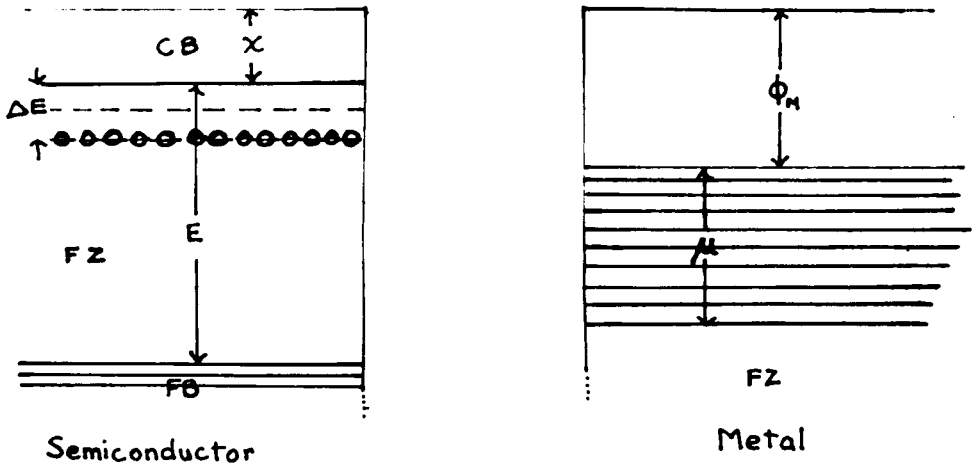

a. BEFORE CONTACT.

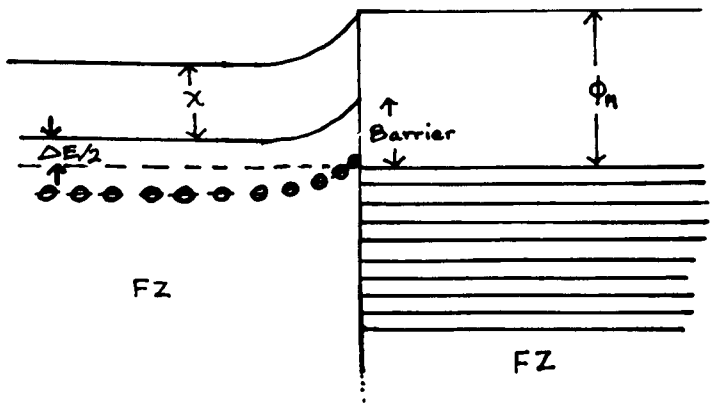

b. AFTER CONTACT.

FIG. 2.5.1.

oxide cathode indicate small rectification effects for an electron current flowing from metal to oxide (Wright[67]). As stated earlier in this section, rectification effects occur even when there is no direct contact of the semiconductor and metal. The thin, high resistance, 'interface layer' sometimes present could therefore be involved in the rectification mechanism. Fan[68] has considered the case of thick interface regions and has concluded that electrons diffuse through the layer.

The conductivity of the oxide itself must now be considered. In the case of alkali halides, migration of ions is considered to make a major contribution to the conductivity (Mott and Gurney[66]). While this process is important when considering activation by electrolysis, it may be neglected when a well activated cathode is considered because it would seem that electrons are principally responsible for the observed conductivity. It will be remembered that the oxide cathode has been described as a very porous body. These pores have a considerable effect on the conductivity of the oxide at high temperatures and this will be discussed later in the section.

The conduction of the electrons through the crystals will now be discussed in terms of the proposed semiconductor model. The specific electronic conductivity is given by equation 2.3.2., while the mobility of the electrons is given by

equation 2.3.5. Using these equations together with equation 2.2.3., and simplifying, we write the specific electronic conductivity as:-

$$\sigma = \frac{4\sqrt{3}\, n_b^{\frac{1}{2}}\, e^2 (g)^{\frac{1}{2}} (2\pi m^* kT)^{\frac{1}{4}}}{3\, h^{3/2}} \exp -\frac{e\Delta E}{2kT} \qquad 2.5.2.$$

The temperature dependence of the exponential term is very much greater than that of the other terms, so that we can compare equation 2.5.2. with the empirical equation:-

$$\sigma = \sigma_{oe}^{-Q/kT} \qquad 2.5.3.$$

It can be seen that a graph of $\log \sigma$ against $\frac{1}{T}$ should be linear if the material behaves as an n-type semiconductor, and that the value of $\Delta E/2$ may readily be obtained from the slope of the graph.

A number of methods have been employed for the measurement of conductivities. Wright[25] used platinum electrodes embedded in the oxide which was deposited on a ceramic base and activated with methane. It is unlikely that these results can be taken as being representative of an actual cathode because of the unusual conditions employed. Young[70], and Loosjes and Vink[71] used a method whereby the oxide material was pressed between two metal electrodes which could be independently, electrically, heated. The cathode material was found to be difficult to activate. In addition, simultaneous measurments of conductivity and electron emission were not easily obtained and were not very reliable because the geometry of the tube was poor. Tomlinson[72] has used a

probe method and also displayed the probe characteristics on a cathode ray oscilloscope.

Sparks and Phillips[73] have used a method whereby the voltage drop across the oxide was determined when emission current was drawn. The author has also tried this method but found, however, that the high potentials which must be applied to the anode produced cathode poisoning. Quite apart from this, only a very small part of the emission current can be used in the conductivity measurements so that measurements at low temperatures are not easy to perform.

The method which is used, almost exclusively, in this laboratory employs a helical probe of platinum or pure nickel. This is incorporated in the body of the cathode so that the resistance of the material between the probe and base can be measured. In common with most of the other methods, the measurement includes the resistance of any interface compounds which are present. Quite apart from this, the system is not symetrical, so that rectification effects are to be expected in addition to those due to the metal to semiconductor contact. These could be overcome by using two identical probes of a material which does not form interface compounds, but in practice this type of system is very difficult to produce. The probe method has the advantage that the cathode is very like a normal cathode, because the very fine probe wire does not appreciably alter the physical structure of the cathode; also, simultaneous measurements of emission and conductivity

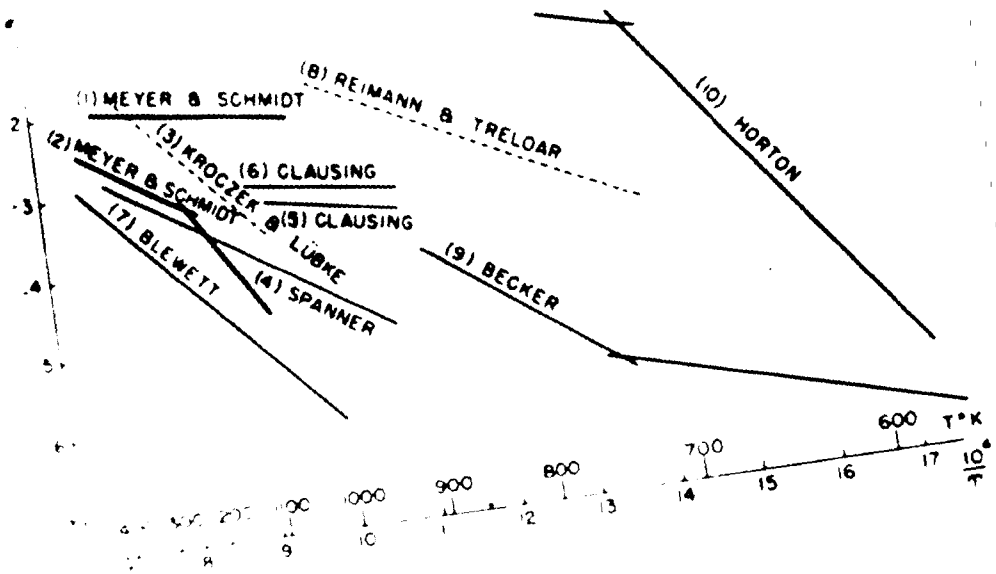
(1) MEYER & SCHMIDT
(2) MEYER & SCHMIDT
(3) KROCZEK
(4) SPANNER
(5) CLAUSING
(6) CLAUSING
(7) BLEWETT
(8) REIMANN & TRELOAR
(9) BECKER
(10) HORTON
LÜBKE
2
.3
.4
5
900
800
700
600 T°K
12
13
14
15
16
17
10⁴/T

FIG. 2.5.2.

can be made.

A review of early conductivity measurments has been made by Blewett[74]. The graph (fig. 2.5.2.) illustrates the diverse results which can be obtained.

Ionic conduction and bulk semiconduction are not the only possible conductivity mechanisms. There is a distinct possibility of a conduction process involving the surface layers of the crystals, which many workers believe to be quite significant. At temperatures where electron emission becomes measurable, the emitted electrons can provide an explanation of the enhanced conductivity observed at higher temperatures. Loosjes and Vink[71] were the first to suggest that electron emission within the pores of the crystals would contribute towards the observed conductivity. The possibility has been investigated by many workers. Hensley[75] and Forman[76] have shown that such a process will depend on three factors:-

(1) The mean free path of the emitted electrons which, under vacuum conditions, will be equal to the pore size.

(2) The space charge within the pores, which provides a retarding potential.

(3) The applied field, which produces a Schottky effect in the pores.

The theory relevant to the last two factors will be discussed in greater detail in the next section. On the basis of the above considerations, pore conduction can be described by an

equation of the type:-

$$\sigma_p = A\, n_o^{-\frac{1}{2}}\, T^{5/4}\, e^{\underline{d}}\, \exp\left[\left(\phi' + V_m - \sqrt{Ee}\right)\Big/ kT\right] \qquad 2.5.4.$$

Here, $\underline{V_m}$ is the mean retarding potential due to space charge, $\underline{E}$ is the applied field, $\underline{\phi'}$ is the work function of the cathode material, $\underline{d}$ is the mean radius of the pores and $\underline{A}$ is a constant.

The retarding potential will depend on both the pore size and the work function and will be given by an expression of the type:-

$$V_m = \text{Constant.exp.}\ -\frac{e\phi'}{RT} \qquad 2.5.5.$$

The pore conduction mechanism will also be affected by the magneto-resistive effect (Forman), which complicates the interpretation of the observed results.

The pore conduction predominates at high temperatures, but at low temperatures, when the number of emitted electrons is small, the semiconductor mechanism becomes predominant. The two processes act in parallel, so that the total specific conductivity can be written as:-

$$\sigma = n_o^{\frac{1}{2}}\left[C \exp -\frac{e\Delta E}{2kT} + B \exp -\frac{eW}{kT}\right] \qquad 2.5.6.$$

Where W includes all the exponential terms of equation 2.5.4. A graph of $\log\sigma$ plotted against $\frac{1}{T}$ should show two linear portions which merge into one another in the temperature range in which pore conduction becomes the dominant process. Experimental curves indicate that this 'break' generally occurs

in the range 700°K to 800°K. The temperature of the 'break' point will depend on the areas of contact between the individual crystals of oxide and their activation states. The slope of the low temperature portion of the graph thus provides a method for the determination of $\frac{\Delta E}{2}$ because at these temperatures the contribution of pore conduction is negligibly small.

Much work has been done in an effort to substantiate the Loosjes-Vink hypothesis. They themselves noted that the high temperature 'activation' energy had a value similar to the Richardson work function. However, these values were calculated from measurements made when the two electrodes were separated and an anode was inserted, which must have modified the oxide coating to some extent. Nakai, Inuishi and Tsung-Che[77] have also claimed similar results. It should be noted that the high temperature slope must be corrected to eliminate the contribution due to solid semi-conduction.

Young[78] and Forman[76] have also provided evidence of pore conduction. Forman has measured the thermo-electric power and the conductivity with an experimental arrangement similar to that of Loosjes and Vink, and found that the two activation energies were in agreement. He also applied a magnetic field of 5,600 oersteds in order to measure the magneto-resistive effect. At low temperatures the conductivity was hardly affected, but in the high temperature range it was reduced by

a factor of six. Additional work has been carried out by Forman with highly porous cathodes. These showed no bend in the conductivity curve and he interpreted this as being due to extremely small areas of contact between the crystals, so that the pore conduction process was predominant at all temperatures. Tomlinson[79], working with probe tubes has also presented evidence which is consistent with the hypothesis.

Some workers, including the author, have observed a third region of the conductivity graph which shows a decrease in slope at high temperatures. One explanation is that this is a saturation effect due to the space charge in the pores.

Higginson[80] has observed a further change in gradient at low temperatures ($\sim 400^{\circ}K$), with an activation energy of about 0.1 eV. He suggested that this might represent the movement of barium ions over the surface of the crystals. An alternative explanation has been given by Metson[81] who suggested that it might instead be due to the migration of negative ions of the residual gas.

6. Thermionic Emission.

Richardson's equation for the electron emission from clean metal surfaces has been shown to apply to semiconductors:-

$$J_o = A_o(1-r)T^2 \exp -\frac{e\phi}{kT} \qquad 2.6.1.$$

J_o is the saturation current density at zero field, r is the reflection coefficient for electrons travelling normal to the surface and A_o is a constant:-

$$A_o = \frac{4\pi m^+ ek^2}{h^3} = \underset{\text{for } m^+ = m}{120 \text{ amp.cm}^{-2}\text{deg.K}^{-2}} \qquad 2.6.2.$$

ϕ is the thermionic work function of the emitter, and can be described, both for semiconductors and metals, as the energy 'gap' between a point in vacuo just outside the metal and the top of the Fermi level.

If the energy zero is taken as being at the impurity levels this can be rewritten for the n-type semiconductor as:-

$$\phi = \chi + \Delta E - \mu \qquad 2.6.3.$$

χ is the electron affinity and is also known as the external, or surface, work function. If we incorporate the value of μ from equation 2.2.1., the equation for the saturation current at zero field can be written as:-

$$J_o = B(1-r)\, N_b^{\frac{1}{2}}\, T^{5/4} \exp - e(\chi + \frac{\Delta E}{2}) / kT \qquad 2.6.4.$$

This is the so called Fowler equation, where $B = \frac{2e(2\pi m^+ k)^{\frac{1}{2}}}{h^{3/2}}$.

Using this equation and plotting $\log \frac{J_o}{T^{5/4}}$ against $\frac{1}{T}$, we find that the graph should have a slope of $\frac{-e(\chi + \frac{\Delta E}{2})}{k}$. In practice it is found that a plot of $\log \frac{J_o}{T^2}$ against $\frac{1}{T}$ has a slope which differs very little from that given by the previous method. On the other hand, the intercept value is different. Both these methods can be employed to obtain a value for $\chi + \frac{\Delta E}{2}$.

Values of r can be calculated by substituting for n_b in equation 2.6.4. Values for n_b can be calculated from chemical analysis results such as those obtained by Prescott and Morrison[82] and Wooten[83].

Similar substitutions enable J_o to be calculated and it is found that the calculated values are considerably greater than those observed during D.C. operation. However, comparable values have been obtained when emission is drawn with the anode voltage applied as pulses a few microseconds in duration (Sproull[84], Coomes[85], Wright[86b]).

7. Emission Decay Effects.

Work with microsecond pulses has thrown some light on the decay of emission observed under D.C. conditions. Rapid decay of emission is also observed when the pulse lengths are longer than a few microseconds. The term 'decay' signifies the reduction of anode current with time at a constant value of anode voltage and cathode temperature. Sproull[84] explained this in terms of the migration of barium ions from the surface to the core under the influence of the applied field. Wright[86a] has shown that a change in interface resistance, suggested by other workers, could not be responsible and that electrolytic and poisoning effects were the most likely cause.

This last explanation invokes the bombardment of the cathode by gas molecules or ions. Metson[87] has reported that critical values of anode potential caused decay of the emission current. The electron energies corresponding to these potentials correspond to the heats of formation of oxides, chlorides,

and sulphates known to be present in the tube.

More recently, Nergaard[88] has postulated another theory for the oxide cathode. He accepts the semiconductor model, but considers that the donor centres are mobile. Thus, while emission is not being drawn from the cathode, the donors are uniformly distributed. When emission is drawn, the donors are transported to give depletion in the layers near the surface. This depletion is offset by back diffusion, so that while an initial decay of emission current is observed an equilibrium state is eventually produced and the emission current attains constant value. On this theory, the position of the Fermi level is dependent on the current drawn from the cathode. While this theory provided an explanation of Nergaard's own experimental results, it has not satisfactorily explained results obtained by other workers.

8. The effect of the Applied Voltage on the Emission Current.

The emission from the cathode is very dependent on the anode voltage and in fact three main types of behaviour are observed. When the anode is negative with respect to the cathode the emission current increases rapidly as the anode voltage is decreased, and electron emission is said to be occuring in a 'retarding field'. When the anode is positive with respect to the cathode, the emission current increases rather slowly with increasing anode voltage, so that now, emission is being obtained in 'an accelerating field'. A

third type of behaviour is observed when the field existing between the anode and cathode is small. Here, the 'space charge' of electrons present between anode and cathode prevents a rapid transition from accelerating to retarding field conditions.

9. Emission in Retarding Fields.

The field existing between the anode and the cathode is dependent upon the value of the applied voltage, the spacing and geometry of the electrodes, and the contact potential difference which exists between the anode and the cathode. When the resultant anode potential is negative with respect to the cathode, the field provides a potential barrier, so that only electrons which have energies larger than the value required to pass over the barrier can reach the anode. The current density for a diode with plane parallel geometry and with an applied anode voltage V_A is:-

$$J_R = A(1-r)T^2.c.\exp\ e\ \frac{(V_A - \phi_A)}{kT} \qquad 2.9.1$$

Here, ϕ_A is the work function of the anode, while c is the anode reflection coefficient. A graph of $\log \frac{J_R}{J_o}$ against V_A should result in two straight lines, the first should have a slope of $\frac{-e}{kT}$, while the second should be a horizontal straight line which intersects the first at $V_A = \phi - \phi_A$. Thus, if ϕ were known, ϕ_A could be determined and vica versa. The slope of the first region of the graph enables the temperature

of the cathode to be determined. Early measurements[89] provided values of temperature which did not coincide with the measured temperature, but agreement has been obtained more recently by Heinz and Hass[90], and Fan[91].

In practice a graph of log i_A against V_A is generally plotted, where i_A is the anode current. The retarding potential region should then be represented by a straight line with a slope related to $\frac{1}{T}$ which intersects a horizontal straight line characteristic of the electrons emitted in the accelerating field. The temperature of the cathode may then be calculated from the slope of the line in the retarding potential region if it is assumed that the distribution of electron energies is Maxwellian. Conversely, the energy distribution of the electrons may be found if the cathode temperature is determined experimentally. When this is attempted, it has been found that the distribution is Maxwellian, except that there is an apparent deficiency of electrons with low energies. (Eisenstein[92], Nottingham[93]). Fan[91] has suggested that this may be due to a large reflection coefficient at the oxide surface due to the presence of patch fields, which are caused by small-scale variations of the work function over the cathode surface. An alternative explanation has been given in terms of the presence of a thin penetrable potential barrier, capable of reducing the number of low energy electrons.

When the transition from a retarding to an accelerating

field is obtained, zero field exists between the anode and the cathode. Thus, the applied anode voltage has a value which is equal and opposite to the voltage drop across the cathode plus the contact potential difference existing between the surfaces of the anode and the cathode. In the case of metallic cathodes, the voltage drop is negligibly small, but in the case of the oxide cathode this can be quite significant. Many workers have neglected this fact and have taken the value of the anode voltage for transition as being numerically equal to the contact potential difference.

10. Space Charge Limited Emission.

Transition between the retarding and the accelerating field regions of a diode characteristic is never sharp. It is modified by a potential barrier, caused by the mutual repulsion of electrons present in the space between the anode and the cathode. This 'space charge effect' increases with increasing current density, and hence with increasing temperature The effects of space charge persist until the anode potential attains a value such that all emitted electrons reach the anode. The value of the current is given by the Langmuir-Child law:-

$$I_{sp} = BV_A^{3/2} \qquad 2.10.1$$

Where B is a constant dependent on the geometry of the tube. If the electrodes are not parallel, the field at the cathode surface is not uniform and the effects of space charge persist over a greater range of anode voltage.

11. Emission in Accelerating Fields.

When an electron is emitted, an image force is created which tends to attract the electron towards the parent surface. Taking this effect into consideration, Schottky[94] has deduced that the applied field will effectively reduce the work function by $\Delta\phi = \sqrt{eE}$: so that the emission current in an accelerating field is given by:-

$$i = i_0 \exp \frac{e^{3/2} E^{\frac{1}{2}}}{kT} \qquad 2.11.1$$

Hence, a graph of $\log_{\wedge} i$ against $V_A^{\frac{1}{2}}$ should give a straight line. This equation is not strictly obeyed by the oxide cathode, because the slope of the line is found to be several times greater than is to be expected from the equation. This is the case regardless of whether steady D.C. fields or pulsed fields are employed. An explanation of this has been given by Rose[95] and Hung[96] in terms of patch fields. A Schottky type equation has been derived for semiconductors by Mogulis[97] on the assumption that the applied field distorts the energy levels situated near the cathode surface. This theory has been extended by Wright and Woods[98], who showed that the current flowing through the cathode must also distort the energy levels. Both the applied field and the current cause a penetration of the cathode surface by the space charge zone. Data obtained from determinations of the Hall coefficient and the conductivity have been found to be in agreement with the theory.

The emission current at zero field can be obtained by

extrapolating the Schottky plots to zero field. From these values, a Richardson type plot can be obtained. The emission current at zero field can also be obtained from the break point of the log I_A/V_A characteristic. As stated previously, the contact potential difference existing between the anode and the cathode can be calculated from the value of V_A at the break point. Hence, if the cathode work function is known a value for the anode work function can be obtained and vice versa. The work function of the anode is seldom that of the pure metal, because the electrode is generally covered with a layer of barium metal or barium oxide which has evaporated from the cathode. Gases which are present in the tube are also responsible for a change in the work function because these are adsorbed onto the anode surface. Champieux[99] used a tunsten filament, which he cleaned by flashing, as an anode. The flashed filament was then supposed to have the work function of pure tungsten and hence, he was able to caluclate the cathode work function from the contact potential difference given by the break point. Heinz and Wagner[100] used a similar method, but found the anode work function by means of a Richardson plot. An alternative method has been used by Hopkins[101] who used a Kelvin vibrating electrode method to determine the cathode work function,

12. The Surface Work Function.

The thermionic work function of a semi conductor is made-up of two terms. The first, the 'depth' of the Fermi level

below the conduction band ($\frac{\Delta E}{2}$), is known as the internal work function, while the second term, the 'depth' of the conduction band below the surface (χ), is known as the surface work function.

If activation is simply caused by the production of donor levels, then any change in the work function is due to a change in $\frac{\Delta E}{2}$. The surface work function should then have a constant value, regardless of the state of activation.

The surface work function can be determined in two ways. The first entails subtracting the value of $\frac{\Delta E}{2}$ obtained from the conductivity plot from the Richardson work function. The second method involves a combination of the emission and conductivity equations to give the equation:-

$$\frac{i_o}{\sigma} = \frac{3(1-r)kT}{4l_o e} \exp\left(-\frac{e\chi}{kT}\right) \qquad 2.12.1$$

A plot of $\log \frac{i_o}{\sigma T}$ against $\frac{1}{T}$ should yield a straight line of slope $\frac{-e\chi}{k}$ if l_o is independent of temperature, so that the surface work function can be readily calculated. It must be noted that this can only be obtained for the temperature range over which semi-conduction predominates. In the high temperature region, where pore conduction is thought to predominate, the slope of the conductivity curve will be related to the work function of the emitting surface by equation 2.5.4.

CHAPTER 3.

The Aims of the Present Investigation.

1. Introduction.

It has been the aim of the present author to investigate several aspects of the behaviour of the oxide cathode, which have received relatively little attention. The first of these is an investigation into the meaning of the results obtained from the Richardson plot which are often quoted as being values of the thermionic work function, together with an investigation into the significance of the intercept values given by the Richardson plot. As an extension of this, the second aim has been to investigate a linear relationship between the Richardson slopes and the intercepts of Richardson plots, which has sometimes been observed by workers investigating the properties of both metallic cathodes with adsorbed layers and oxide-coated cathodes. The third aim has been to investigate the claim, which has been made by several workers, that the surface work function of the oxide cathode does not change with the state of activation.

While these are the main aims of the investigation, it has been possible to examine other aspects of cathode behaviour and these will be discussed in the chapters devoted to experimental results and conclusions.

2. The Surface Work Function.

If the oxide cathode is considered simply as a semiconductor and the possible presence of adsorbed layers on the surface of the crystals is ignored, it is plain that the

activation process would involve only the production of donor levels below the conduction band. The surface work function of the oxide cannot be modified by such a change in the bulk properties, but it could change locally if surface states are produced. These surface states will be caused by the adsorption of foreign atoms or ions onto the surface of the crystals. If a very large number of these states exist, there may even be conductivity over the surface of the crystals to the detriment of bulk conductivity. The conductivity mechanism would involve the migration of ions or transfer of electrons from one surface state to another. Even a small number of surface states will inevitably modify the thermionic and photoelectric work functions of the crystals and hence the value of the contact potential which exists between the cathode and anode.

When the adsorbed species is electropositive with respect to the semiconductor, electrons will be gained by the semiconductor and will set-up a space charge layer near the surface. This results in the formation of dipoles which modify the work function of the semiconductor in the same manner as described in Chapter two. If the adsorbed atoms are electronegative, a positive space charge layer will be formed inside the semiconductor due to the loss of electrons to the adsorbed layer. This will also result in the production of dipoles which, in this case, increase the work function.

Many workers have neglected to take into account the effects produced by adsorbed atoms and have attempted to explain the properties of the oxide cathode on the basis of

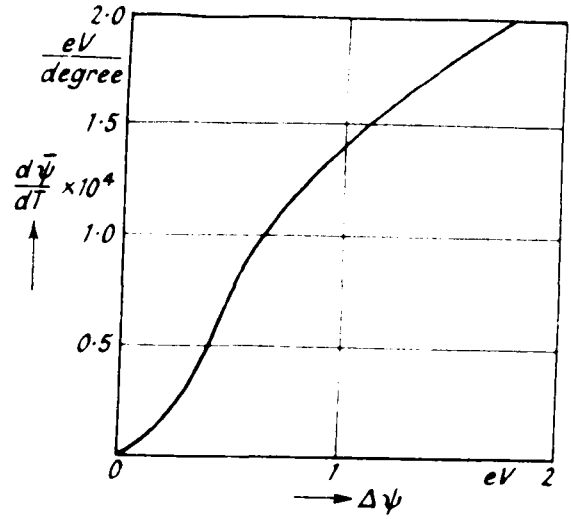

FIG. 3.5.1. Temperature Coefficient $d\bar{\psi}/dT$ of the Emissive Mean Value of Work Function as a Function of the Maximum Variation $\Delta\psi$ of Work Function.

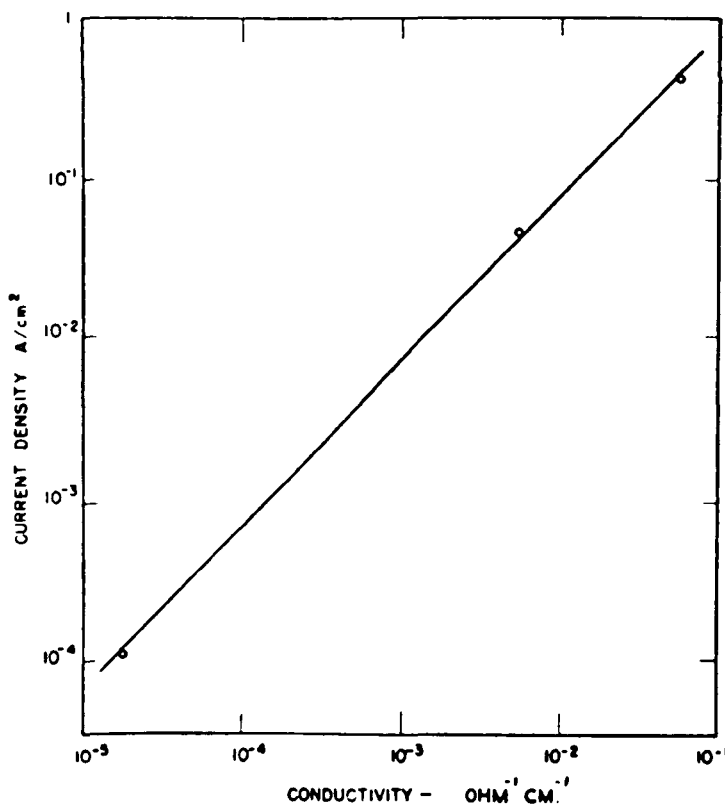

FIG. 3.2.1.—Correlation of electron emission current density and the coating conductivity, see text.

the simple semiconductor model described in Chapter two. Consequently, when studying the behaviour of the cathode, they have attempted to provide experimental evidence to show that, while the value of $\frac{\Delta E}{2}$ alters during activation, χ remains constant.

The equation which can be used to determine the value of χ, from emission and conductivity measurements, has been given as:-

$$\frac{i_o}{\sigma} = \frac{3(1-r)kT}{4l_o e} \exp - \frac{e\chi}{kT} \qquad 3.2.1.$$

Thus for a constant value of temperature, a plot of i_o against σ for different activation states, should result in a straight line if χ and l_o are both independent of the state of activation. Such a relationship was first obtained by Nishibori and Kawamura[102] and was later confirmed by Hannay, MacNair and White[103]. More recently, Hopkins[101] has claimed such a relationship from one of his experimental tubes in the low temperature conductivity region, (a typical experimental line is given in fig.3.2.1.).

Most of this experimental work was performed before the formulation of the Loosjes-Vink hypothesis, which is outlined in Chapter two, and consequently, these workers did not realize that the slope of the conductivity plots at high temperatures represented the activation energy of the pore-emission conductivity process, rather than the depth of the Fermi level below the conduction band of the semiconductor. The values of the emission current and the conductivity, which were used

in plotting these lines, were obtained in the high temperature range, probably because values of the emission current density at zero field and the conductivity are more easily obtained, by experiment, at high temperatures. Consequently, the conductivity values which the earlier authors plotted, represent the pore-emission conductivity process and not solid semiconduction as was assumed.

The emission current density at zero field has already been given as:-

$$J_o = A_o(1-r) \quad T^2 \quad \exp.\ (-e\phi/kT) \qquad 3.2.2.$$

The exponential term is dominant, so that at constant temperature, J_o can be regarded as dependent upon the value of ϕ, the Richardson work function. The conductivity of the oxide cathode has been given as:-

$$\sigma = N_o^{\frac{1}{2}} \left[C_1 \exp-(e\Delta E/2kT) + B \exp - (eW/kT) \right] \qquad 3.2.3.$$

At high temperatures the exponential term containing W is much larger than the other exponential term, so that the value of σ is determined, to a first approximation, by the value of W. The value of W has been given as:-

$$W = \phi + Vm - \sqrt{Ee} \qquad 3.2.4.$$

Vm, the mean retarding potential due to space charge, has a small value compared with ϕ over the temperature range considered, while E, the applied electric field, is also very small. Hence, the value of the conductivity in the high temperature range can be stated as being mainly dependent on the value of the Richardson work function.

We see that both J_o and σ are dependent on the value of

ϕ, so that a linear relationship is to be expected when J_o or $\ln J_o$ is plotted against σ. Thus, the linear relationship observed by the workers named above does not show that the surface work function is constant for all states of activation. On the other hand, their results do provide additional evidence in support of the Loosjes-Vink hypothesis.

The above discussion indicates that evidence in support of the constant surface work function hypothesis could only be obtained from emission and conductivity results obtained at low temperatures, where semiconduction is thought to be the main conductivity mechanism. The results obtained at low temperatures during this investigation have been analysed, but a linear relationship between J_o and σ has not been found. It was this that led the present author to investigate, in detail, the results of the workers who had obtained the linear relationship. The results obtained will be discussed in detail in later chapters, but it can be suggested here that the emission process cannot simply be examined in the light of the simple semiconduction model which was outlined in Chapter 2.

3. <u>The Richardson Equation and Experimental Results.</u>

The derivation of the emission equation by the use of statistical mechanics was first given for metals by Sommerfeld[104] and Nordheim[105]. Their form of the Richardson equation can be written as:-

$$J_o = A_o(1-r)T^2 \exp(-e\phi/kT) \qquad 3.3.2.$$

Where $A_o = \frac{g(2\pi m^* k^2 e)}{h^3} = g(60 \text{ amp/cm}^2\text{degree})$. The term 'g', which as stated previously is the occupation number, is

usually put equal to two, because the highest occupied energy band in the metals generally used for emission work is the s-band, but it is feasible that values other than two are possible in some metals, due to the overlapping of the highest energy bands. The generally accepted theoretical value of A_o is therefore taken as 120 amp/cm^{2}degree^2. The mean value of r, the reflection coefficient, has been calculated by means of wave mechanics, and the values obtained by Nordheim[105] and MacColl[106], assuming a continuous variation of the potential at the metal surface, gave a value of $r \simeq 0$. The more recent theoretical work of Herring and Nichols[107] also indicates a very small value. Thus, deviations from the theoretical value of the intercept will not normally be due to the values of g and r. The deviations could perhaps be explained if the electrons could not be regarded as completely free, but this is unlikely.

As stated in Chapter two, an equation exactly similar to equation 3.3.2 can be derived for semiconductors, if the simple model assumed in that chapter is used. In this case the work function is now the sum of two terms, the first being the external work function and the second the internal work function. The values of g and r are usually regarded as being the same as for metals.

From the above discussion, it would appear that if Richardson plots are made for the experimental results obtained from metals and the oxide cathode, the thermionic work function can be obtained from the value of the slope, while the antilog of the intercept value should have the theoretical

value of 120 amp/cm^{2}degree^2. In practice, determinations made over many years, by many different workers, have generally given values of the intercept which are inconsistent with the theoretical value. Values both larger and smaller than the theoretical value have been obtained. Determinations carried out on platinum have given values of $A_o(1-r)$ which have been as small as 11.7 amps/cm^{2}degree^2 and as large as 1.07×10^7 amp/cm^{2}degree^2, with corresponding values of the work function, 6.63eV and 4.69 electron volts respectively. Intercept values as large as 5×10^{11} have been obtained for oxygen on Tungsten (Kingdon). The oxide cathode has given values as large as 2.8×10^4 amps/cm^{2}degree^2 and as small as 10^{-3} amp/cm^{2}degree^2 with work functions of 1.03eV and 1.04eV respectively.

4. Possible Explanations of the Experimental Results

Several possible explanations of the experimental results outlined above have been given by various workers and these will be summarised below.

The method of measuring the value of $A_o(1-r)$ is, in itself, not very accurate; for example, consider the error in A due to 1% error in temperature measurement. If the temperature considered is 1,000°K and the work function of the surface is 5eV, then $\frac{\delta A}{A} = \frac{e\phi}{kT} \times \frac{\delta T}{T} = 0.58$, so that the emission constant can only be ascertained to an accuracy of about $\pm$ 50%.

Another factor which must be considered, is the actual area of the emitting surface. Many workers do not state how they determined the true emitting area and, assuming it to be constant, plot $\log \frac{i_o}{T^2}$ instead of $\log \frac{J_o}{T^2}$, so that the

logarithm of the area is included in the intercept value. But, quite apart from this, it can be appreciated that the actual emitting area may not be equal to the measured macroscopic area, so that, regardless of whether the emission current density or the emission current is plotted, the intercept value will depend upon the emitting area, which cannot readily be determined.

In addition, the work function may itself be temperature dependent and modify the intercept value in some way. Another factor which is generally completely ignored is the possibility that the work function may not be constant over the cathode surface. Variations could result from individual crystals or crystal faces having different work functions, or the presence of adsorbed layers on the surface, or both. These different work function areas will have a considerable effect on the intercept value in that the overall work function of the emitting surface will be temperature dependent. The patch fields resulting from contact potentials on the surface will produce electric fields on the cathode surface for zero applied field. Thus, the value of i_o obtained experimentally will not be the value for zero field. Surface roughness will also produce a variation in field over the cathode surface and modify the value of i_o.

5. The Temperature Dependence of the Work Function.

It can be seen from the above discussion that the temperature dependence of the work function might be an important factor in producing experimentally observed values of the intercept which differ from the theoretical value.

This has been discussed by Schottky[108], Becker and Brattain[109] and Wigner[110]. A linear dependence on temperature has commonly been assumed when:-

$$\phi_T = \phi_o + \frac{d\phi}{dT} \cdot T \qquad 3.5.1.$$

Replacing this in the emission equation, we obtain:-

$$i_o = A_o(1-r)\, ST^2 \exp -e(\phi_o - d\phi/dT \cdot T)/kT \qquad 3.5.2.$$

Where is the emitting area.

This equation can be rearranged to give:-

$$i_o = A_o(1-r)\, ST^2 \exp -(\frac{d\phi}{dT} \frac{e}{k}) \cdot \exp -(\frac{e\phi_o}{kT}) \qquad 3.5.3.$$

The slope of the Richardson plot enables the value of ϕ_o, (the Richardson work function at ^oK), to be calculated. The intercept will have the value $\log \left[A_o(1-r)S\right] - \frac{d\phi}{dT} \cdot \frac{e}{k}$, so that, values smaller than the theoretical value might represent the effect of the temperature dependence of the work function. If the temperature dependence is not linear, a curvature of the Richardson line should be observed. In practice it is likely that the curvature will generally be masked by experimental inaccuracies.

The simple treatment given above assumes an emitter of uniform work function. If the work function, ϕ, is a function of the co-ordinates x and y of the surface, the arithmetic mean value of the work function will be given by:-

$$\bar{\phi}_a = \frac{1}{S} \iint \phi(x,y)dx.dy. \qquad 3.5.4.$$

which is the work function which would be obtained by a contact potential difference method. The exponential term of the emission equation results in a different form of mean value when the work function is determined by emission

measurements. The mean value of the work function, as determined from emission measurements, is given by:-

$$\bar{\phi}_e = \frac{kT}{e} \log \frac{S}{\iint \exp. - e\phi(x,y)/kT.dx.dy.} \qquad 3.5.5.$$

In which the low work function areas are given a greater weight than the high work function areas.

If we consider that only two work functions ϕ_{min} and ϕ_{max}, exist at the cathode surface and that the areas of these are S_{min} and S_{max} respectively, the 'emissive mean' work function will be given by:-

$$\bar{\phi}_e = \frac{kT}{e} \log \left[\frac{S_{min}}{S} \exp - \frac{\phi_{min}}{kT} - \frac{S_{max}}{S} \exp - \frac{e\phi_{max}}{kT} \right] \qquad 3.5.6$$

The mean value, $\bar{\phi}_e$, varies with temperature even if the relative areas remain constant, because the large work function areas contribute relatively more to the emission at high temperatures.

This temperature dependence has been estimated by Gysae and Wagener[111], and fig. 3.5.1., shows the results obtained for a temperature of 1,000°K, in terms of the difference in work function of the two cathode areas. At this temperature it can be seen that the temperature coefficient is of the order of 10^{-4} eV/degree. The effect of the temperature dependence of area changes will be developed by the author (for a simple model) in the next chapter.

6. Determinations of the Temperature Dependence of the Work Function.

Determinations of the temperature dependence of the work function were first carried out by Gysae[112], from the

displacement of the log I_A/V_A characteristics. This method gave a value of the arithmetic mean work function. A temperature coefficient of about 1 x 10^{-3}eV/degree was found for temperatures above 800°K with considerable variation from one experimental tube to another. Below 800°K Gysae found a negative temperature coefficient, varying between -2 x 10^{-3} and -15 x 10^{-3}eV/degree.

Other determinations have been carried out by Huber[113], using the intersection method which gives the emissive mean work function, when values between 2 x 10^{-5} and 8.8 x 10^{-4}eV/degree were obtained. Little other work has been done and it is not possible to decide whether these values of the temperature coefficient are caused by a temperature dependence of the mean work function, either directly due to area changes or by a temperature dependence of the individual work functions of the various emitting areas.

7. <u>The Relationship Sometimes Found Between Intercept Values and the Richardson Slope.</u>

The results of different workers in connection with this relationship are very contradictory. Detels[114], Huxford[115], and Petai and Frank[116] are among the authors who have obtained results indicating that both the intercept value and the Richardson work function vary during the activation of an oxide cathode. But on the other hand, Espe[117] has claimed that ϕ remained constant while the intercept value altered. Detels, Kniepkamp and Nebel[118], and Veenemans[119] are among those who have found a linear relationship between the

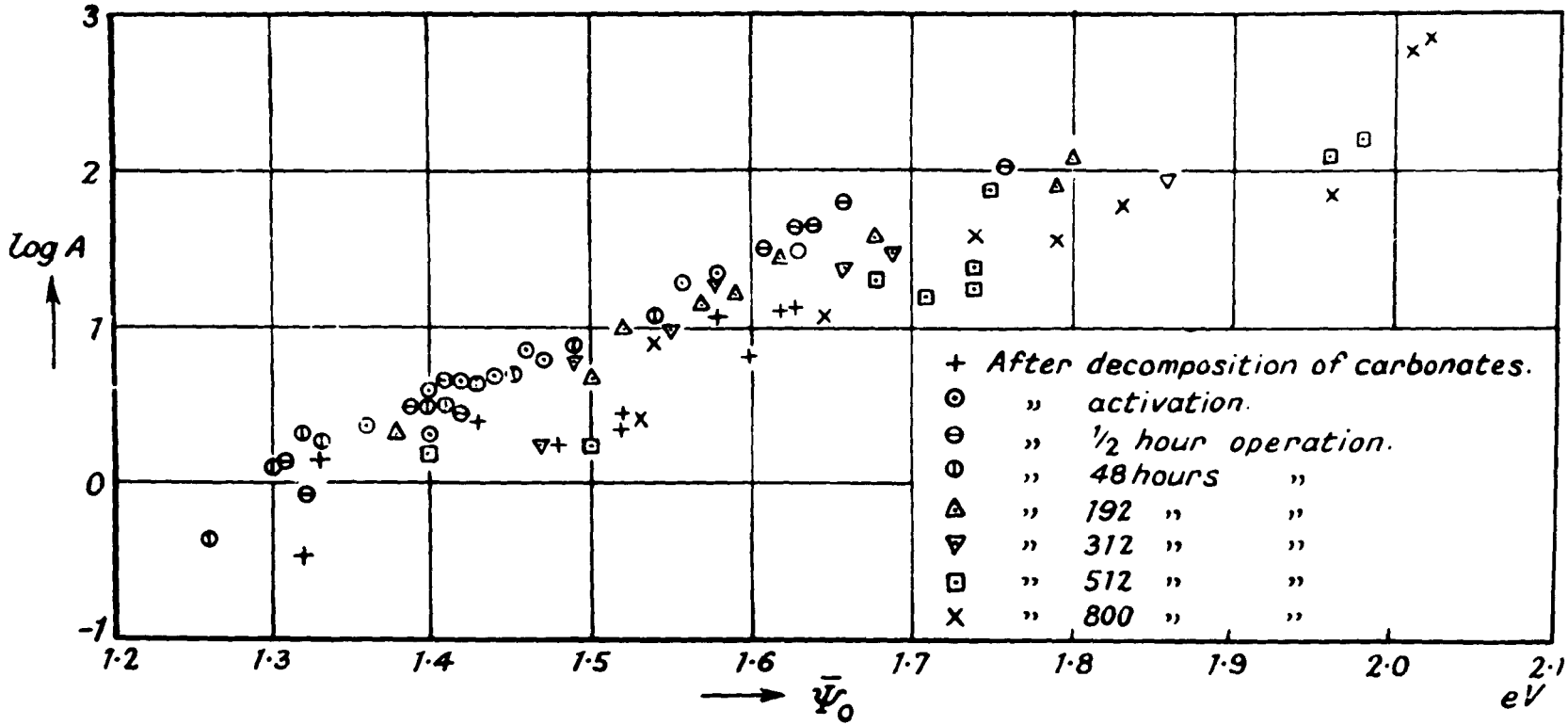

—Relationship between Emission Constant A and Work Function $\bar{\Psi}_0$ of Oxide Cathodes (Veenemans [1]).

Fig. 3.7.1.

intercept value and the Richardson work function, (see fig. 3.7.1.). If the intercept value is represented by log A, then this relationship may be written as:- $\log A = a\phi + b$, where a and b are constants. This relationship has also been obtained by Jacobs, Rees and Crossley[120], for different stages in the life of an oxide cathode.

Many explanations have been proposed in an attempt to account for this relationship. According to Hermann and Wagener[121], it may be due to an increase in the density of impurity levels within the crystals of the oxide as activation proceeds. Other explanations have involved an increase in the temperature coefficient of the work function as activation proceeds, but no mathematical treatments have been given. It has also been considered (Veenemans), that this relationship might provide proof of the thermal ionisation of barium atoms on the surface of the cathode, as described by de Boer. Theories of the above type have been worked out in considerable detail and two of these will be discussed below. An explanation proposed by the author will be given in the next Chapter.

8. The Interference Density Theory.

This theory has been proposed by Hermann and Wagener and the theory given below involves terms which are literal translations from the original German. Some of these terms are not in common use in this country, so that some explanation of the terminology used will now be given.

The term 'Interference Level' represents a level within a band of energies caused by the interaction of the impurity levels of the individual excess atoms. Similarly, the term

'Interference Band' represents the energy difference between the interference levels of highest and lowest energies, and is also used to refer to a system of interference levels. 'Interference Strip' is a term used to denote an energy gap, of width kT, within the interference band. Thus, if we have an interference band of width $e\Delta H$, (units of kT), containing n_H interference levels, the 'Interference Density' is the number of interference levels in an interference strip of width kT, that is,

$$n_{(kT)} = n_H kT/e\Delta H \qquad 3.8.1$$

This theory is based on the fact that the relationship between log A and ϕ is very similar in form to the one which is sometimes found to apply to conductivity measurements at different activation states of a semiconductor, (Meyer[122]). Thus:- $\beta = K_1 \log \alpha + K_2$, where K_1 and K_2 are constants with $K_1 > 0$, (Meyer's rule), and the relationship is said to be valid for $\beta \geqslant 0.06$ eV. α and β are given by the empirical conductivity equation, which can be written as:-

$$\sigma = \alpha \exp - (e\beta/kT)$$

The authors claim that changes in the slope of this line may occur at certain temperatures, and attribute this to a change in the number of electrons in the conduction band (thus ignoring the Loosjes-Vink hypothesis). β is found to decrease with the increasing number of excess atoms and a plausible explanation of this fact has been given by Mott and Gurney[123].

Let us now assume that the concentration of excess atoms is such that the impurity levels, due to the excess atoms, interact to give a band of levels. This interference band

Will have a width ΔH which will depend on the number of excess atoms and their degree of interaction. The interference level of lowest energy will be located at a depth H below the bottom of the conduction band. Thus, the number of electrons in the conduction band will be given by:-

$$n_f = gc^{\frac{3}{4}} n_{(kT)}^{\frac{1}{2}} T^{\frac{3}{4}} \exp - [e(H - \Delta H)/2kT].$$

g is, as before, a weighting factor; $c = \frac{2\pi m^+ k}{h^2}$; $n_{(kT)}$ is the number of interference strips in an interference band of width kT.

An increase in ΔH is produced as the number of excess atoms increases. This causes a decrease in the exponent of the equation and hence a corresponding decrease in β in the conductivity equation. The equation involving β and $\log a$ is more difficult to explain. a can be calculated from the equation for n_f and the equation:-

$$\sigma = \frac{N e^2 l_o}{2m^+ \bar{v}},$$

where N is the number of electrons/unit volume, $\bar{v}$ is their average velocity and l_o their mean free path.

β can be expressed in terms of the equation for n_f, when:-

$$\sigma = K_1 \log \frac{1}{l_o^2 n_{(kT)}} + K_2(T).$$

If this and the equation:-

$$\beta = K_1 \log a + K_2$$

are to be satisfied, a decrease in l_o or $n_{(kT)}$ with increasing ΔH or an increasing number of excess atoms n_H must be assumed. A decrease in $n_{(kT)}$ is the most likely cause.

In the above treatment, $\frac{H-\Delta H}{2}$ is the depth of the Fermi level below the conduction band. Hence, if we write the value of the work function in the Richardson equation in terms of the external and internal work function, the term $n_{(kT)}$ will be included in the non-exponential part of the equation, while $\frac{H-\Delta H}{2}$ is included in the work function. Thus, it is possible that changes in intercept value and work function will result in the same sort of linear relationship which has been indicated for the intercept and slope of the conductivity plot.

In this treatment, possible changes in the external work function χ have been ignored, so that, such a relationship could only be obtained for experiments in which there was no change in surface conditions. It has been indicated in an earlier section, that a constant value of surface work function cannot be expected for all activation states and therefore, the above argument does not provide a full explanation of the linear log A/Ø relationship.

9. The Influence of Changes in Surface Covering.

The most recent and the most comprehensive treatment of the linear log A/Ø relationship, in terms of changes in surface covering, has been given for metallic film cathodes by G. Haas[124]. This treatment was given for cathodes of the thoriated tungsten type and, if extended to the oxide cathode, would necessitate changes in surface work function without changes in the internal work function. Simpler treatments have been given by Richardson[125], de Boer[126], Veenemans[127] and Zwicker[128], all of which involved similar ideas. These will not be considered here.

If we consider the emitting surface to be non-homogeneous with respect to work function, electric fields will exist on the surface. These fields have been referred to earlier in this chapter, as 'patch fields'. Let the fraction of the total area covered by active centres (areas of low work function) be θ, and η the fraction of a monolayer of adsorbed atoms on the surface. We can express the equation for electron emission from a homogeneous surface, as:-

$$J_o = A(1-r)T^2 \exp-(eP_{max}/kT) \qquad 3.9.1$$

Where P_{max} is the potential barrier, measured with respect to the Fermi level, which electrons must surmount to be collected at the anode. If we modify this equation for a cathode having regions of different work function, we can write the total current density as:-

$$J_o = \sum_i AT^2\theta_i(1-r_i)\exp(-eP_{i\,max}/kT) \qquad 3.9.2.$$

Neglecting the emission from the higher work function patches, which is a small proportion of the total, we may write:-

$$J_o = AT^2 \exp\left(\frac{-e}{kT}\sum_{i=1}^{i=n}\theta_i\phi_i\right)\exp\left(\frac{-e}{k}\sum_{i=1}^{i=n}\theta_i\alpha_i\right)\sum_{i=1}^{i=j}\theta_i(1-r_i) \qquad 3.9.3.$$

Where ϕ_i is the work function of the i^{th} patch.

Hence, the value of the work function of the Richardson plot, if J_o is measured at zero field as indicated by the characteristic, will be:-

$$\phi\,(J_o) = \sum_{i=1}^{i=n}\theta_i\,\phi_{oi} \qquad 3.9.4.$$

which is independent of temperature.

The value of the intercept is given by:-

$$A_{(Jo)} = A\exp\left(\frac{-e}{k}\sum_{i=1}^{i=n}\theta_i\alpha_i\right)\sum_{i=1}^{i=j}\theta_i\,(1-r_i) \qquad 3.9.5$$

which includes the theoretical A value, the temperature coefficient of the work function, the reflection coefficient and the surface coverage. The above equations are for a constant surface coverage.

The effect of migration over the surface will now be considered. For this a new variable η must be defined, such that:-

η = Number of atoms of active material on the surface / Number of atoms of active material in a monolayer.

An equation for the thermionic emission current density can now be derived for zero field conditions:-

$$J_o = AT^2\theta(1-r_i)\exp\left\{\frac{-e}{kT}\left[\phi_{o2} - \eta(\phi_{o2} - \phi_{o1}^+)\right]\right\} \exp$$
$$\left\{\frac{-e}{k}\left[\alpha_2 - \eta(\alpha_2 - \alpha_1^+)\right]\right\} \qquad 3.9.6.$$

Where the values marked $^+$ are for $\eta = 1$ and the equation is for the simple case of areas of only two different work functions. ϕ_{o1} and ϕ_{o2} are respectively, the work functions of the clean surface and that surface covered by adatoms at absolute zero. α_1 and α_2 are the temperature coefficients of ϕ_{o1} and ϕ_{o2} respectively.

Similarly for the high field case:-

$$J_o = AT^2\theta\,(1-r_i)\exp\left\{\frac{-e}{kT}\left[\phi_{o2} - \frac{\eta}{\theta}(\phi_{o2} - \phi_{o1}^+)\right]\right\}$$
$$\exp\left\{\frac{e}{k}\left[\alpha_2 - \frac{\eta}{\theta}(\alpha_2 - \alpha_1^+)\right]\right\} \qquad 3.9.7$$

which gives values:-

$$\phi_{(J_o')} = \phi_{o1} = \phi_{o2} - \frac{\eta}{\theta}(\phi_{o2} - \phi_{o1}^+) \qquad 3.9.8$$

$$A_{(J_o')} = A\theta\,(1-r_i)\exp\left\{\frac{-e}{k}\left[\alpha_2 - \frac{\eta}{\theta}(\alpha_2 - \alpha_1^+)\right]\right\} \qquad 3.9.9.$$

Both $\phi_{(J'o)}$ and the exponential part of $A_{(J'o)}$ have the same dependence on surface covering, therefore the slope of a plot of $\log_{10} A_{(J'o)} / \phi_{(J'o)}$ will be

$$\simeq - \frac{-e}{2.3\ k} \frac{(\alpha_2 - \alpha_1^+)}{(\phi_{o2} - \phi_o^+)}$$

Though for higher values of $\phi_{(J'o)}$ this will not be the case, as the non-exponential part of $A_{(J'o)}$ becomes dominant.

Haas has claimed that this has been verified for the case of thorium on tungsten, but it must be noted that the equation for zero field did not yield a linear relationship between the intercept and the work function.

The two theories outlined above, seek to explain the linear log A/ϕ relationship in two different ways. The first, by considering changes in the internal work function with constant surface work function, and the second by considering changes in the external work function only. It is unlikely that explanations of this type could explain the linear log A/ϕ relationship for the oxide cathode, where considerable evidence indicates that both these quantities alter with the state of activation.

CHAPTER 4.

An Explanation, by the Author, of the Linear Relationship sometimes Observed between the Slope and Intercept of the Richardson Plot for the Oxide Cathode and Metallic Cathodes.

1. The linear $\log_{10} A/\phi$ relationship.

The equation for the emission current at zero field, i_o, from a surface of work function ϕ and area S, has been derived by Richardson and others, and can be written as

$$i_o = A_o(1-r)ST^2 \exp - \frac{e\phi}{kT}, \qquad 4.1.1.$$

where $A_o = \frac{4\pi mek^2}{h^3}$, and r is the reflection coefficient. The other symbols have the usual meaning.

If the values of $\log_{10} \frac{i_o}{T^2}$ are plotted against values of reciprocal temperature $\frac{1}{T}$, a straight line should be obtained. The slope is $-0.4343 e\phi/k$ and intercept $\log A_o(1-r)S$. In practise values of $\frac{10^3}{T}$ are usually plotted, instead of $\frac{1}{T}$, to simplify the graph. When such a plot is made for an actual complex cathode, values of slope and intercept are obtained which are often inconsistent with theoretical values. The slope of the Richardson plot gives a different value of work function than that determined for the same surface by other methods. Some workers (see Chapter 3), including the author, have observed a relationship between the intercept, (which can be symbolised by $\log_{10} A$), and the Richardson work function, ϕ, of the form $\log_{10} A = a\phi + b$. It was thought that an investigation of this relationship would throw some light on the reasons for the abnormal values of $\log_{10} A$ and ϕ.

In order to simplify the mathematical treatment, let $\log_{10} \frac{i_o}{T^2} = y$ and $\frac{10^3}{T} = x$. A plot of y against x will have slope m and intercept p. Hence, the equation for emission can be written as

$$y = mx + p. \qquad 4.1.2$$

The $\log_{10} A/\emptyset$ relation now becomes

$$p = mc + b. \qquad 4.1.3$$

In these equations $m = -\frac{e\emptyset}{k10^3 \cdot 0.4343}$, $c = -\frac{k10^3 a}{e \cdot 0.4343}$ and $p = \log_{10} A$. The symbol b retains the same meaning.

Equations 4.1.2 and 4.1.3 can be combined by eliminating p, to give:-

$$y = mx + cm + b. \qquad 4.1.4$$

This is the general equation for all straight lines which obey equation 4.1.3 for given values of c and b. Hence we have to solve the differential equation, $y = mx + f(m)$ where $f(m) = mc + b$.

Differentiating this with respect to x:-

$$m = m + x \frac{dm}{dx} + f^1(m) \frac{dm}{dx}. \qquad 4.1.5$$

But $f^1(m) = c$, so that:-

$$0 = x \frac{dm}{dx} + c \frac{dm}{dx}. \qquad 4.1.6$$

It follows that either $\frac{dm}{dx} = 0$ or $x = -c$. Now $\frac{dm}{dx} = 0$ when m is not a function of x and hence the equation $y = mx + mc + b$ represents a series of straight lines having slopes m and intercepts $mc + b$. Considering the solution $x = -c$ and substituting in equation 4.1.4 we find that $y = b$. Hence the singular solution of equation 4.1.4 is the point $(-c, b)$ and all straight lines represented by the equation $y = mx + mc + b$ (where m has a different

constant value for each straight line), must pass through this point. We also see that the slope of the $\log_{10} A/\phi$ plot has a value of $\frac{0.4343e}{kT^+}$ ie $a = \frac{10^3}{0.1985\ T^+}$.

Interpreting this point in terms of the original equation we see that the point has co-ordinates $(\frac{1}{T^+}, \log \frac{i_o^+}{T^{+2}})$. T^+ is the temperature corresponding to the intersection of all the lines. Hence, at temperature T^+, all the cathodes give the same emission current at zero field (i_o^+).

2. A simple model involving adsorption.*

Consider now a cathode, uncontaminated by adsorbed layers, which has a work function ϕ_2. If a gas or vapour of partial pressure p is introduced into the experimental tube, it will attain equilibrium with the production of adsorbed layers on all the surfaces. The area occupied by the adsorbed layer on the cathode will be a function of the temperature of the cathode. The number of molecules adsorbed per unit area has been given by de Boer[129] as $\sigma = \frac{Np}{\sqrt{2\pi MRT}}\ t_o \exp. \frac{-Q}{RT}$. Here N is Avagadro's number, M the gram. molecular weight, and R the gas constant for one gram molecular weight. t_o is the time of oscillation of an adsorbed molecule at absolute zero. If we assume that the area occupied by each molecule is independent of the number adsorbed and that the molecules are adsorbed as a monolayer, we can write an equation for the fractional area covered by the layer on the cathode. The fractional area is,

$S_1 = \frac{K^1 p}{\sqrt{T}} \exp \frac{-H}{kT}$, where K^1 is a constant and H is the

* This is modified in a paper to be published shortly.

heat of adsorption for one molecule. The fraction of cathode area which is uncovered is, $S_2 = \frac{K^1 p}{\sqrt{T}} (1-\exp-\frac{H}{kT})$.

Using the theoretical Richardson equation, the emission currents at zero field will be:-

$i_1 = A_o(1-r_1)T^2 S.S_1 \exp-\frac{e\phi_1}{kT}$, for the adsorbed layer and,

$i_2 = A_o(1-r_2)T^2 S.S_2 \exp-\frac{e\phi_2}{kT}$, for the clean surface.

ϕ_2 is the work function of the clean surface.

Replacing for S_1 and S_2, we can write the equation for the total emission as:-

$$i_o = i_1 + i_2 = A_o(1-r)ST^2 \frac{K^1 p}{\sqrt{T}} \exp \frac{-(H+e\phi_1)}{kT} + \exp \frac{e\phi_2}{kT} - \exp \frac{-(e\phi_2 + H)}{kT}$$

Here, r_1 has been taken as being equal to r_2. Herring and Nichols[107] have shown that r is always small compared with unity. Hence, the approximation is justified.

This simplified picture of a cathode will represent actual cathodes to a first approximation. Significant quantities of gases and vapours always exist in the most highly evacuated tubes. Variations of work function over the clean cathode surface are neglected, but actual variation will be small compared with the effect of the adsorbed layers.

The solution of the differential equation indicates that, for all cathodes giving a particular linear $\log_{10} A/\phi$ relationship, a temperature T^+ exists where the emission current at zero field is a constant. Hence, for a particular adsorbent and surface,

$$p\left[\exp\frac{-(H+e\phi_1)}{kT}+\exp\frac{-e\phi_2}{kT}-\exp\frac{-(e\phi_2+H)}{kT}\right] \qquad 4.2.2.$$

must be a constant.

This condition can be satisfied if p and $\left[\exp\frac{-(H+e\phi_1)}{kT}+\exp\frac{-e\phi_2}{kT}-\exp\frac{-(e\phi_2+H)}{kT}\right]$ are both constants or if the product of the two terms is a constant.

3. The significance of the relationship for metallic cathodes.

For a metal cathode and a given adsorbent, H, ϕ_1 and ϕ_2 must all be constants, so that p must also be a constant if the above condition is to be satisfied. This means that for metallic cathodes there can only be one Richardson plot which satisfies the necessary conditions. In practice the linear $\log_{10}A/\phi$ relationship has been observed when the values of ϕ, calculated from the slope and the intercept of tangents to a single curved Richardson plot, are plotted. This curve must describe the way in which the relative areas of the two different work function regions of the cathode surface vary with the cathode temperature and the partial pressure of the contaminant. Obviously, the tangents to such a curve cannot pass through a common point. Calculated values of $\log_{10}A$ and ϕ do, however, exhibit the relationship because, for the fairly limited temperature range considered, the tangents will, to a first approximation, pass through a common point.

When the oxide cathode is considered, the same sort of relationship is to be expected from a single plot, if these same conditions are satisfied.

4. The Linear $\log_{10}A/\phi$ relationship for the oxide cathode.

The work function of the clean cathode surface ϕ_2 can have any value between fairly wide limits, depending upon the

depth of the Fermi level below the conduction band. Adsorbed layers will modify the surface work function χ, because H and ϕ_1 will also be changed as the nature of the surface changes with ϕ_2. Hence, the oxide cathode will only exhibit the linear $\log_{10} A/\phi$ relationship for a series of differnt activation states, when the variables p, H, ϕ_1 and ϕ_2 are such that the value of the function given above (4.2.2.) is a constant. If a more complicated model is considered, the condition will be exactly similar and differ only in that more variables are involved.

The fact that so many variables are involved indicates why the linear $\log_{10} A/\phi$ relationship is so seldom observed. On the other hand, all valves which have received similar treatment during manufacture and activation, will give values of this function (equation 4.2.2.), which are of the same order of magnitude (Fig 3.7.1 page 54). Hence it is likely that a plot of $\log_{10} A/\phi$ for a large number of cathodes, having different states of activation, will indicate a trend towards a straight line.

5. The Values of the Intercept and Richardson Work Function

The equation of the saturation current at zero field from the idealized "two work function emitter" has been given as:-

$$i_o = A_o(1-r)T^2 S \sqrt{\frac{K^I}{T}} p \left[\exp\frac{-(H + e\phi_1)}{kT} + \exp\frac{-e\phi_2}{kT} - \exp\frac{-(H + e\phi_2)}{kT} \right]$$

Hence, a normal Richardson plot of $\log_{10} \frac{i_o}{T^2}$ against $\frac{10^3}{T}$ should exhibit curvature. This will be due to (a) the temperature dependence of the sum of the exponential terms, (b) the $T^{-\frac{1}{8}}$ term and (c) the temperature dependence of p.

The slope of the Richardson plot at any temperature T_t

can be obtained by substituting T_t in the first derivative with respect to $\frac{1}{T}$ of the logarithmic form of the equation. Hence the first derivative can be obtained from,

$$\frac{d \log_{10} \frac{i_c}{T^2}}{d \frac{1}{T}} = \frac{d}{d\frac{1}{T}} \frac{1}{2.303} \log_e p\left(\frac{1}{T}\right) \sqrt{\frac{1}{T}} \left[\exp -\frac{(H + \phi_1)}{kT} + \exp - \frac{o\phi_2}{kT} - \exp - \frac{(H + e\phi_2)}{kT} \right] \quad 4.5.1$$

Neglecting $T^{-\frac{1}{2}}$, which is small compared with the exponential terms, we obtain the following value for the first derivative:-

$$\frac{d \log_{10} \frac{i_c}{T^2}}{d\frac{1}{T}} = \frac{1}{2.303} \left\{ \left[\exp -\frac{(H + e\phi_1)}{kT} + \exp \frac{-\phi_2}{kT} - \exp - \frac{(H + e\phi_2)}{kT} \right] p^1\left(\frac{1}{T}\right) + p\left(\frac{1}{T}\right) \left[\frac{-(H + e\phi_1)}{k} \cdot \exp - \frac{(H + e\phi_1)}{kT} \frac{-e\phi_2}{k} \cdot \exp \frac{e\phi_1}{kT} + \frac{(H + e\phi_2)}{k} \cdot \exp - \frac{(H + e\phi_1)}{kT} \right] \right\} \div p\left(\frac{1}{T}\right) \left[\exp \frac{(H + e\phi_1)}{kT} + \exp \frac{e\phi_2}{kT} - \exp - \frac{(H + e\phi_2)}{kT} \right] \quad 4.5.2.$$

or:-

$$\frac{1}{2.303} \frac{p^1\left(\frac{1}{T}\right)}{p\left(\frac{1}{T}\right)} + \frac{1}{2.303} \frac{\left[\frac{-(H + e\phi_1)}{k} \exp - \frac{(H + e\phi_1)}{kT} - \frac{e\phi_2}{k} \cdot \exp \frac{-e\phi_2 + (H + e\phi_2)}{kT} \exp \frac{-(H + e\phi_2)}{kT} \right]}{\left[\exp - \frac{(H + e\phi_1)}{kT} + \exp \frac{-e\phi_2}{kT} - \exp - \frac{(H + e\phi_2)}{kT} \right]} \quad 4.5.3.$$

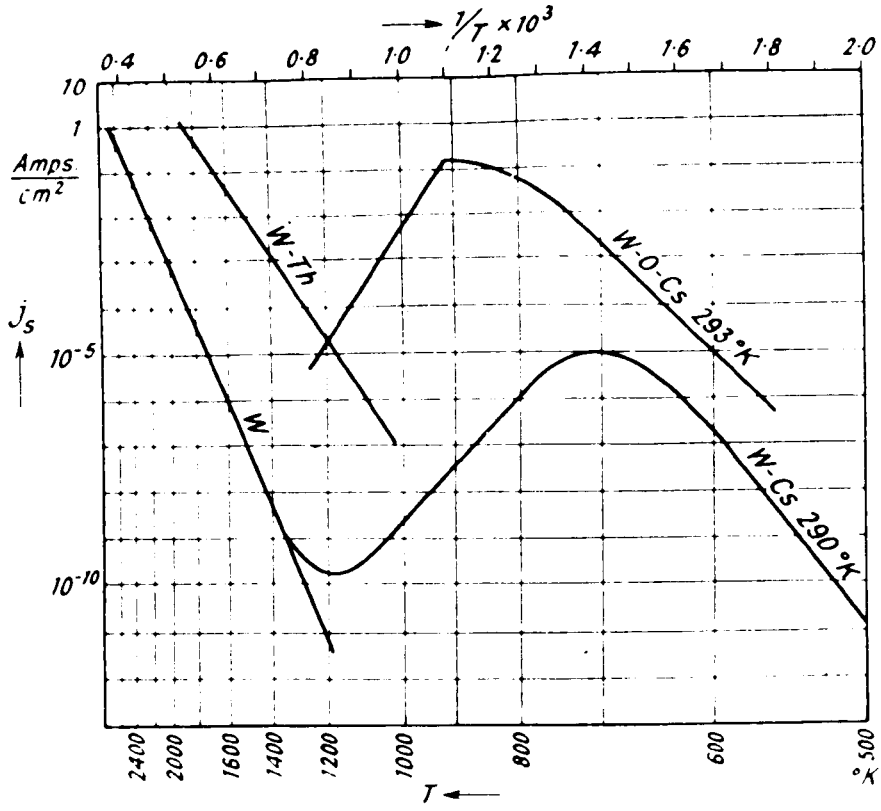

—Electron Emission of different Atomic Film Cathodes as a Function of Temperature.

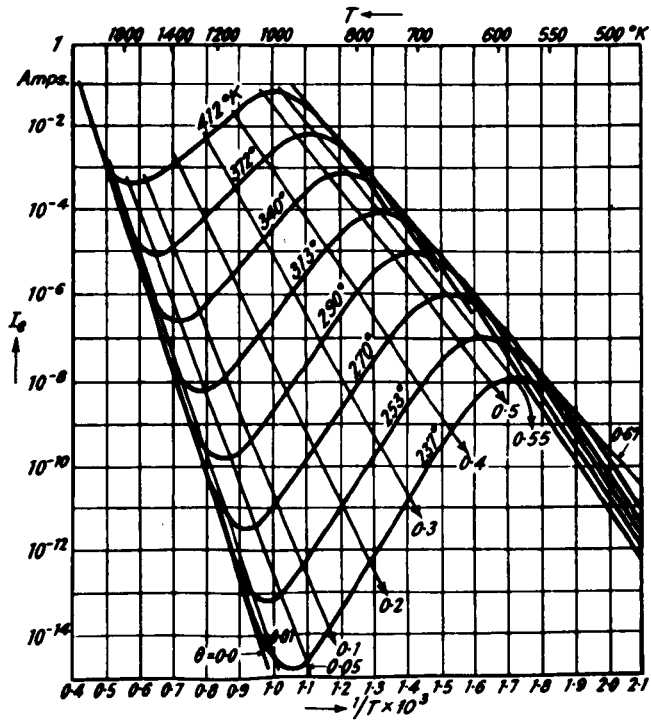

—Electron Emission of the W-Cs Cathode as a Function of Temperature (Temperature of the Valve as Parameter) (Langmuir and Taylor[9]).

FIG. 4.5.1.

We note that the slope and intercept at any temperature is very dependent on the form of $p(\frac{1}{T})$.

If p is constant during the determination, the slope of the line corresponds to the right-hand term. The Richardson work function is obtained from the slope by multiplying by $\frac{-k}{e}$.

The intercept value can be readily obtained from the value of the slope by substituting T_t for T in

$$\frac{1}{2.303}\frac{p^{I}(\frac{1}{T})}{p(\frac{1}{T})} + \frac{1}{2.303}\frac{\left[\frac{-(H+e\phi_1)}{k}\exp\frac{-(H+e\phi_1)}{kT} - \frac{e\phi_2}{k}\exp\frac{-e\phi_2}{kT} + \frac{(H+e\phi_2)}{k}\exp\frac{-(H+e\phi_2)}{kT}\right]}{\left[\exp\frac{-(H+e\phi_1)}{kT} + \exp\frac{-e\phi_2}{kT} - \exp\frac{-(H+e\phi_2)}{kT}\right]} \times \frac{1}{T} + \log_{10}\frac{i_o}{T^2} \qquad 4.5.4.$$

Where $\log_{10}\frac{i_o}{T^2}$ has the value given by the Richardson equation.

Hence, it may be seen that in the presence of an adsorbent, the intercept and the slope of the Richardson plots do not give the theoretical values. There is every reason to expect that positive or negative values of intercept $(\log_{10} A)$ could be obtained depending upon the values of $p(\frac{1}{T})$, H, ϕ_1, ϕ_2 and T. For example see fig. 4.5.1.

Positive values of slope are to be expected when the following are satisfied (a) ϕ_1 is small compared with ϕ_2; (b) H is small; (c) T is large. Large positive values of intercept will be obtained when the adsorbent is electronegative and the pressure is fairly high. The value will, however, decrease with increasing temperature and, in fact, would be

equal to the theoretical ~~value~~ value when $P(\frac{1}{T})$ tends to zero, or at extremely high temperatures. Small positive, or small negative, values of the intercept with small negative values of slope are to be expected when ϕ_1 is smaller than ϕ_2 and the temperature is low, or H is very large.

It may seem from this treatment that the Richardson method is not suitable for obtaining a value of work function for a particular surface. It certainly does not provide a method for determining the work function of the clean surface, except when the temperature is very high or the effects of the adsorbed layer are very small. The Richardson work function will, however, give a measure of the energy required to thermionically remove an electron from the surface, under the conditions present in the experimental tube.

The curvature of the Richardson plot will depend on the value of the heat of adsorption and the quantity of the adsorbent present. It may well be that a Richardson plot approximating to a straight line will be obtained if the pressure in the experimental tube rises exponentially with temperature and the adsorbent is electronegative. This may be the case only when the gas or vapour present in the experimental tube is in equilibrium with adsorbed layers on all the surfaces. Since the temperature of all surfaces in the tube have a functional dependence on the temperature of the cathode, the pressure will rise exponentially with the cathode temperature.

Linear characteristics will also be obtained at low temperatures, when the surface coverage is almost complete.

The characteristics will also be linear at very high temperatures when the surfaces are only slightly contaminated.

In the case of contaminents which are present in large concentrations, for example, caesium in caesium/tungsten cathodes, the pressure is the vapour pressure corresponding to the temperature at the coldest bulk substance. In these cases the pressure will rise only slightly with cathode temperature, because of the limited temperature increase of the bulk substance which is situated at the extremities of the glass envelope.

Barium getters, which are fired to reduce the pressure of the gas in experimental tubes by chemical combination, will provide barium vapour, which may be adsorbed onto the cathode surface and the cathodes themselves produce a film of active metal. The exact amount adsorbed at any temperature will, of course, depend on the vapour pressure of the barium and the heat of adsorption. This strongly electropositive substance may well produce a large reduction in the work function of the oxide cathode and may, in fact, be responsible for the low work function generally observed. If this is the case, the behaviour of the oxide cathode should be very similar to that of the caesium/tungsten cathodes and might exhibit a negative value of the Richardson work function at temperatures when the adsorbed layer is being removed very rapidly. (fig 4.5.1)

These hyptheses will be discussed later in the light of results obtained in the present investigation.

6. <u>The Values of Work Function Obtained by Other Methods.</u>

Two other methods of obtaining the work function of surfaces are commonly used. The first of these is the contact

potential difference method discussed in earlier chapters. The work function obtained by this method is called the arithmetic mean work function and, for the 'two work function emitter' considered above, will be given by:-

$$\left\{\left[\frac{k^1 p(\frac{1}{T})}{T}\right]\left(\exp\ \frac{-H}{kT}\right).\ \phi_1\right\} + \left\{\left[\frac{k^1 p(\frac{1}{T})}{T}\right](1 - \exp - \frac{H}{kT}).\ \phi_2\right\} \quad 4.6.1$$

It is unlikely that values obtained by this method will correspond to values obtained by the Richardson method, except when surface contamination is either almost complete or almost absent.

Determination of work function by the photoelectric effect will give values corresponding to the low work function surfaces, subject to the Frank-Condon effect. In this case, the work function will be bigger by $\frac{\Delta E}{2}$ than could be obtained from the same section of the surface by the Richardson method. The value of $\frac{\Delta E}{2}$ can, of course, be determined from conductivity measurements as described in an earlier chapter. It would seem therefore, that agreement between the values obtained from these different methods will only be obtained at very low or very high temperatures.

THE VACUUM SYSTEM

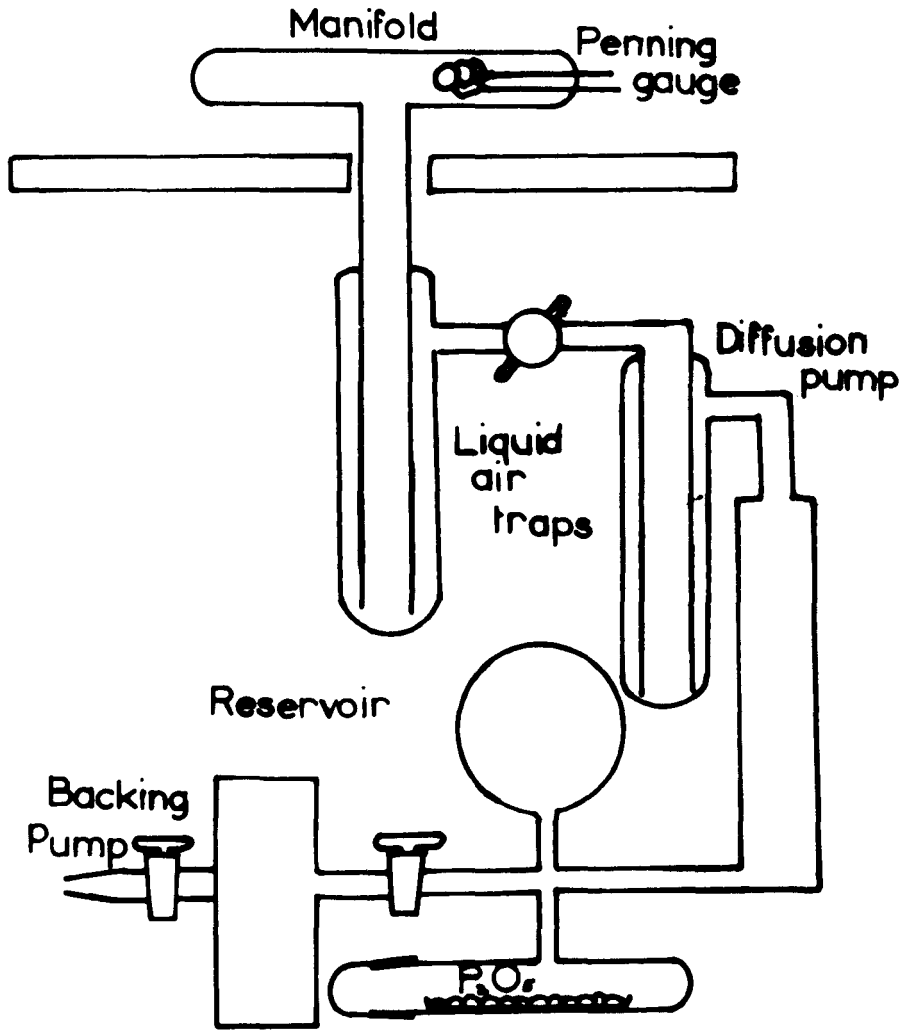

FIG. 5.1.1.

Chapter 5.

Apparatus and Techniques.

1. A general description of the techniques involved in the manufacture of an oxide cathode has been given in chapter 1. The manufacture of the necessary processing equipment and experimental tubes constituted a large part of the research programme. The processing apparatus consisted of a vacuum system, an oven, and suitable power supplies built into a steel frame. Apparatus for carrying out various measurements on the experimental cathodes was mounted on a bench adjacent to the processing apparatus.

2. The Vacuum System.

Reproducible results can only be obtained if a suitably low pressure is maintained in the experimental tube during its processing. Hence, a vacuum system having a high pumping speed and producing an ultimate vacuum of at least 10^{-6} mm.Hg. is required. The high pumping speed is needed to remove, as rapidly as possible, the carbon dioxide liberated during the processing. If this is not accomplished, the 'life' of the experimental tube is drastically reduced.

The vacuum system was constructed of Pyrex glass and is illustrated in schematic form in fig. 5.1.1. The glass used in the system was cleaned by treatment with concentrated nitric acid, washed with distilled water and dried in an electric oven. All metal parts involved in the construction of the system were cleaned by hydrogen furnacing, while the mercury used in the mercury diffusion pump was purified by vacuum distillation after treatment with nitric acid and

distilled water. By these precautions, possible contamination of the experimental tubes was minimised. Clean conditions were maintained by rebuilding the system twice during the course of the investigation.

The system consisted of a two stage mercury diffusion pump with a pumping speed of about one litre per second. This was 'backed' by a Metropolitan-Vickers rotary oil pump. The taps of the 'backing' system were greased with Apiezon 'N' grease, while the main tap was greased with Apiezon 'T' which has a higher melting point and is not affected by heat from the oven. The main tap was eliminated when the system was rebuilt for the second time.

A drying tube, containing phosphorous pentoxide, in the 'backing' system prevented water from entering the oil pump. Two liquid nitrogen traps were provided so that the carbon dioxide produced in the breakdown process could be readily removed from the system. Liquid nitrogen was initially applied to the trap nearest to the diffusion pump to prevent mercury vapour from entering the system. Carbon dioxide, produced in the breakdown process, was retained as the solid in this trap and its vapour limited the pressure which could be attained by the system to about 10^{-5} mm.Hg. This carbon dioxide was removed by applying liquid nitrogen to the second trap and allowing the temperature of the first to increase, so that the carbon dioxide sublimed and was pumped away without causing any undesirable increase in pressure. The ultimate pressure of the system was reduced to a minimum (lower than

10^{-6}mm.Hg.) by eddy current heating the metal parts of both the experimental tube and the system and by baking the glass of the experimental tube and the manifold to a temperature of about 450°C for about twelve hours.

3. Pressure Measurement.

Two types of pressure gauge have been used during the present investigation. In all the experimental work undertaken, a Penning gauge built into the manifold enabled pressure changes during breakdown and processing to be monitored. This gauge consisted of a nickel ring anode mounted half way between two nickel discs, 2cms. in diameter and 1cm. apart, which together constituted a cathode. A permanent magnet provided a field of 600 oersteds in a direction perpendicular to the electrodes. A D.C. potential of 2000 volts was applied to the electrodes from a high impedence power supply running from the A.C. mains. The electric field caused an electric discharge and produced positive ions from the gas molecules present in the system. The magnetic field caused the ions and electrons to move in helical paths between the electrodes, thus greatly increasing the possibility of further ionization by collision. The current passing between the electrodes was measured by means of a Tinsley multi-range galvanometer. This current, which was limited by the high impedence source [redacted] to a value below 100 microamps, was approximately proportional to the pressure in the range 10^{-5}mm.Hg to 10^{-6}mm.Hg.

A second type of gauge was sometimes employed to enable

Alpert Gauge, Diagramatic.

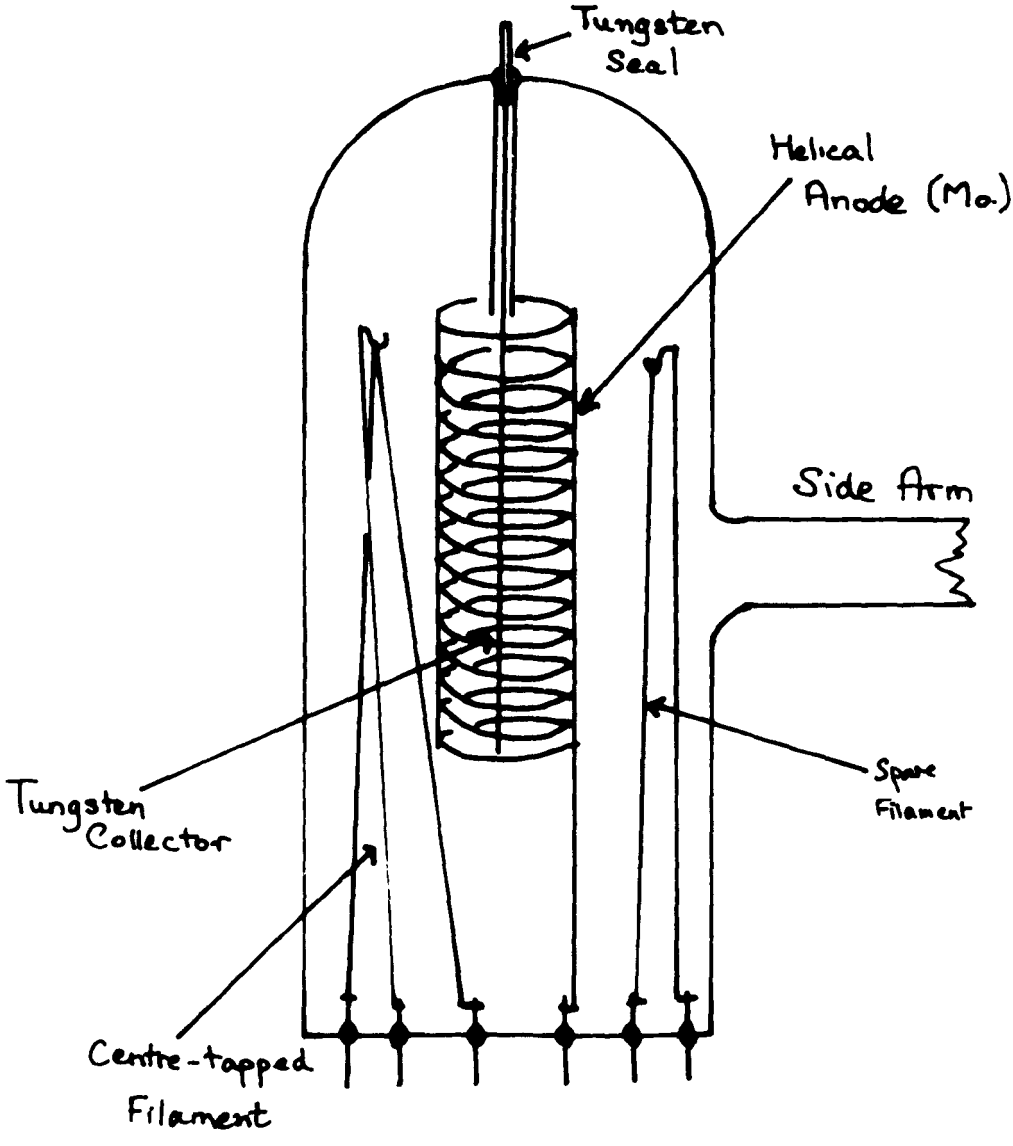

FIG. 5.21.

pressure changes in the experimental tube to be observed both before, and after, the tube had been isolated from the pumping train. This second type of gauge was attached to the experimental tube by means of a side-arm. A diagram of the gauge is shown in fig. 5.2.1. These gauges were of the Bayard-Alpert[130] type, first specified in 1950, and may best be described by the name 'inverted ion gauges'. A central collector, consisting of a fine tungsten wire, was mounted coaxially within a grid anode, while an electrically heated tungsten filament cathode was placed outside the grid. Thus, the area of the ion collector was very small and electron emission produced by the incidence of soft X-rays was reduced to a minimum. The grid and filament were mounted on a standard C9 pinch and sealed into a C9 envelope. The collector was mounted on a tungsten seal, sealed into the top of the envelope. The grid was construced of 0.25mm diameter molybdenum wire which was wound into a helix 2cm. in diameter and 4cm. long and welded onto four nickel wire supports. Two separate tungsten filaments were fitted, one of which was centre-tapped, so that a spare filament was available for use. Quite apart from this, the second filament had two other possible functions. Firstly, the electron emission characteristics of the filament could be used as a separate indication of the pressure, and secondly, the flash filament technique could be used to estimate the pressure. In the present investigation the pressures inside the experimental tube were too high for these facilities to be employed.

The tungsten seal and collector wire were protected by

a glass tube of such a length that only the wire actually within the grid was exposed. This prevented X-rays from striking the large diameter tungsten seal, and increased the leakage path, thus preventing the charges, which accumulated upon the envelope of the gauge, from causing a false reading of collector current. The ion collector was made from 0.19mm diameter tungsten wire which was electrolytically tapered in a caustic soda cell so as to minimise the effects of bombardment by soft X-rays.

The gauge was out-gassed during the vacuum processing of the experimental tube by heating the filaments to about 2,000^{o}C. The resultant electron emission simultaneously out-gassed the collector. The grid was out-gassed by heating with eddy currents. An accurate calibration of the gauge, built to the above specification, was not attempted, but previous workers in this laboratory have indicated that the ratio of the collector current to the grid current (measured in amps) is approximately a factor of ten greater than the pressure as indicated in mm.Hg. by a Penning gauge. This was verified by the author on numerous occasions while processing several experimental tubes.

The inverted ionisation gauge can also be used as an ion pump, providing that the pressure in the system is below about 10^{-6}mm.Hg. Two distinct processes are responsible for the pumping action, the first involves chemical reactions and the second is physical in origin. Chemical reactions occur between the gas atoms or molecules present in the tube and the

hot tungsten cathode, but these are usually restricted to the chemically active gases. The second process involves the entrapment and neutralisation of positive ions by the glass of the envelope and the thin tungsten film which is evaporated onto the glass. The pumping action of the gauge is quite efficient providing that no small leaks are present, either in the glass or in the tungsten seals, and that there is no source of gas in the experimental tube. Some workers have claimed pressures of the order of 10^{-10}mm.Hg. Small leaks, which cannot be detected by the usual techniques, can prevent the ion pump from reducing the pressure below about 10^{-7}mm.Hg.

Whether used as a pump or a gauge, the filament was heated to about 2,000°C by means of a large step-down transformer The collector was held at a potential of 100 volts positive, and the grid at a potential of 50 volts negative, with respect to the cathode, by means of high tension batteries. The currents to the electrodes were measured by means of the galvanometer or the electrometer as appropriate.

4. The Manifold.

A number of different systems have been employed in order that the experimental tube might be sealed from the pumping train and reconnected as necessary. Most of the experimental tubes were sealed onto a simple manifold by means of the pumping stem built into the base of the standard C9 pinch used for all the experimental tubes. When this method was employed, the experimental tube was sealed off and removed from the system by fusing the glass of the stem,

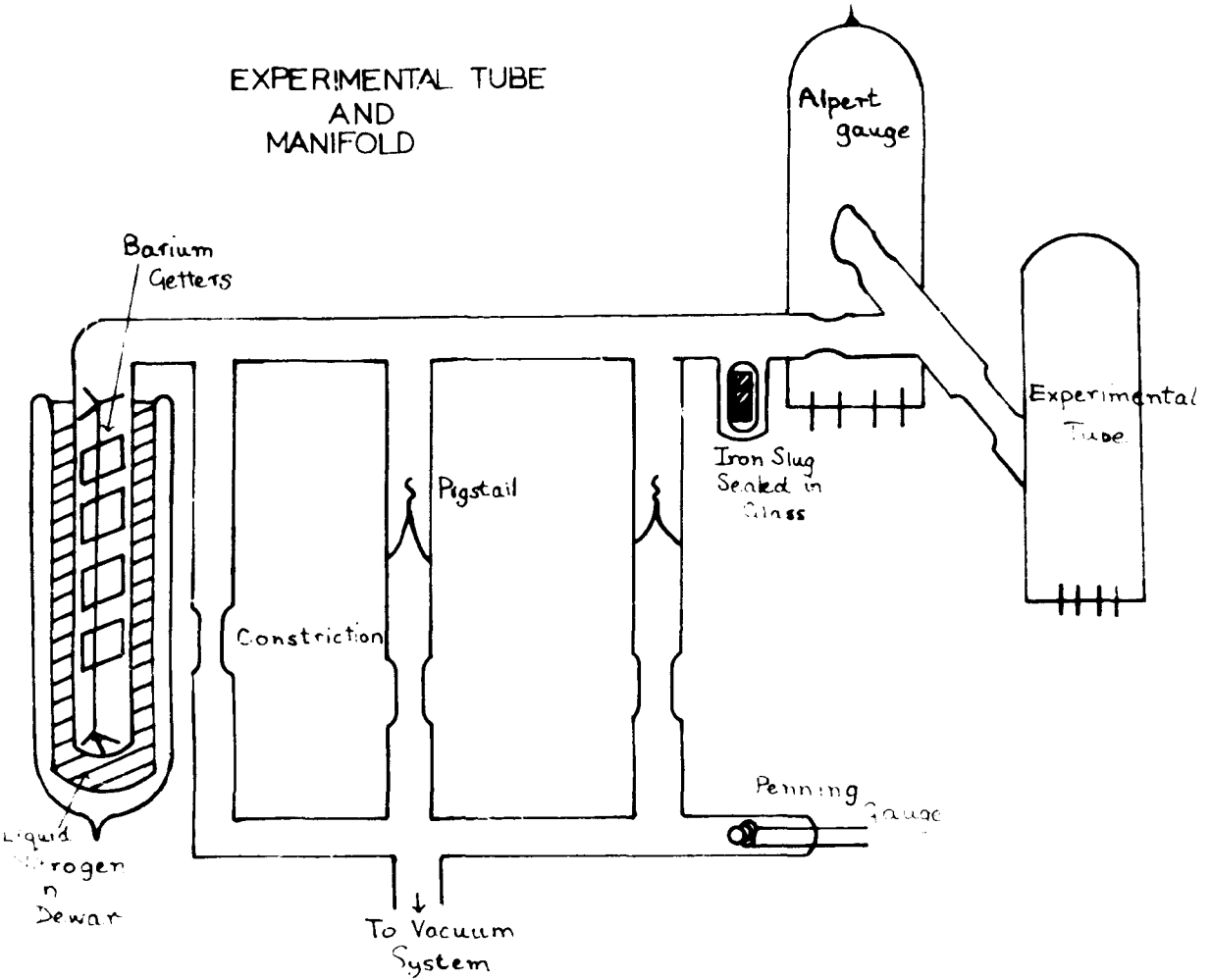
EXPERIMENTAL TUBE
AND
MANIFOLD
Alpert
gauge
Barium
Getters
Experimental
Tube
Iron Slug
Sealed in
Glass
Pigstail
Constriction
Penning
Gauge
Liquid
Nitrogen
in
Dewar
To Vacuum
System

FIG 5.4.1.

drawing off the tube and finally annealing the fused stem.

In some of the more recent experimental work it was required that the tube should be capable of being reattached to the pumping system. These tubes were sealed off by means of constrictions which could be sealed by a hand torch. The tubes were reattached to the vacuum system by mean of glass pigs-tails which could be broken open by the action of an iron slug which was sealed in glass and opperated by an external magnet. Such a system is illustrated in fig. 5.4.1. When these manifolds were employed, the experimental tubes were attached to the manifold by means of a suitably constructed side-arm which was fused into the envelope of the experimental tube. The tube could be finally removed from the pumping train by sealing the constriction. Tubes, containing getters capable of being fired by means of eddy current heating, were also used in conjunction with these manifolds. In these cases, low pressures were achieved by gettering and cobling the getter film with liquid nitrogen before the Alpert pump was operated.

5. Leak Detection.

Conventional methods have been employed to discover the position of any leaks in the experimental glassware. Large leaks were found at backing pressures (10^{-3} mm.Hg.) by means of a Tesla coil discharge through the 'pinhole' responsible for the leak. Smaller leaks were discovered by coating suspect glass with carbon tetrachloride and noting the pressure increase produced when the vapour passed through

the pinhole. Some leaks, which prevented low pressures from being attained, were undetectable by any of the methods which are available in this laboratory and it was thought that porosity of the tungsten, which constituted the tungsten seals, was responsible.

6. The Experimental Tubes.

A number of different types of experimental tube have been built, each type being designed for a specific purpose. The basic techniques involved in the preparation of all types of experimental tube were very similar, so that a general description will be given below.

Nearly all the metal parts involved in the construction of the tube were shaped from pure nickel sheet, but the base metal employed for the cathodes was '0' nickel. In certain of the experimental tubes other metals were used and these will be mentioned where appropriate.

A framework of glass rod was always used to support the electrodes because it possessed several advantages over ceramic materials and mica. Ceramic insulators have insulating properties which are inferior to those of glass. In addition, the large pore spaces present in mica and ceramic materials contain large quantities of gas which may be released after the tube has been processed and removed from the vacuum system. The framework of pyrex glass, the envelope and the pinch of C9 glass were cleaned by treatment with concentrated nitric acid and distilled water after which they were dried in an air oven. Strips of thin nickel

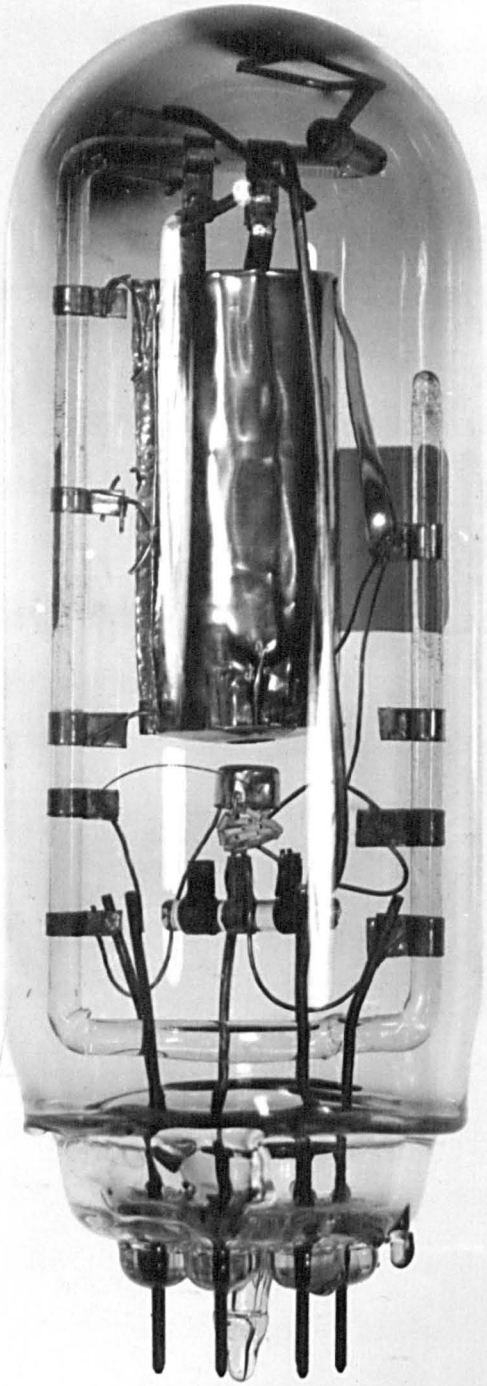

Tube R1.

FIG 5.6.1.

sheet were then shaped around the glass framework in appropriate positions and welded into place by means of an electric spot welder to serve as supports for the electrodes. The appropriate electrodes were then shaped from nickel sheet and welded as necessary. These were then carefully cleaned by hydrogen furnacing and stored in a 'clean' box until required during assembly.

Two main types of cathode were used in the construction of the experimental tubes:-

(a) Button Cathodes.- These were basically a cup of '0' nickel containing a commercial helical tungsten heater insulated from the base by means of a ceramic body. The depth of the cup was 5mm. and the wall thickness was 0.2mm. The cups had a flat bottom 9mm. in diameter, onto which the cathode coating was sprayed. A tungsten thermocouple wire 0.095mm. in diameter was welded onto the bottom of the cup, so that the cathode temperature could be measured. The cold junction of the thermocouple was made by welding the wire onto a pin of the C9 base so that the temperature of the cold junction was as near room temperature as possible. This procedure was also adopted for the cold junctions of the thermocouples used with cylindrical probe cathodes. The cup, complete with thermocouple and heater, was mounted upon a small glass support, hydrogen furnaced, and stored in the clean box until required for spraying and mounting in the experimental tube. The form of this type of cathode can be seen from the photograph of tube R1, fig. 5.6.1.

(b) Cylindrical Probe Cathodes.- These cathodes were prepared from a hollow '0' nickel sleeve 7.0 cm. in length and 2.5mm. in diameter and having a wall thickness of 0.2mm. A tungsten thermocouple wire 0.095mm. in diameter was threaded through the sleeve together with a tightly fitting copper mandrel specially shaped to accommodate the tungsten wire. A weld was then made at the centre of the sleeve to form the hot junction of the thermocouple. Next, before removing the mandrel, two thin strips of nickel sheet were welded at both ends of the sleeve, at distances of 3mm. and 17mm. from the ends. These strips provided supports for hollow ceramic tubes 2.5cms. long which each contained a 25s.w.g. nickel wire. Each wire was held firmly in position by a weld to a thin strip of nickel welded round the ceramic tube. The ceramic tubes were mounted onto the cathode by means of the nickel stirps previously welded onto the sleeve, in such a way that 3cm. of the centre of the sleeve could be used as the cathode base. 2mm. of the wire in the ceramic tube was exposed so that welded connections could be made to the probe which was embedded within the cathode material. Two 26 s.w.g. nickel wires were welded to the ends of the sleeve to act as supports. The mandrel was then removed and replaced by the insulated heater. The thermocouple was then insulated with ceramic sleeves and the whole assembly was hydrogen furnaced to remove contamination. The cathode base was then stored in the 'clean box' until required for spraying.

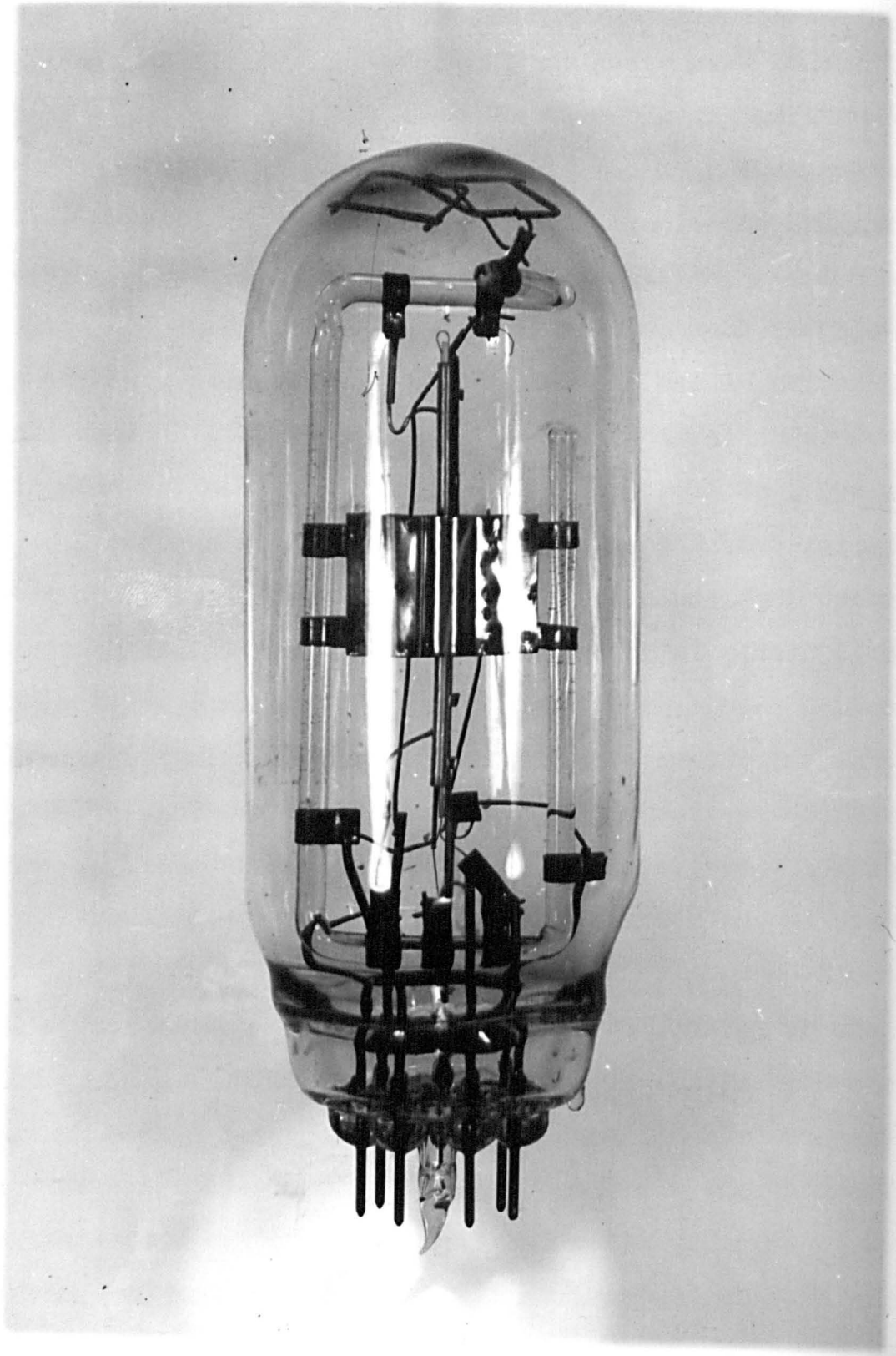

Tube P2

FIG. 5.6.2.

7. Coating the Cathode.

(a) Button cathodes were mounted behind a mask and the flat surface was coated to a thickness of 100 microns by spraying with the suspension of barium carbonate specified in Chapter 1.

(b) Probe cathodes were mounted in a rotating jig behind a mask and the central 2.5cms. of the sleeve was coated, by spraying, with the barium carbonate suspension to a thickness of 50 microns. The probe supports were shielded during spraying by two lengths of rubber tubing mounted at the ends of the sleeve. When the cathode material was dry, the probe wire was wound and attached to the probe supports as follows. One end of a 5cm. length of pure nickel probe wire, .0005 inches in diameter, was attached to one probe support by welding. Because the probe wire was so fine as to be difficult to see, a short length of 29 swg nickel wire was next welded to the other end of the probe wire to facilitate handling. The probe wire was then allowed to hang from the first probe support and the cathode was slowly and carefully rotated to wind on five or so turns of the wire over the first coating. The probe wire was then welded to the second probe support so that the turns of wire were held firmly in place. The excess wire was then cut off. This assembly was remounted in the rotating jig and a final sprayed coating of the carbonate was applied to give a total thickness of 100 microns. The constructional details can be seen from the photograph of tube P2, Fig. 5.6.2. The thickness of the coating was determined by projecting an enlarged image of the finished cathode onto a screen and

comparing the coated and uncoated regions.

Next, the cathode and other electrodes were assembled onto the glass framework by welding to the nickel supports. Tweezers were used wherever possible to prevent contamination. One end of the cathode probe was supported telescopically so that the thermal expansion of the cathode did not alter the electrode geometry. At this stage, two barium getters were welded to the glass support and the framework was then attached, by welding, to the pins of a C9 glass pinch. The necessary welded connections, from the pins of the pinch to the different electrodes, were then made with 26 swg. nickel wire. Connections to additional tungsten seals were also made at this stage. The pinch, complete with the electrode assembly, was then suitably located in a C9 envelope in such a manner that the envelope could be 'drop-sealed' onto the pinch with an oxy-coal gas flame.

The additional tungsten seals, which were sometimes necessary, were normally fused into the envelope before the electrodes were attached to the glass framework.

After completion, the tubes were sealed onto the manifold of the vacuum system. The backing pump was then switched on and any leaks present were investigated by the methods described in section 5.5. When the locations of the pinholes were discovered, the vacuum system was 'let down' to air and the leaks were sealed by means of a small flame. The leak-free system was then evacuated by means of both pumps and the processing of the cathode was commenced.

8. Cathode Processing.

After the pressure inside the experimental tube had been reduced by the pumps, to about 10^{-5}mm.Hg, the manifold and experimental tube were baked for several hours at 450°C. The oven was then switched off, and removed, and the metal parts of the tube and manifold were heated by eddy currents while the glass was still hot (~100°C). This treatment allowed a large proportion of the gases adsorbed on the surfaces within the experimental system to be pumped away. A slowly increasing potential difference was next applied across the cathode heater, by means of a motor driven Variac, so that the cathode temperature increased slowly (from room temperature to ~900°K in 24hrs.) This treatment decomposed the organic binder and the carbonate layer on the cathode. Most of the evolved gas was pumped away but, as stated above, some of the carbon dioxide was retained by the nitrogen trap. This carbon dioxide was removed by means of the method described in section 5.1.

When the 'break-down' was completed, the heat treatment of the glass and metal was repeated in order to pump away a large proportion of the gases adsorbed on the surfaces within the system. The electrolytic activation process was then commenced by applying a small anode voltage while the cathode was at temperatures within the range 900°K to 1200°K. When the desired degree of activation had been attained, the tube or manifold was 'sealed off' and the getters fired as required. Measurements could then be commenced on the finished tube.

SCREENED BOX CIRCUIT

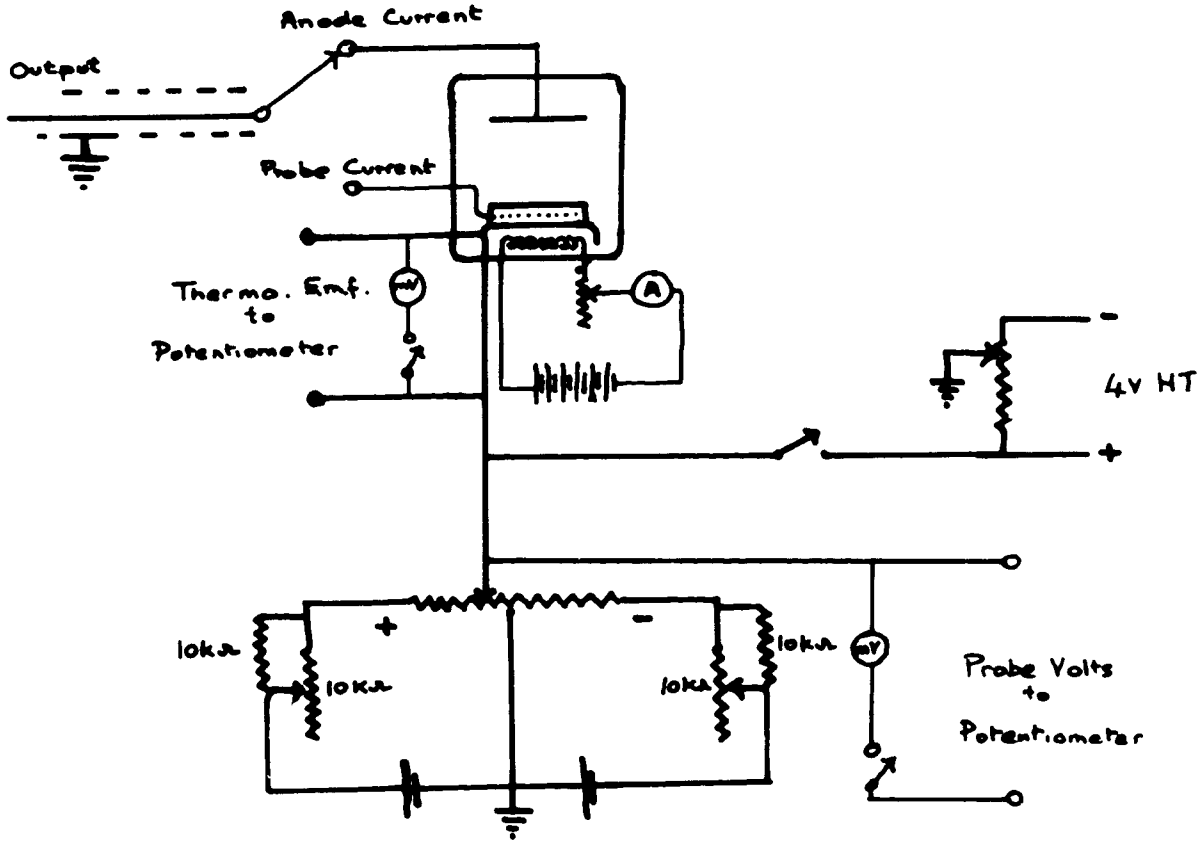

FIG. 5.9.1

9. Measurements.

The principal measurements made on the experimental tubes were of the anode currents, for a series of applied anode voltages, and the conductivities of the cathode coatings. These measurements were carried out at a number of cathode temperatures for a number of different states of cathode activity. Some of the currents involved were very small in magnitude and were easily masked by the electrical disturbances which arose from the use of other electrical apparatus in the laboratory. It was therefore necessary that the experimental tubes should be electrically shielded. This was accomplished by mounting the tubes in a metal screening box. Screened cable was used for electical connections. A specially designed screen box was built for measurements on the probe tube and the circuit of this is shown in fig. 5.9.1. Similar screened boxes were used for the tubes of different design.

Quite apart from the electrical screening, it was necessary to ensure that the tubes were screened from light. For this reason the boxes were made 'light-tight'. Radiation incident on the cathodes produced photoemissive and photoconductive effects which, though interesting, confused the measurements of the conductivity and the thermionic emission. These photoelectric effects have been investigated by another worker in this laboratory (Mee[131]). In the case of experimental tubes mounted on the pumping manifold, electrical screening and the exclusion of light were achieved by the use of aluminium foil shaped around the experimental tube.

TUNGSTEN NICKEL THERMOCOUPLE CALIBRATION

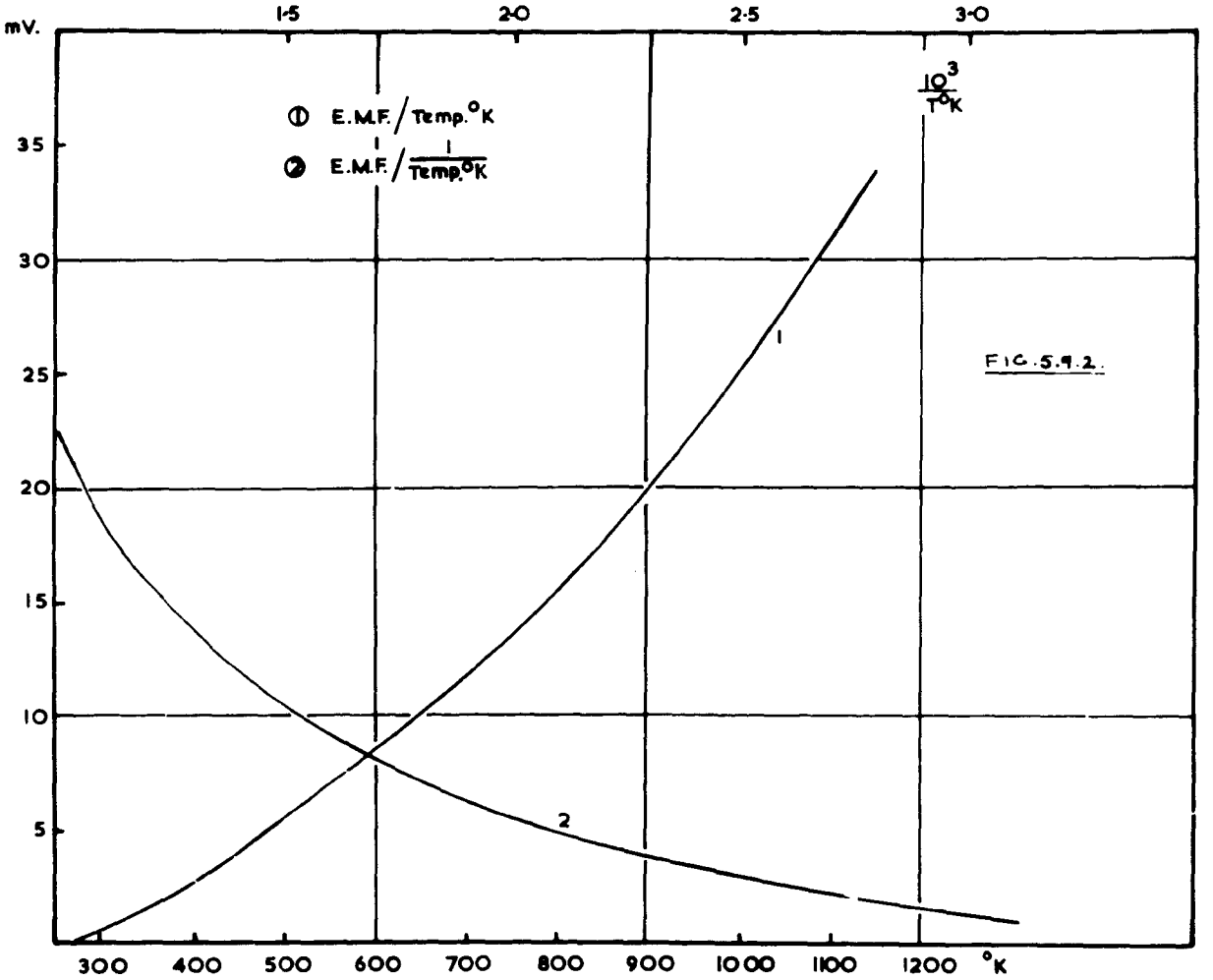

FIG. 5.9.2.

THE ELECTROMETER

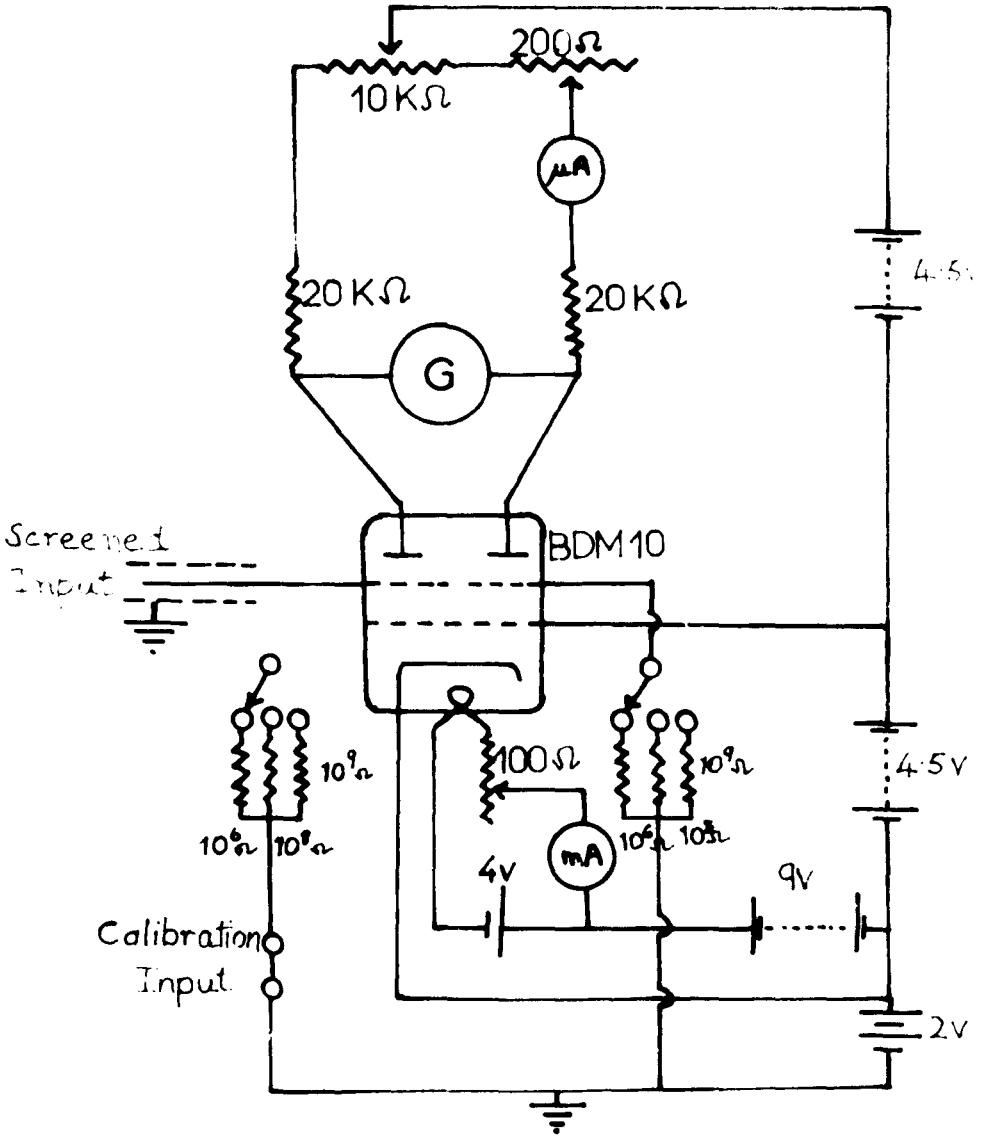

FIG 5.9.3.

The cathode temperatures were measured by means of the tungsten/nickel thermocouples already described. Measurements of the thermo-e.m.f. generated were made by means of a Muirhead potentiometer. The temperature indicated by these thermocouples were those of the base metal. A temperature gradient existed in the cathode material but the error was estimated as being not greater than 1%. A calibration graph of the thermo-e.m.f. against the cathode temperature is shown in fig.5.9.2. The cold junction was situated as near the pinch as possible so that its temperature was very nearly the same as the temperature of the room, therefore it is unlikely that this would constitute any appreciable error in the measurement of temperature. The larger values of the anode current and the current between the probe and the base were measured by means of a sensitive galvanometer (1cm. = 10^{-8}amps.) while the smaller currents were measured by means of an electrometer. The electrometer was of the 'out-of-balance' type and incorporated the Ferranti B.D.M. 10 electrometer valve and high stability resistors. The circuit of this electrometer, which was built in this laboratory, is shown in fig 5.9.3. It will be seen that one section of the valve was used as a reference circuit. Any potentials developed across the grid resistance of the other section of the valve caused a change in the anode current which in turn produced an 'out-of-balance' current through the galvanometer connected between the two anodes. Three sets of grid resistors were provided to cover the current range 10^{-8} amp. to 10^{-13}amp. An input

of 1mV. gave an out-of-balance current of 4×10^{-8}amps. Power supplies were provided from dry batteries. The heater current was supplied from an accumulator housed in a separate screened box.

The conductivities of the probe tubes were determined from the slope of probe current/voltage characteristics. These characteristics were obtained by applying small potentials (0 to $\pm$ 100mV) between the cathode base and probe, and by measuring the resultant currents be means of the galvanometer or electrometer. The circuit which provided these small potentials was incorporated in the screened box (fig.5.9.1.). The conductivities of the retarding potential tubes were obtained by measuring the current to the collector electrode for particular values of anode potential. These methods will be described in greater detail in the next chapter.

The experimental cathodes were heated by an A.C. current from a Variac transformer supplied by a constant voltage transformer operating from the A.C. mains. Although A.C. was used, the heater cathode insulation was sufficient to insure negligable interference with measurements. The fluctuations in the heater voltage were not sufficiently large as to cause a measurable change in cathode temperature.

10. <u>The Pen Recording Apparatus</u>.

An attempt was made to measure the anode currents and thermo-e.m.fs of an experimental tube automatically. The currents were measured by amplifying the D.C. voltages produced by the passage of the currents through a resistor in

DC. Amplifier for Recorder.

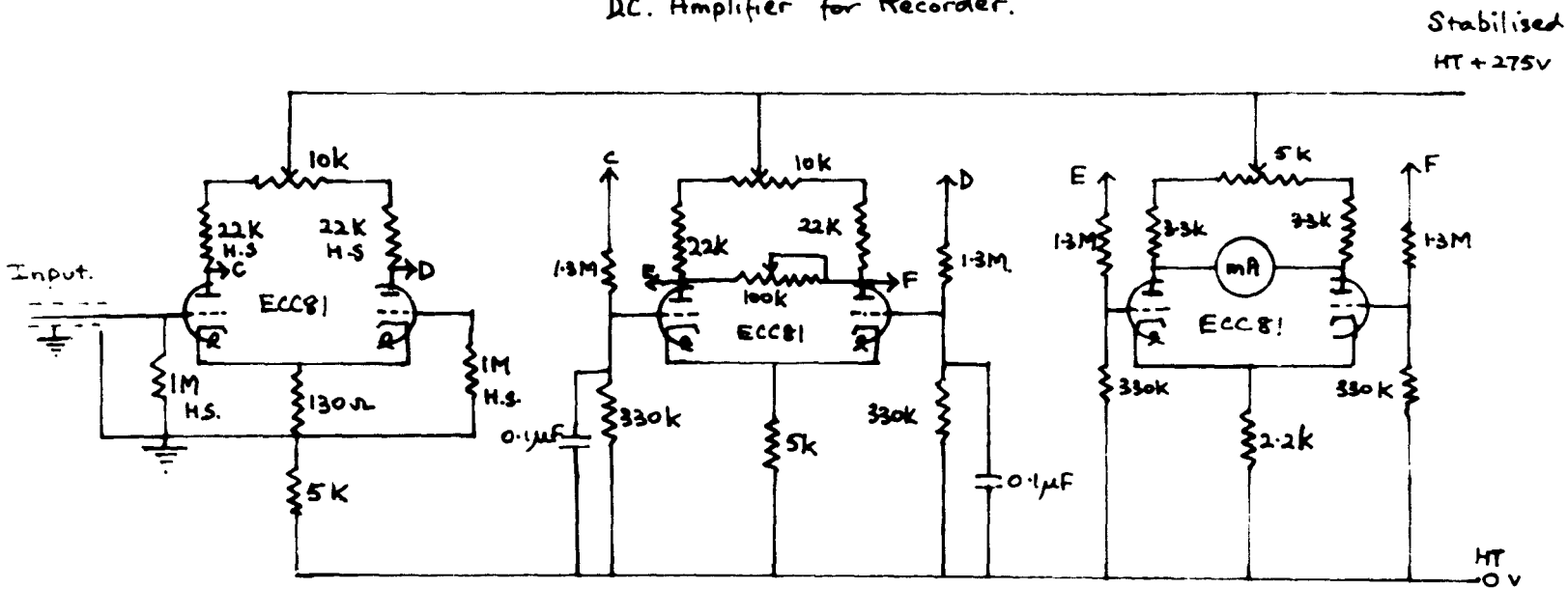

FIG. 5.9.4.

in the grid circuit of a out-of-balance type D.C. amplifier. The out-put of the amplifier was fed into a pen recorder. The circuit of this amplifier is shown in fig. 5.9.4. Other voltages and currents were recorded by the same pen recorder by means of a series of rotating contacts which connected the appropriate circuits for fixed time intervals.

This method provided an accurate record of the readings of anode currents obtained from the heated anode/heated cathode tube (HNN_1) described later. The main disadvantage was that the currents had to be limited to a small range of values. The method was thus restricted to the values of the anode current obtained over a relatively small temperature range and for this reason the method was discontinued.

CHAPTER 6.

Experimental Results

1. Introduction.

The experimental results discussed in this chapter were obtained from a number of different types of tube. The construction of the different types of experimental tube, together with the experimental results obtained, will generally be described in different sections, each section being devoted to a particular experimental tube. This method of setting out the experimental results has a number of distinct advantages. The development of techniques and the tube design can be presented chronologically and the reasons why a particular new design of experimental tube was chosen will, it is hoped, become clear when the shortcomings or interesting results obtained from the previous tube are described. This method of presentation also has an advantage in that repetition of the descriptions and the results is avoided. It is hoped that the experimental work will thus appear as a logical development of ideas, though the description of early work will naturally be modified in the light of experience obtained as the work has progressed. On the other hand, the more important conclusions which can be drawn from the experimental results will be discussed in the next chapter, from the point of view of different aspects of the behaviour of particular cathodes. The discussion will be simplified by ascribing particular code letters and numbers to each tube. Tubes, in which measurements of the conductivity of the coating is carried out by the use of a probe wire embedded in the cathode

material will be described as probe diodes and will be designated by the letter P. A number following this letter will indicate which probe diode is being considered. Thus, for example, P_1 will represent the first probe diode constructed and P4 the fourth. This numbering system will also be used for all other types of tube. When an Alpert pump has been used with a probe diode it will be indicated by the letter A. For example, PA1 represents the first of this type of system constructed. Tubes in which the conductivity was measured by means of a retarding potential method will be represented by the letter R followed by the appropriate number. Tubes with a heated anode will be indicated by the letter H while N will indicate that the anode was constructed of nickel and W that the anode was constructed on tungsten. A further type of tube, in which the cathode consisted of two heated electrodes separated by a coating of barium oxide, will be described by the letter D. The state of activation, for a particular series of measurements, will be indicated by Roman numerals. Thus, for example, R2 III will refer to measurements carried out on the second retarding potential tube, in the third state of activation.

A large number of the graphs plotted from experimental results are similar in form and therefore only typical experimental curves will be included. The information obtained from other similar experimental curves will normally be collected together in tabular form. Experimental curves which illustrate a particular type of behaviour will also be included where appropriate.

2. The Methods Used in the Determination of Cathode Conductivity.

It will be noted that attempts have been made to measure the conductivity of the coating by means of three different types of experimental tube. The most successful of these types was the probe diode.

(a) Probe Diodes.- The method of construction for this type of experimental tube has been described in section 5.6. and a photograph of tube P2 has been given in fig. 5.6.2.

In this type of tube a probe wire was inserted into the cathode coating and the current between the probe and the base was measured for a number of applied potentials. The current/voltage characteristics for potentials in the range 0 to ± 100mV were determined for all the probe tubes, at different temperatures and for various activation states. These have been plotted so that the values of apparent conductivity of the cathode coating could be calculated from the slope of the characteristic. Examples of these curves will be given in latter sections. Small potentials must be applied in order that the equilibrium conditions are not upset. Determinations of the conductivity of the coating were normally made after the determinations of the emission current. It was assumed that the cathode was in the same physical state for both measurements. Most of the probe characteristics approximated to a straight line, indicating the absence of rectification effects, but slight curvature has been found for several of the determinations carried out on a number of probe tubes. The most marked curvature of the probe characteristics was obtained for the first activation state of P1 and this is

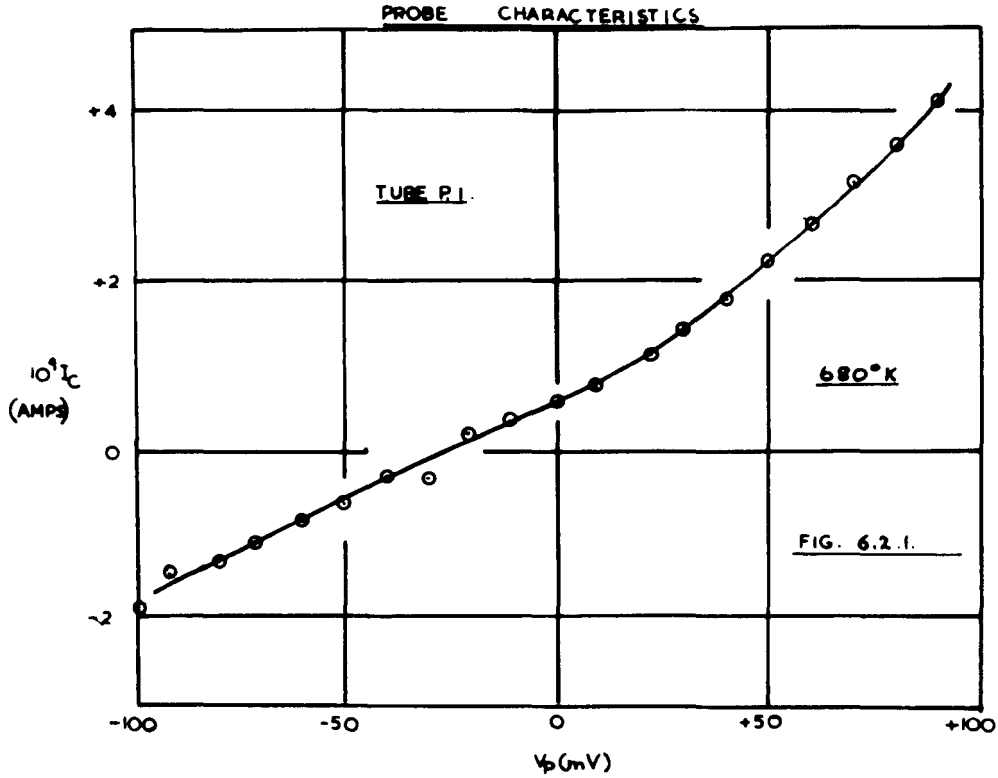

Basic Conductivity Circuit.

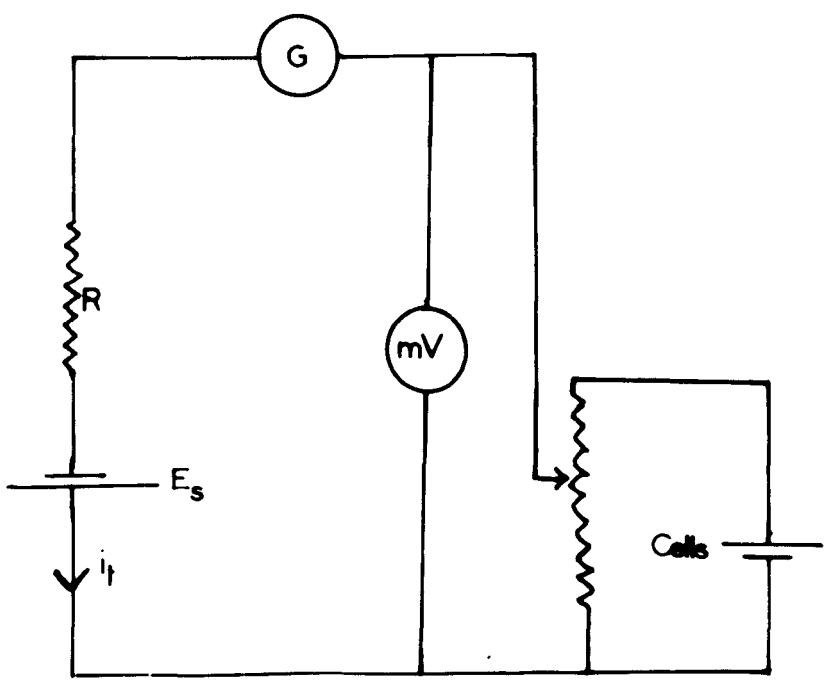

FIG. 6.2.2.

illustrated in fig. 6.2.1. for a temperature of 680°K. In general it can be stated that at low temperatures the characteristics were approximately linear and that the curvature, when present, became more marked as the cathode temperature increased. The apparent conductivity of the coating was, in all cases, calculated from the slope of the characteristic at the origin.

The specific conductance of the coating can be calculated from the apparent conductivity by use of the equation:-

$$\sigma = \frac{1}{R} \quad \frac{\text{Cosh}^{-1} t/a}{2\pi l} \qquad 6.2.1.$$

where, a is the radius and l is the length of the probe wire. t is the thickness of the coating between probe and base. The equation holds for $t > a$, a condition which is satisfied by the probe tubes built in this laboratory, because for these $t \simeq 10a$. In practice, this correction has seldom been applied because when the plot is made of the logarithm of the conductivity against $\frac{1}{T}$, it is the value of the slope which is of interest, not the intercept value. The correction term merely adds a constant (characteristic of the particular probe tube) to the value of the intercept.

Examination of fig. 6.2.1 indicates that a current is observed for zero applied voltage. This can be attributed to the Seebeck e.m.f., which is caused by the fact that the probe is at a lower temperature than the base metal. In this particular characteristic the Seebeck e.m.f. has a value and a sign consistent with an n-type semiconductor model. The temperature difference between the probe and cathode base

cannot be determined for this type of experimental tube, so that information as to the depth of the Fermi level cannot be obtained by this method. The Seebeck e.m.f. is generally consistent with the n-type semi-conductor model, but results have been obtained from tube PA2 at low temperatures which are consistent with a transition from n-type to p-type semiconduction as the temperature is decreased. This will be discussed in greater detail in a later section.

When measurements of probe current are made, it is important that the resistance of the galvanometer, or the electrometer, used to measure the current should be taken into account. The following treatment indicates the effect of the measuring instrument on the results obtained, and indicates the correction which must be applied. The experimental arrangement of the measuring instruments and the electrical supplies used are indicated diagramatically in fig. 6.2.2.

The resistance between the probe and the base of the experimental cathode is symbolised by the series resistance R. The Seebeck e.m.f. E_s produced by the temperature difference existing between the probe and the base is represented by the cell E_s. The resistance of the galvanometer or electrometer is indicated by G, while the millivoltmeter which is used to measure the applied probe potential, is symbolised by mV. The applied potential will be symbolised by V. The applied potential is supplied by means of potential divider, fed from dry cells. The resistance of the millivoltmeter and the potential divider and cells, all of

which are connected in parallel, can be neglected compared with the resistance of the galvanometer or electrometer and the resistance between the probe and cathode base. The total current flowing through the probe resistance and the galvanometer or electrometer is the sum of two currents. The first current i_1 is due to the applied e.m.f. V, so that:-

$$i_1 = \frac{V}{(G+R)}$$

The current i_2, due to the Seebeck e.m.f., is given by:-

$$i_2 = \frac{E_s}{(G+R)}$$

So that, the total current i_T is:-

$$i_T = i_1 + i_2 = \frac{1}{(G+R)} V + \frac{E_s}{(G+R)}$$

Now, when the probe characteristics are plotted, the total current i_T is plotted against the applied e.m.f. V. Thus the slope of the line (assuming that the probe system is ohmic) is $\frac{1}{(G+R)}$ and the intercept on the i_T axis is $\frac{E_s}{(G+R)}$, while the intercept on the applied e.m.f. axis is $-E_s$, the Seebeck e.m.f. with the sign changed. Thus the sign and the magnitude of the Seebeck e.m.f. can be readily obtained from the graph. The slope of the characteristics does not represent the conductance between the probe and the cathode base. The value of the galvanometer or electrometer resistance must be subtracted from the value of (G+R), obtained from the slope of the curve, before the conductivity of the cathode is calculated. This correction has been applied, where necessary, to the results given in this chapter.

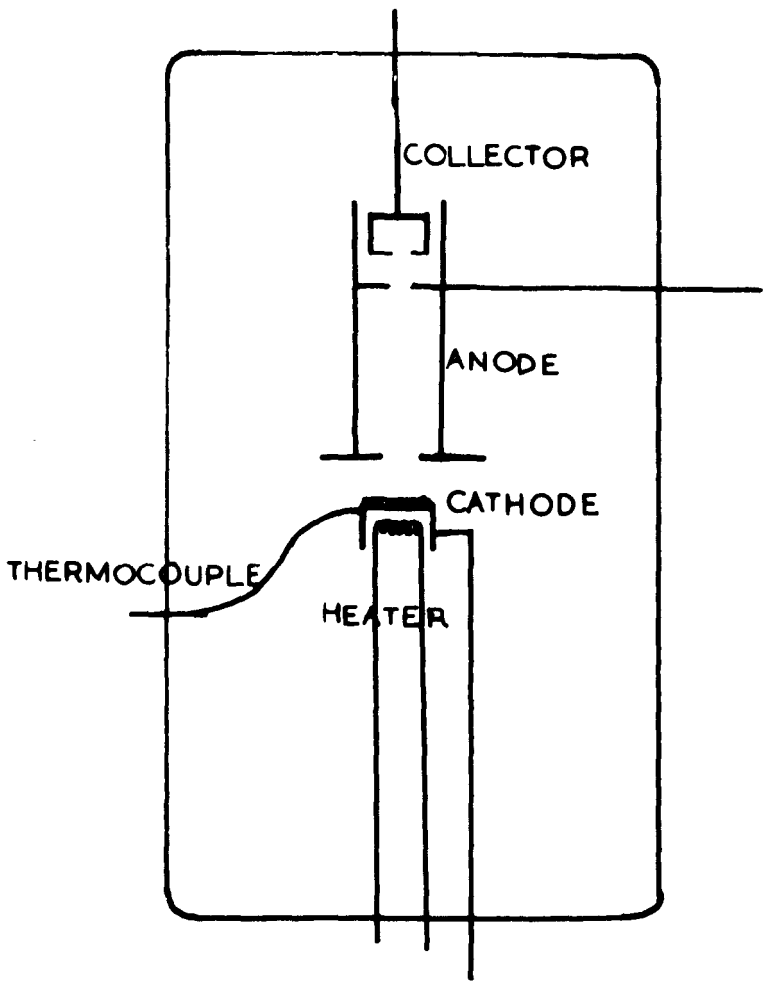

TUBE R.I. DIAGRAMATIC.

FIG. 6.2.3.

(b) The Retarding Potential Tubes.- Specially designed retarding potential tubes can be used to measure the conductivity of the oxide cathode. Such tubes have been used by Sparks and Phillips[73], and a detailed account of the relevant theory can be found in their paper. The tubes built during the present investigation consisted of a button cathode, an accelerating anode and a collector electrode. A photograph of tube R1 has been given in fig. 5.6.1., and the electrode configuration is given diagramatically in fig. 6.2.3. The anode is made with a hole in its centre, 6mm. in diameter, so that electrons emitted by the cathode will pass through the anode system to be collected by the collector electrode. Electrons reaching the collector have energies which are dependent on the collector potential with respect to the cathode surface. If the potential of the collector (including the contact potential difference) is positive with respect to the cathode surface, all the electrons passing through the centre of the anode will reach the collector and the collector current should have a constant value. When the collector potential is negative with respect to the cathode surface, only electrons with high enough energies to pass over the potential barrier will be collected. Thus the graph of the logarithm of the collector current against the collector potential should show a break when the potential is equal to that of the cathode surface.

If a potential is now applied to the anode, the surface barrier of the cathode is reduced by the Schottky effect and a larger collector current flows. The collector character-

istics are thus modified by being displaced by an amount $(\Delta\phi_{c1} - \Delta\phi_{c2}) + (V_{1R2} - V_{1R1})$, where $(\Delta\phi_{c1} - \Delta\phi_{c2})$ is the change in the height of the potential barrier and $(V_{1R2} - V_{1R1})$ is the change in the collector voltage at the 'break' of the collector characteristics.

If corresponding values of collector potential are determined for a constant value of collector current and different values of anode voltage, a plot of V_c against I_A should give a straight line and the slope should have a value R which is the resistance of the cathode coating. If the thickness of the coating t and the area A are known the specific conductivity can be calculated from the equation:-

$$\sigma = \frac{t}{RA} \qquad 6.2.2.$$

The most apparant advantage of this method is that the values of the anode current and the collector current can be determined simultaneously. Thus the cathode should be in the same physical state both for the emission and the conductivity measurements.

(c) The Double Cathode Tube. One tube was built in which the cathode material was sandwiched between two small nickel boxes which could be independently heated. Both the nickel boxes were provided with thermocouples. The conductivity of the oxide could then be determined in a manner similar to that employed for probe diodes. The results obtained, together with a description of the experimental tube, will be given in a later section.

3. Emission Measurements.

A circuit diagram of the experimental arrangement used

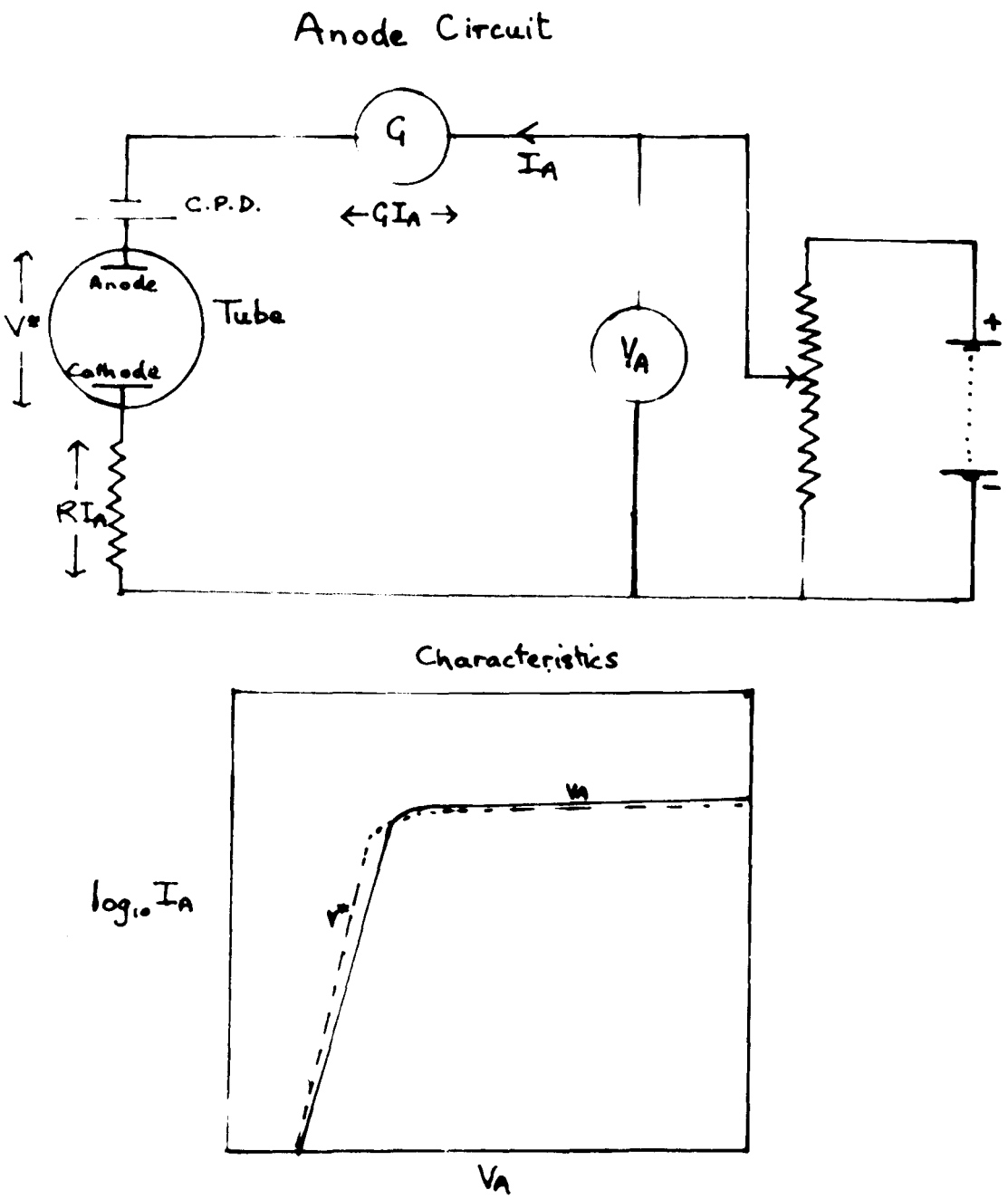
Anode Circuit
G
I_A
C.P.D.
$\leftarrow GI_A \rightarrow$
Anode
Tube
Cathode
V_a
RI_A
V_A
+
−
Characteristics
$\log_{10} I_A$
V_A

FIG. 6.3.1.

during the determination of emission currents is given in fig. 6.3.1. Anode characteristics were obtained by plotting the logarithm of the emission current against the applied voltage V_A. From the circuit, it will be seen that the emission current causes a voltage drop to occur across the cathode material and also across the current measuring instrument, so that the actual potential applied between the surfaces of the anode and cathode is not that indicated by the voltmeter V_A.

Most workers neglect to correct for the 'lost volts' developed across these resistances, and consequently, wrongly take the value of applied voltage for the break in the anode characteristics as being numerically equal to the contact potential difference. If the cathode material obeys Ohms law and if I_A is the anode current, R is the resistance of the cathode and G the resistance of the current measuring instrument. The effective potential difference V^+, which exists between the surface of the anode and cathode is given by:-

$$V^+ = V_A - \Delta\phi - RI_A - GI_A \qquad 6.3.1.$$

Thus the anode characteristic will suffer a displacement along the voltage axis which is dependent upon the anode current.

The value of the effective voltage V^+ becomes correspondingly smaller than V_A as the anode current increases. This gives a curvature to the anode characteristics in the retarding potential region, which becomes more pronounced as I_A increases. Several workers have obtained experimental results which they have interpreted as indicating a

deficiency of low energy electrons (Chapter 2). It will be noted that this observed effect could perhaps be explained in tems of the displacement of the characteristics produced by the voltages dropped across the current measuring instrument and the cathode material.

The current density in the retarding field portion of the emission characteristics has been given in a previous section as:-

$$J_R = A(1-r)T^2 . c. \exp e(V_A - \phi_A)/kT \qquad 6.3.2.$$

This equation does not take into account the voltage drop produced across the measuring instrument and the cathode material. If this is incorporated into the equation together with the value of the saturation current at zero field, we can obtain an equation for the retarding field current,

$$I_A = I_o \exp (eV^+/kT) \qquad 6.3.3.$$

or

$$I_A = I_o \exp \left[e (V_A - \Delta\phi - RI_A - GI_A)/kT \right] \qquad 6.3.4.$$

Using logs.,

$$\text{Log } I_A = \log I_o + e (V_A - \Delta\phi - RI_A - GI_A)/kT \qquad 6.3.5.$$

It will be seen that a plot of log I_A against V_A should only give a straight line when RI_A and GI_A are small compared with $V_A - \Delta\phi$. Thus if the best straight line is drawn through experimental points obtained in the retarding potential region of the characteristic, the value of the slope should not coincide with the theorectical value of e/kT. This provides one possible explanation of the fact that workers in

this field have not always obtained values of temperature from the slopes of the retarding potential lines which coincided with the measured temperature of the cathode. The voltage drop across the cathode material and the current measuring instrument will also modify the value of the slope of the Schottky plot, if the value of $(R+G)I_A$ is significant when compared with the value of the applied anode voltage.

At first glance it might appear that determination of the anode current under retarding field conditions should provide a method for the determination of the conductivity of the cathode, but this cannot readily be done because the value of the anode current is mainly determined by the height of the potential barrier and not the resistance of the cathode coating.

It is clear that the value of the contact potential difference, as obtained from the break point of the anode characteristic, will include the voltage drop across G and R, so that these values must be treated with reserve. It is possible that at high cathode temperatures the voltage drop across the coating will be of the same order as the indicated contact potential difference. For this reason, the value of the contact potential difference obtained from the break point of the emission characteristics will be called the 'apparent contact potential difference'.

4. Tube P1.

The first probe tube to be successfully completed and processed was manufactured in the manner described in section 5.6.2. The tube was mounted directly onto the vacuum system. Breakdown was accomplished by raising the

cathode temperature from room temperature to 900°C over 24 hours by means of the motor driven Variac transformer. After breakdown the carbon dioxide was removed from the traps and the cathode temperature was reduced slowly (over 3 hours), by hand control of the Variac, to room temperature. The experimental tube was then baked and the metal parts were eddy-current heated. An attempt was made to measure the conductivity of the coating while the tube was still on the vacuum system, but the resistance was too high for a measurable current to be obtained even with the electrometer operating on the most sensitive range. At this stage, one of the two barium getters, mounted within the experimental tube, was fired and the tube was then sealed off and the second getter fired. The experimental tube was then connected up within the screened box and, after the temperature of the cathode had been raised to 680°K, a measurement of the conductivity was made using the electrometer as the current measuring instrument. This probe characteristic has already been given in fig. 6.2.1. and the rectification effects obtained have been discussed in section 6.2. An emission characteristic was then determined at 620°K using the electrometer. An attempt was then made to determine emission and conductivity characteristics at higher temperatures, but during the second of these measurements the cathode heater failed and experiments had to be discontinued. The tube thus provided only a few experimental results but the experience obtained was very valuable.

It had already been decided that measurements of the conductivity of the oxide cathode should be attempted by a number of different methods, to see whether or not the results obtained were comparable and to decide upon the best type of experimental tube. With this aim in view, the next experimental tube made was of the retarding potential type.

5. Tube R1.

The photograph of this tube, shown in fig. 5.6.1, illustrates the cathode design quite well, but the design of the anode and collector cannot be readily seen and therefore the tube design has been illustrated diagramatically in fig. 6.2.3.

The techniques involved in the construction of this type of tube have already been described in section 5.6.4 while the method used for the determination of the conductivity has been outlined in section 6.2. The tube was fitted with two getters and the breakdown procedure was identical to that used for P1, with the exception that the breakdown was accomplished over twelve hours instead of twenty four hours.

Partial activation was achieved by drawing emission with a cathode temperature of 1,110°K. The collector electrode was connected to the anode during this process with a anode potential of 12 volts. During the first hour of the activation process, the anode current increased from a very small value to 0.5 mA. Activation for a further 48 hours, at the same cathode temperature and anode voltage, caused the anode current to increase to 1.58 mA. The cathode was then cooled to room temperature over a period of three hours.

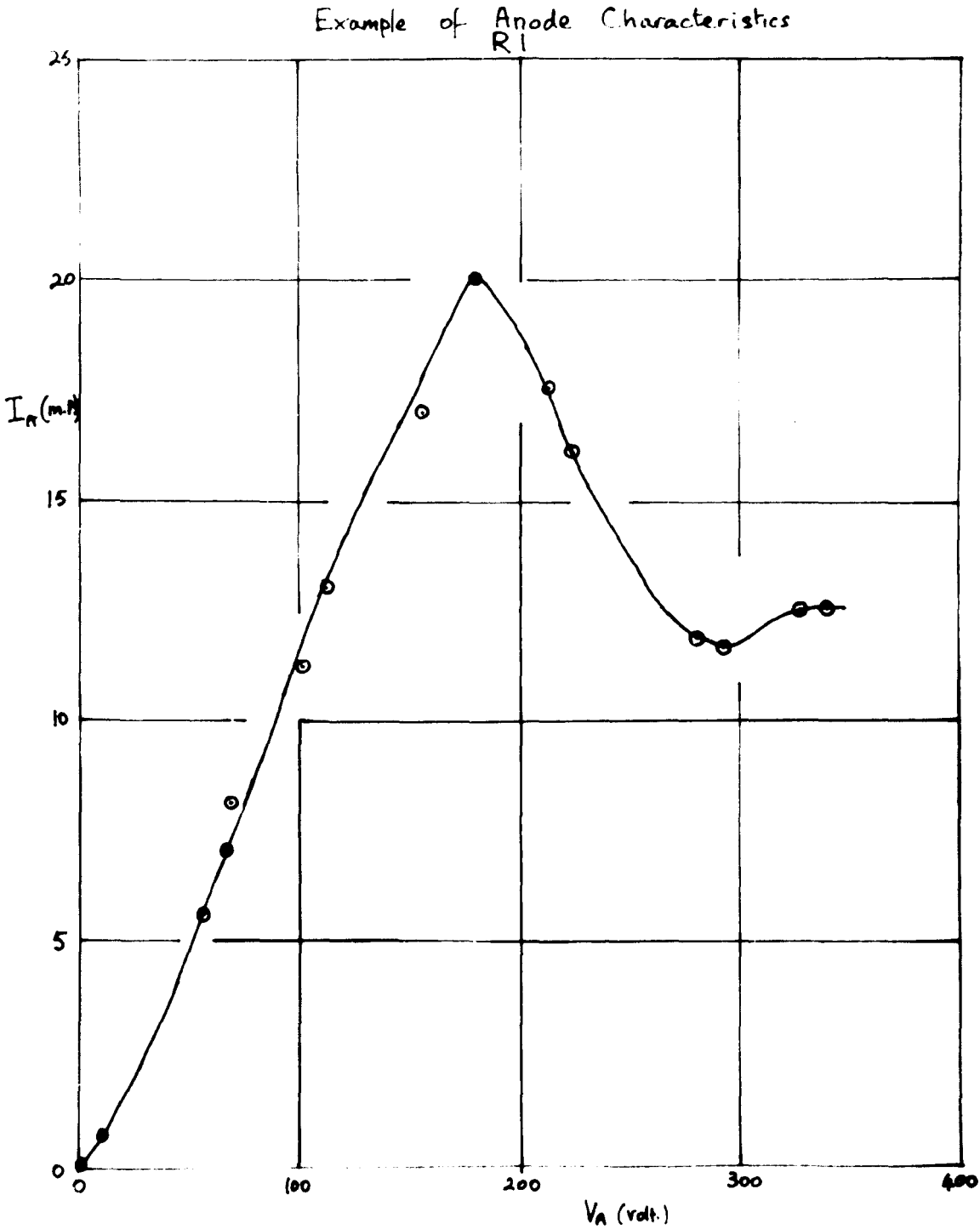
Example of Anode Characteristics
R1
25
20
15
10
5
0
I_A (m.A)
0
100
200
300
400
V_A (volt.)

FIG. 6.5.1.

When cool, the cathode was found to be a greenish blue colour. The valve was then baked overnight after which the metal parts were heated with eddy currents. One getter was then fired, the tube was sealed off and the second getter fired.

A determination of the anode and collector characteristics was then attempted at a known cathode temperature. The form of the anode and collector characteristics were not as expected from the theory. For example, an experiment with the collector connected to the anode showed a marked decrease in anode current when the anode voltage was increased beyond about 180 V (fig. 6.5.1.). The behaviour at smaller values of anode voltage was as predicted by the theory. The observed 'slumping' of the anode current could be attributed to the removal of an electronegative substance from the anode and collector by bombardment with electrons having energies of approximately 180 eV. If some of this substance was readsorbed on the cathode an increase in the work function would be produced, which in turn would reduce the emission current.

A series of collector characteristics were next determined at a number of constant temperatures, for a number of different anode voltages between 100 and 400 volts. The collector voltage was increased from 0 to 50volts, when curved characteristics were obtained. A typical curve is given in fig. 6.5.2. At first this behaviour was puzzling, but it was realized that it could be attributed to the dynatron effect. This effect can also be observed with the simple triode valve when the grid is more positive than the anode.

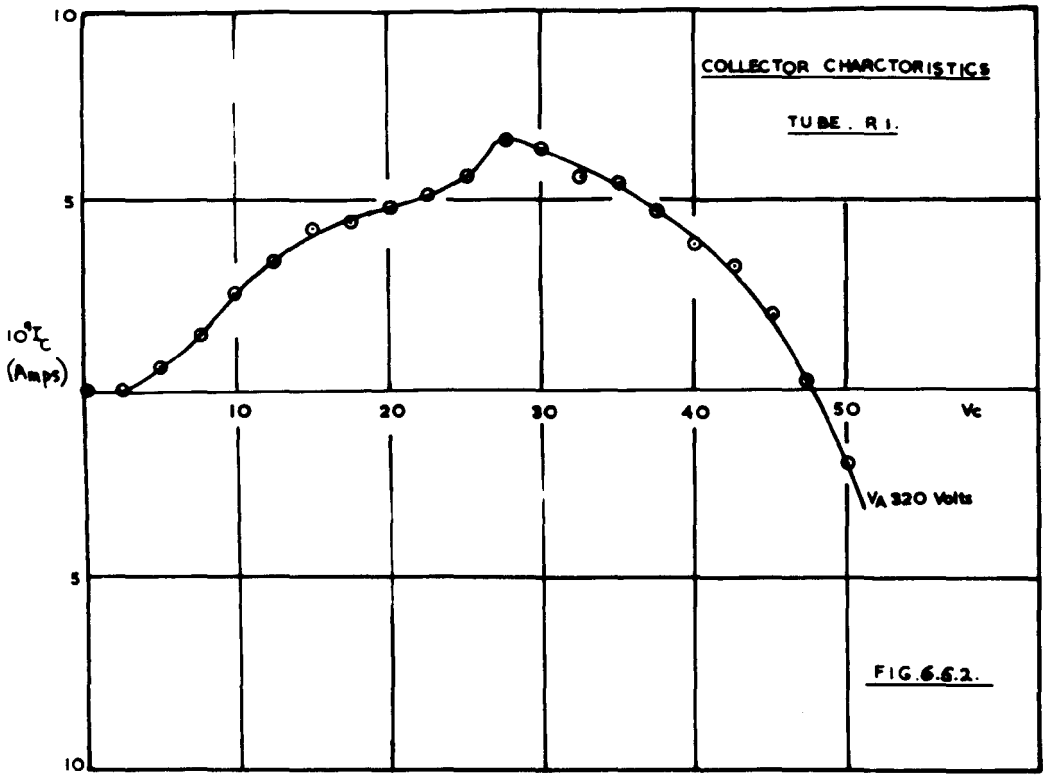
COLLECTOR CHARCTORISTICS
TUBE . R1.
10
5
$10^6 I_c$
(Amps)
10
20
30
40
50
Vc
V_A 320 Volts
5
10
FIG.6.6.2.

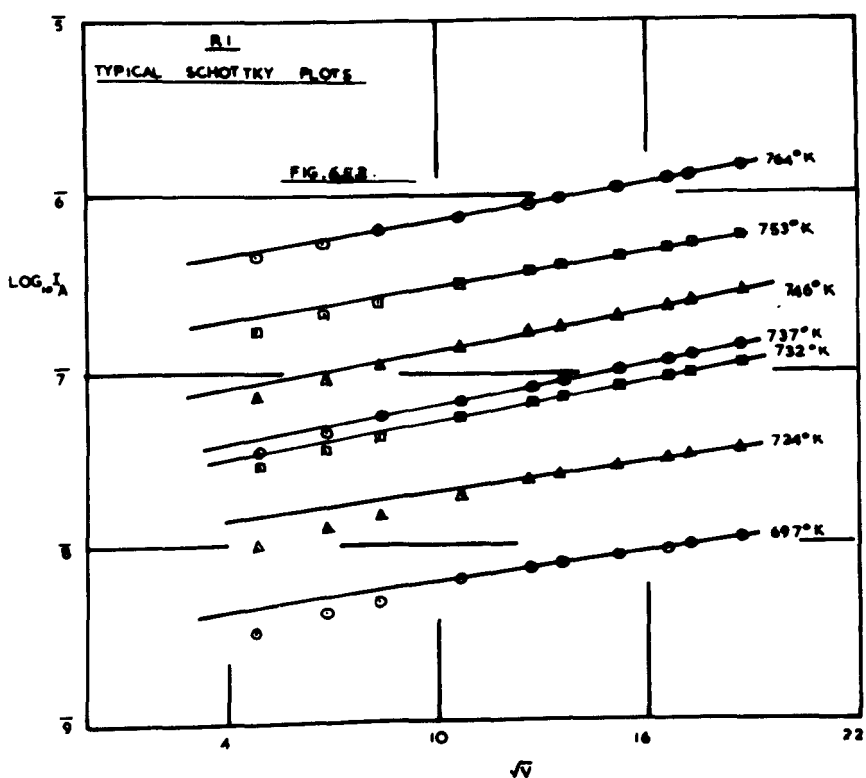
R1
TYPICAL SCHOTTKY PLOTS
FIG. 6.6.3.
$\overline{5}$
$\overline{6}$
$\overline{7}$
$\overline{8}$
$\overline{9}$
$LOG_{10} I_A$
764°K
753°K
746°K
737°K
732°K
724°K
697°K
4
10
16
22
$\sqrt{V}$

Thus, initially, the collector current increases at the expense of the anode current, but as the proportion of secondary electrons, liberated from the collector by electron bombardment increases, the resultant current to the collector decreases, while that to the anode increases. Under such conditions, the experimental tube acts as a source of power because the differential resistance of the tube is negative.

The large number of secondary electrons produced made measurement of the conductivity of the cathode quite impossible and it was realized that the design of the collector electrode would have to be improved if conductivity measurements were to be obtained. For this reason, no more conductivity measurements were attempted with this tube, but determinations of the emission characteristics were continued, in an attempt to investigate the changes of the Richardson work function and the intercept of the Richardson plot. The effects of secondary emission were reduced by connecting the collector electrode to the anode. The variation of the anode current with voltage was then investigated at a series of different temperatures for different states of activation.

The emission currents at zero field were obtained by making Schottky plots, an example of which is given in fig. 6.5.3. Activation between determinations was accomplished by drawing emission. No further slumping of the anode current was obtained at high anode voltages.

Richardson plots were drawn for each state of activation, when the values of the work function and intercept were:-

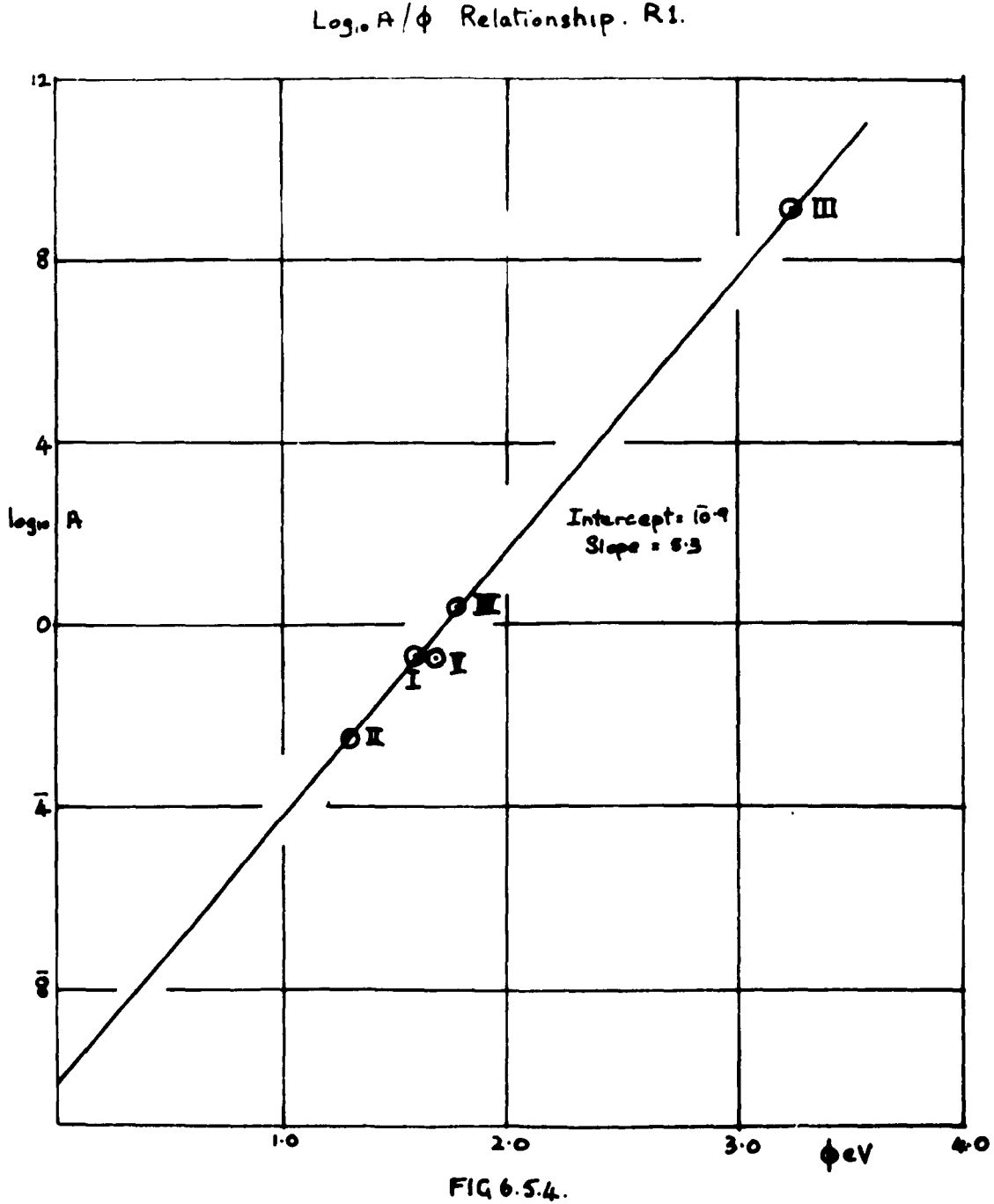
Log10 A/ϕ Relationship. R1.
12
8
4
log10 A
0
4̄
8̄
Intercept: 1̄0·9
Slope = 8·3
III
II
I
I
II
1·0
2·0
3·0
ϕeV
4·0

FIG 6.5.4.

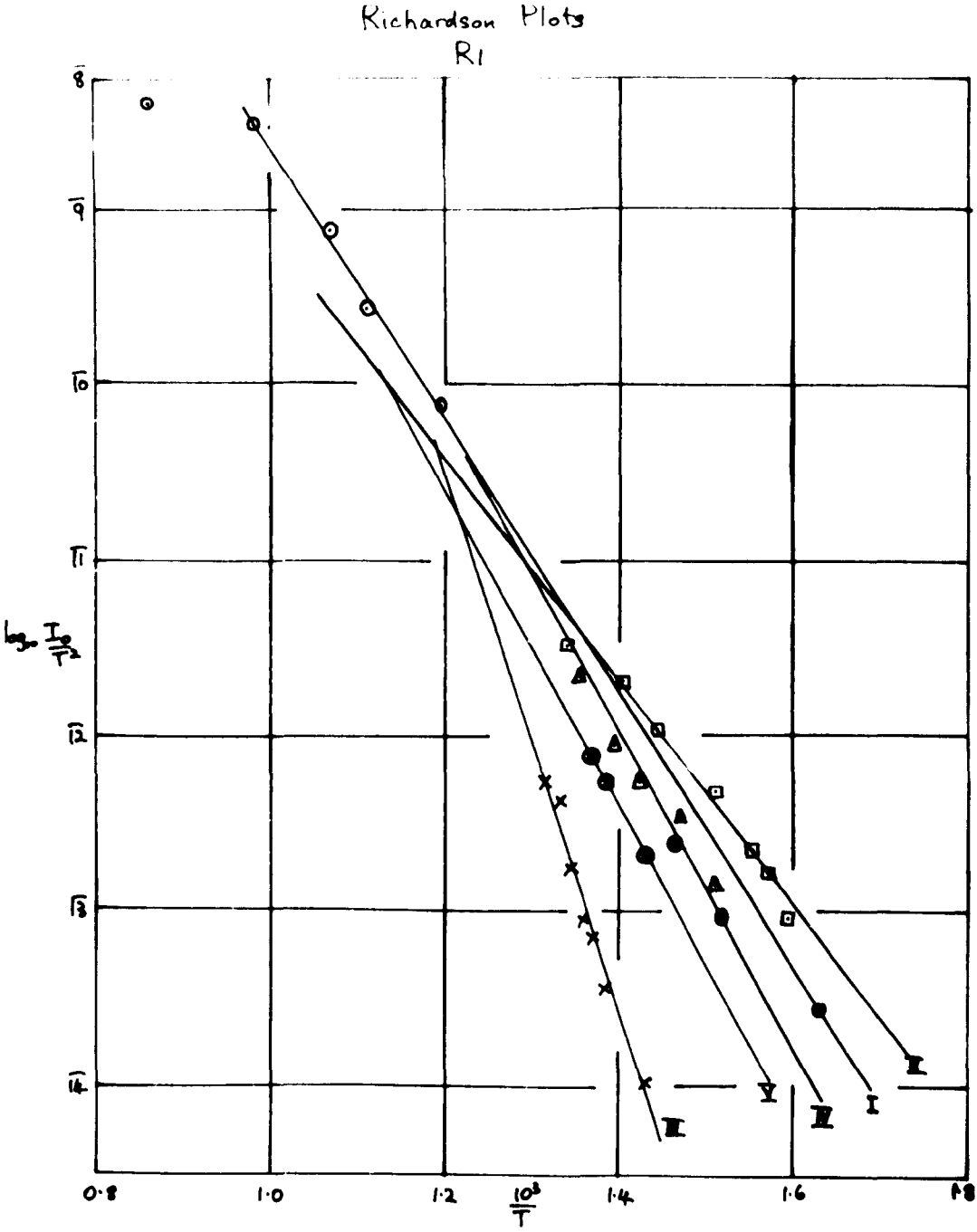
Richardson Plots
R1
$\log_{10} \frac{I_s}{T^2}$
$\frac{10^3}{T}$
0·8
1·0
1·2
1·4
1·6
1·8
$\bar{8}$
$\bar{9}$
$\bar{10}$
$\bar{11}$
$\bar{12}$
$\bar{13}$
$\bar{14}$
I
II
III
IV
V

FIG 6.5.5.

	Activation State I	Activation State II
ϕ(eV)	1.57	1.29
$\log_{10}A$.	$\bar{1}.27$	$\bar{3}.37$

After the second determination the cathode temperature was rapidly changed and this caused the top layer of the cathode coating to become detached. A marked increase in work function resulted, but this was reduced as emission was drawn and the remaining film of barium oxide became activated (III, IV and V).

	Activation State III	Activation State IV	Activation State V
ϕ(eV)	3.25	1.77	1.66
$\log_{10}A$	9.02	0.33	1.12

This last value was the result of many hours activation so that no further determinations of work function were attempted.

A plot of $\log_{10}A$ against ϕ was made and a straight line relationship was observed (fig. 6.5.4). Theory given in Section 4.1. indicates that all five Richardson plots should intersect at a common point. The numerical value of $\frac{10^3}{T}$ calculated from the $\log_{10}A/\phi$ plot was 1.2 and examination of the Richardson plots (fig. 6.5.5.) shows that the lines cross at values of $\frac{10^3}{T}$ of this order of magnitude. Similarly the value of $\log_{10}\frac{I_o}{T^2}$ given by the intercept of the $\log_{10}A/\phi$ plot has a value of the same order of magnitude as that given by the Richardson plots. No further determinations were made with this experimental tube, but another similar retarding potential tube was constructed with an improved collector design.

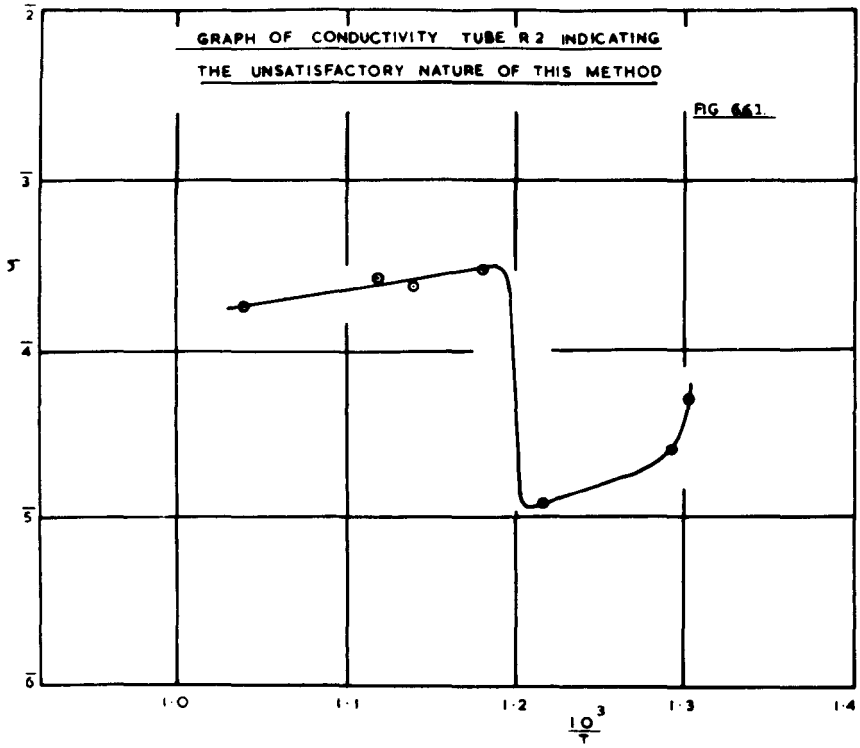
GRAPH OF CONDUCTIVITY TUBE R 2 INDICATING
THE UNSATISFACTORY NATURE OF THIS METHOD
FIG 661.
$\bar{2}$
$\bar{3}$
$\bar{4}$
$\bar{5}$
$\bar{6}$
1·0
1·1
1·2
1·3
1·4
$\frac{10^3}{T}$

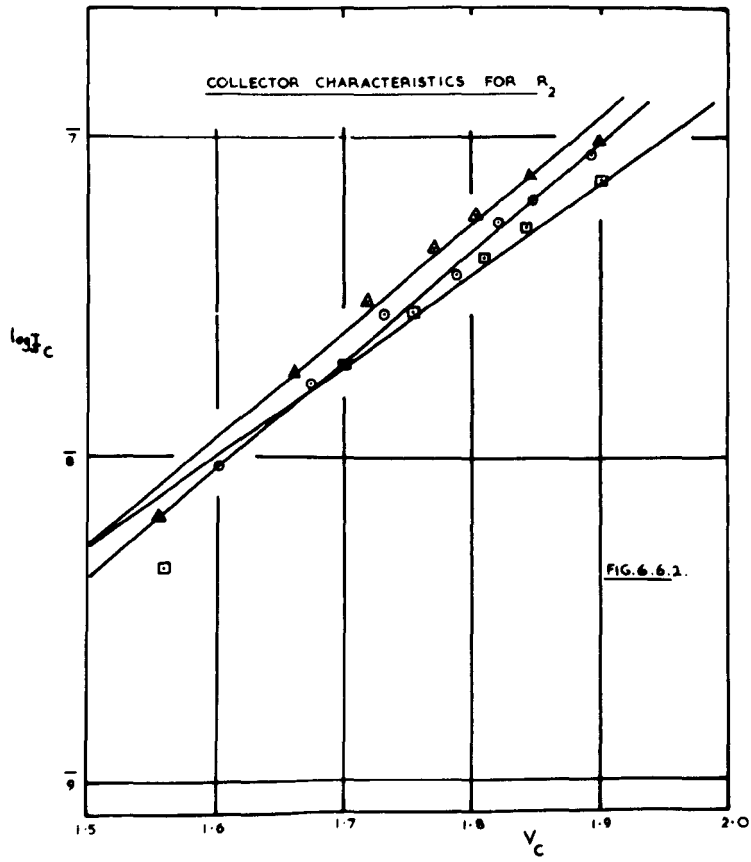
COLLECTOR CHARACTERISTICS FOR R_2
$\log I_C$
$\bar{7}$
$\bar{8}$
$\bar{9}$
1·5
1·6
1·7
1·8
1·9
2·0
V_C
FIG. 6.6.2.

6. Tube R2.

The structure of the anode and cathode of this tube were very similar to those of R1, but the collector was carefully designed so as to reduce secondary emission. Because of the similarity, no photograph or diagram of R2 will be given. The collector consisted of a nickel cylinder closed at one end with a collinator at the end nearest to the cathode. Thus most of the secondary electrons were reflected internally and were not able to proceed to the anode.

The finished tube was processed in exactly the same way as tube R1, after which the anode and collector characteristics were determined for several states of activation. Activation was accomplished by drawing emission between the determinations.

When the logarithms of the conductivities, measured at each temperature for a particular activation state, were plotted against $\frac{10^3}{T}$ the points appeared to be scattered about a straight line and were generally very unsatisfactory. The curve with most scatter is given in fig. 6.6.1.

Three such conductivity plots were obtained for three different activation states. Examples of the collector characteristics are shown in fig. 6.6.2. The dynatron effect was not obtained with the new design of collector electrode.

The values of the activation energies from the slopes of the conductivity curves for the first three activation states were:-

	Activation State		
	I	II	III
Activation energy (eV)	1.9	2.1	1.8

These values cannot be classed as being reliable, but it may be noted that the values of the activation energies are of the order of 2 eV, and can therefore be compared with the values of the Richardson work functions obtained for the same three activation states (see below). This is to be expected as the conductivity plots were obtained in the temperature range 800°to 1,000°K where, according to the Loosjes-Vink hypothesis, pore conductivity by emission should predominate. It was apparent that only order of magnitude values of the conductivities and the activation energies could be obtained with this particular type of experimental tube. In addition, the determinations made were necessarily in the high temperature region, because the currents were not measureable with the electrometer at lower temperatures.

The low temperature region of the conductivity plots are of much greater value than those of the high temperature region because values of $\frac{\Delta E}{2}$, and hence χ, can be obtained from the slope. For these reasons, no further conductivity measurements were made with this type of experimental tube, because the dosign of R2 was such that no great improvement in results would have been possible.

Emission measurements from this tube appeared to be quite reliable, so further determinations of the anode characteristics were attempted for different states of activation. As with tube R1, the geometry of R2 was such that the Schottky method was the best for determining the saturation current at zero field. The examples of these

RICHARDSON PLOTS TUBE R_2

FIG 6.6.4

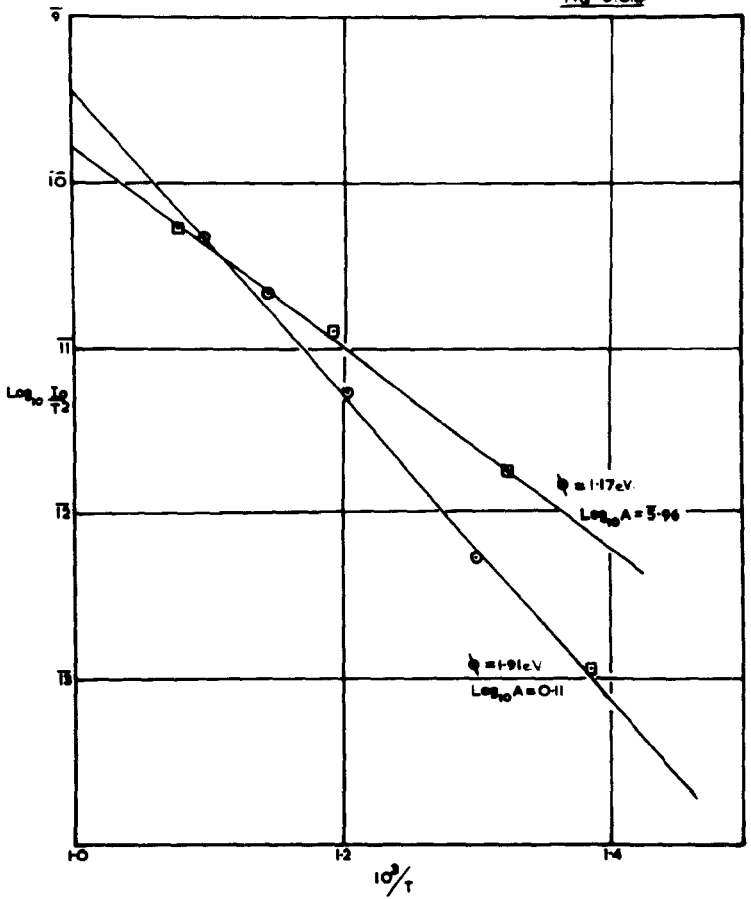

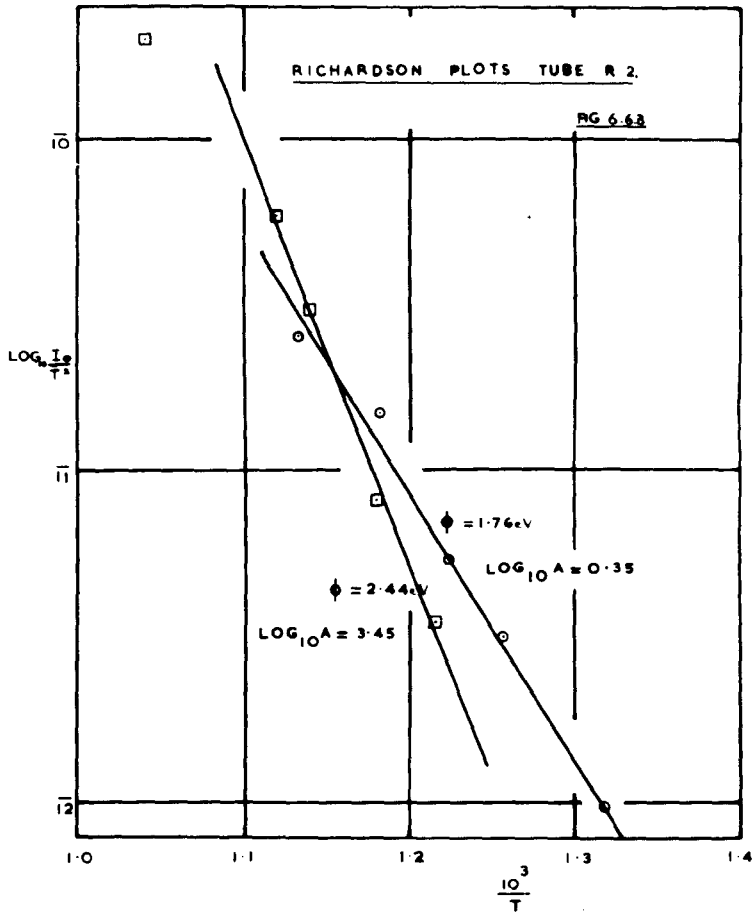

$\log_{10} A / \phi$ Relationship R_2

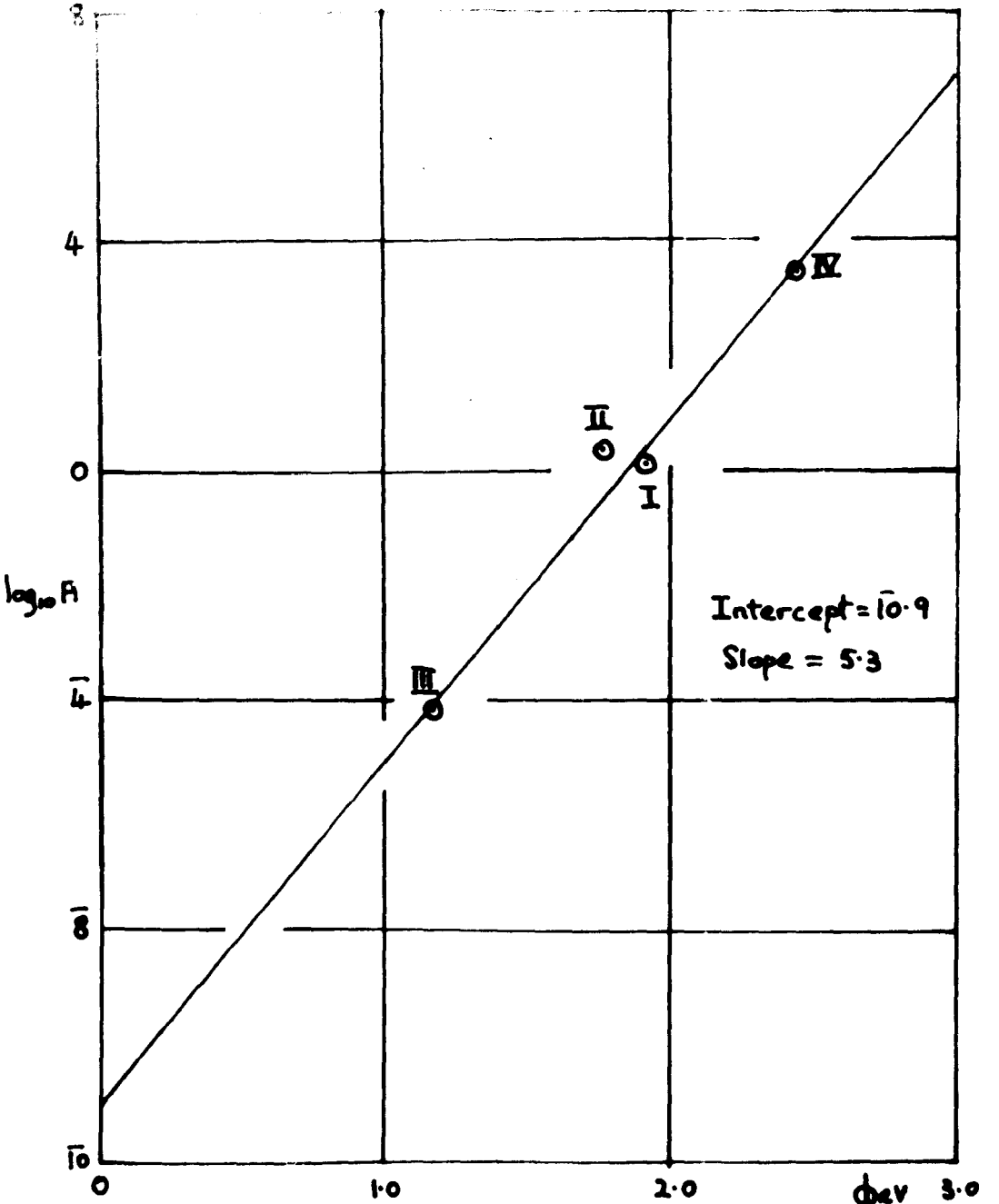

FIG. 6.6.5.

plots given for R1(fig. 6.5.3) are exactly similar to those obtained from R2. The values of Richardson work function and the corresponding values of intercept are as follows:-

	Activation State			
	I	II	III	IV
ϕ(eV)	1.91	1.76	1.17	2.44
$\text{Log}_{10}A$	0.11	0.35	$\bar{5}.96$	3.45

The first three decreasing values of work function were obtained when the activation of the cathode was increased by drawing emission. The fourth value was obtained after eddy current heating the nickel anode to approximately 1,200°K. It is likely that such heat treatment caused the removal of an electronegative adsorbed layer on the anode, part of which was adsorbed on the cathode to give an increased work function. In all probability the electronegative substance is oxygen.

The Richardson plots obtained are given in figs. 6.6.3, 6.6.4. It will be noted that these intersect at $\frac{10^3}{T} \simeq 1.15$ and $\log_{10} \frac{I_b}{T^2} \simeq \bar{10}$. $A \overset{\text{linear}}{\wedge} \log_{10} A/\phi$ relationship was obtained (fig. 6.6.5) with intercept $\bar{10}$ and slope 5.3. From the value of the slope the value of $\frac{10^3}{T}$ for the intersection of the plots was calculated as being 1.06. Hence, these results also conform with the theory of the $\overset{\text{linear}}{\wedge} \log_{10} A/\phi$ relationship proposed in Chapter 4.

7. Tube P2.

This probe tube was built to the same specification as tube P1. The same pre-breakdown treatment was given and

the cathode was broken down over a period of 24 hours. The tube was then baked and the metal parts were out-gassed by eddy current heating. Activation was then commenced with an anode voltage of 12 volts and a cathode temperature of 1,040°K. The anode current increased from a very small value to 50 mA over a period of one hour. The rate of activation then slowed considerably with a further increase in anode current of only 17 microamps in two hours. The slow increase was thought to be due to poisoning effects and it was wondered whether the electrons striking the anode possessed energies high enough to cause removal of adsorbed oxygen. The anode voltage was therefore reduced to 4 volts when the anode current increased to 0.71 mA in 17 hours.

In an attempt to test the hypothesis that poisoning was being produced by the higher values of anode voltage, the anode voltage was again increased to 12 volts and readings of the anode current were taken at regular intervals:-

	Anode at 4 volts				
Current in mA	0.71	2.0	0.42	0.29	0.27
Time after application of 12 volts to anode.		0mins.	2mins.	4mins.	6mins.

After the last reading, the anode voltage was altered back to 4 volts, when the anode current slowly increased over a period of 2 hours to 0.76 mA. It can be seen that the initial increase in anode current produced by the increase in anode voltage is offset by poisoning of the emission. It is apparent that for some value of anode voltage in excess of 4 volts, poisoning of the emission commences.

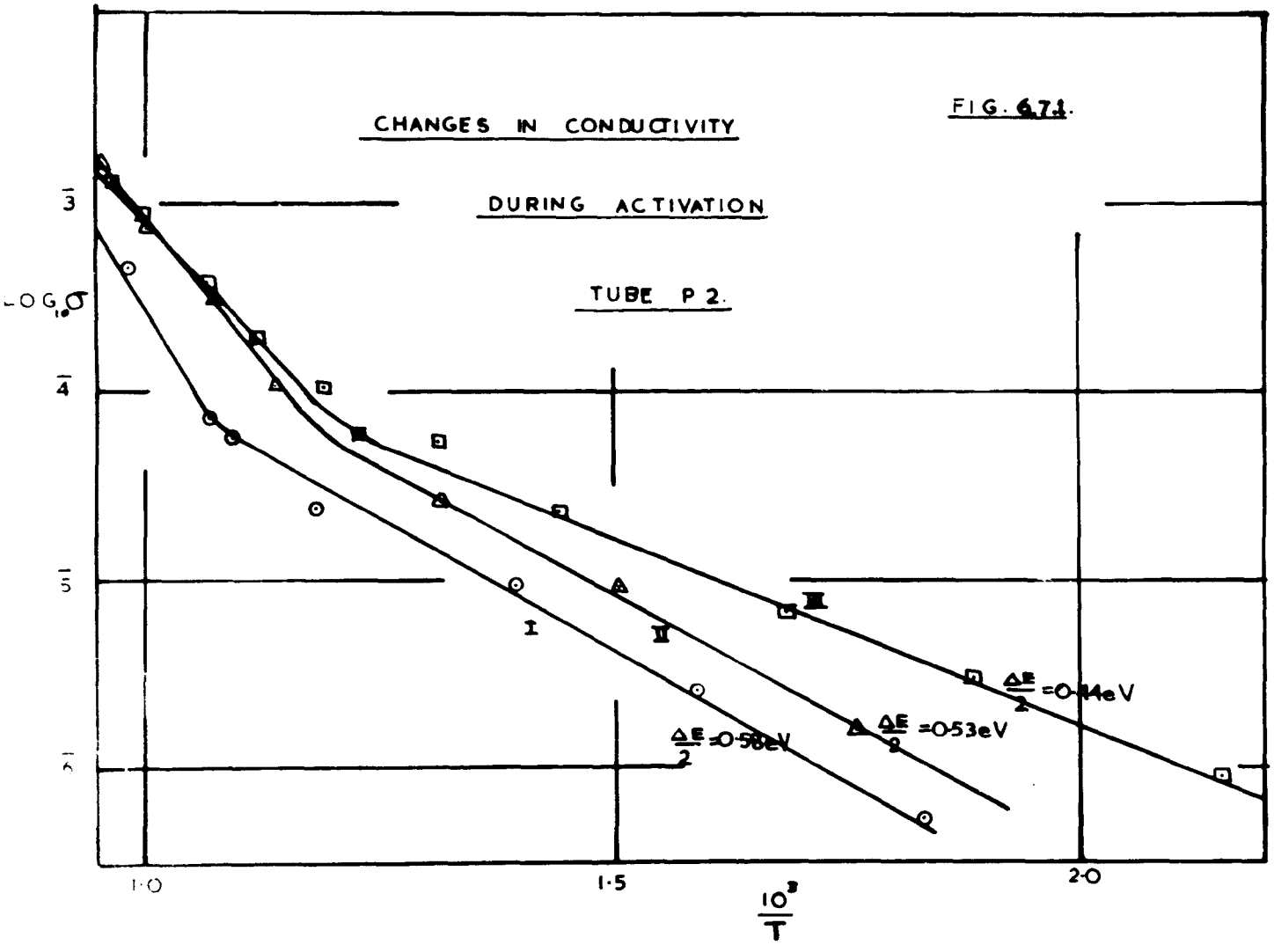
CHANGES IN CONDUCTIVITY
DURING ACTIVATION
TUBE P 2.
FIG. 6.7.1.
LOG10σ
1/3
1/4
1/5
1/6
I
II
III
ΔE/2 =0·58eV
ΔE/2 =0·53eV
ΔE/2 =0·44eV
1·0
1·5
2·0
10³/T

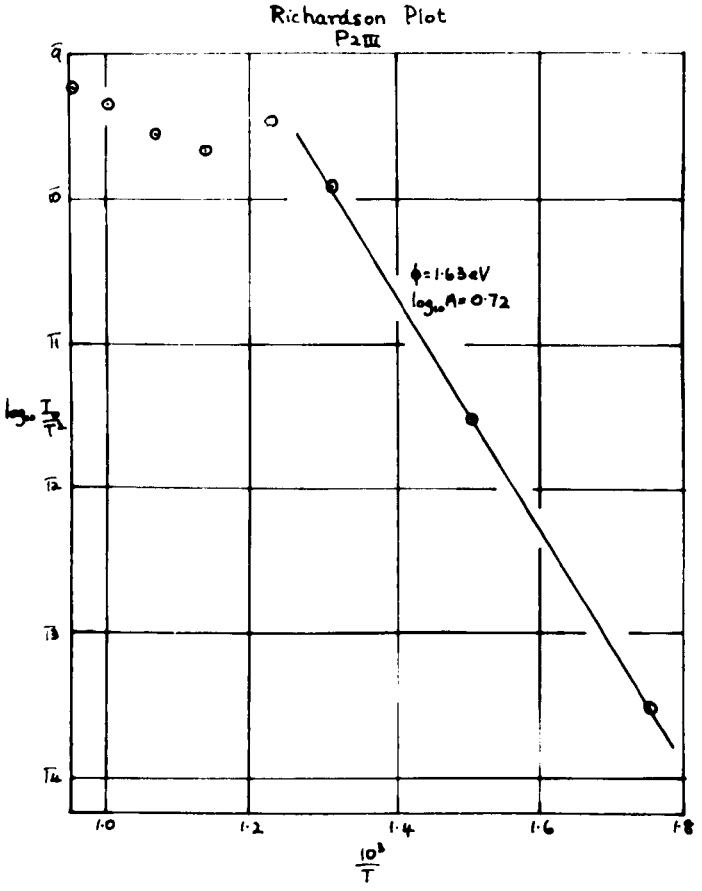
Richardson Plot
P2III
ϕ=1·63eV
$\log_{10}A$=0·72
$\log_{10}\frac{I_s}{T^2}$
$\frac{10^3}{T}$
1·0
1·2
1·4
1·6
1·8

FIG. 6.7.3.

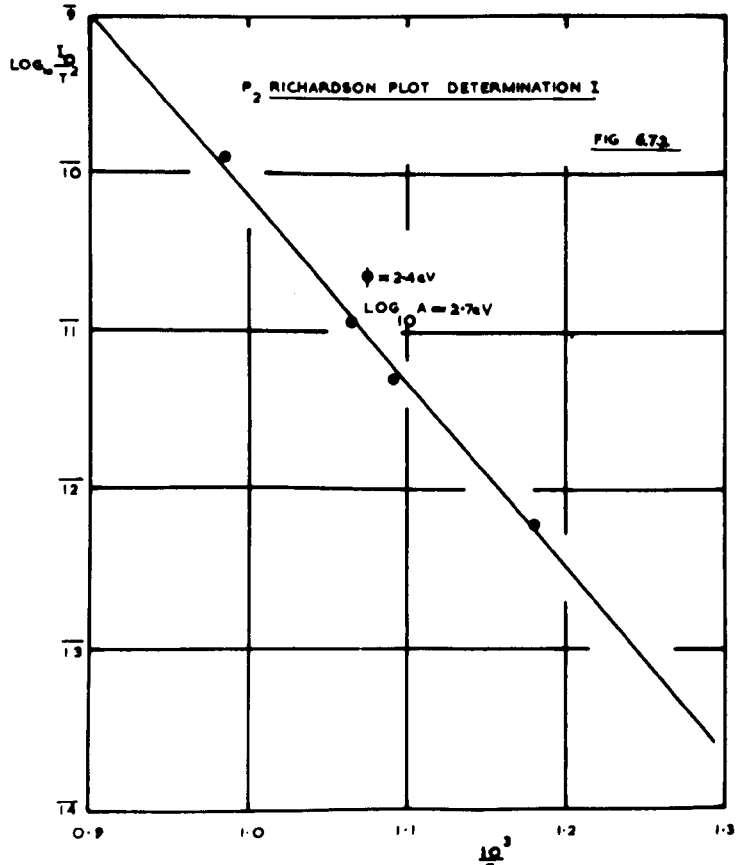
P_2 RICHARDSON PLOT DETERMINATION I
FIG 6.7.3
ϕ = 2·4eV
LOG$_{10}$A = 2·7eV
LOG$_{10}\frac{I_s}{T^2}$
$\frac{10^3}{T}$
0·9
1·0
1·1
1·2
1·3

The experimental tube was next cooled to room temperature after which one getter was fired. The tube was then sealed from the vacuum system and the second getter fired. The experimental tube was then connected up inside the screened box. An attempt was then made to measure the conductivity at room temperature, when it was found that the characteristic passed through the current and voltage zero, thus indicating, as expected, zero Seebeck e.m.f. A slight curvature of the probe characteristic was observed in the same sense as the curve obtained for tube P1. The conductivity was found to have a value of 1.62×10^{-8} mho. The temperature of the cathode was then increased and conductivity and emission measurements were carried out using the electrometer. This procedure was carried out for other values of cathode temperature. Determinations were also carried out for other activation states. In all cases the cathode was activated by drawing emission.

Three conductivity curves were obtained for different states of activation, but further measurements were prevented when the probe wire and metal base came into contact, thus producing a short circuit. The variation of conductivity with reciprocal temperature is given in fig. 6.7.1. for the three activation states. One example of the Richardson plots obtained is given in fig. 6.7.2, Most of the Richardson plots indicated that the emission current was being limited in some way at high temperatures, fig. 6.7.3. This effect is easily noticable if the anode characteristics obtained

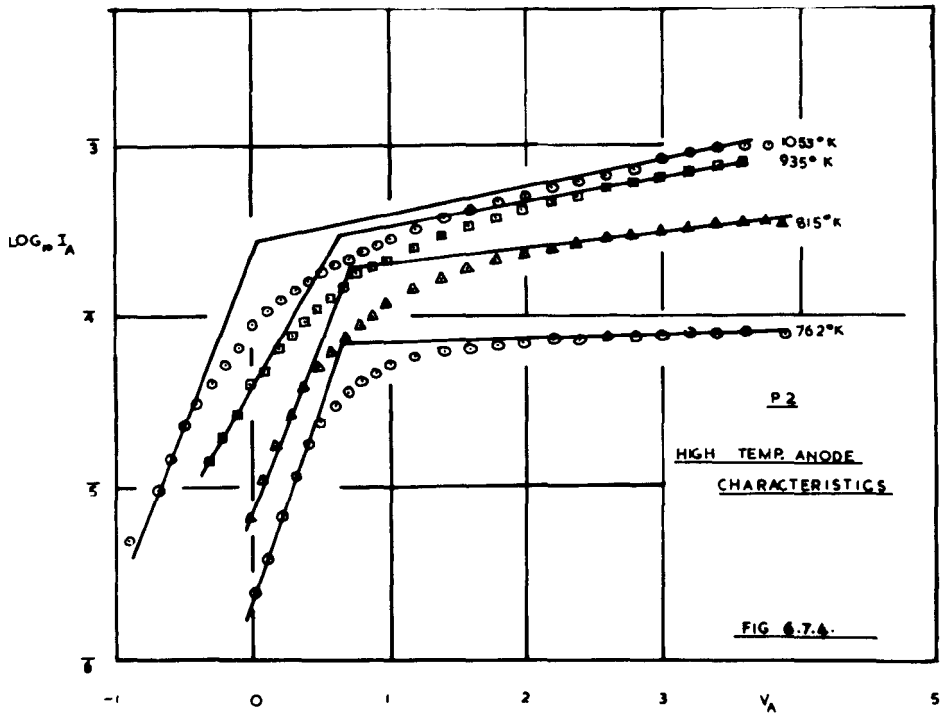
$\bar{3}$
$\bar{4}$
$\bar{5}$
$\bar{6}$
$LOG_{10} I_A$
1053°K
935° K
815°K
762°K
P 2
HIGH TEMP. ANODE
CHARACTERISTICS
FIG 6.7.4.
-1
0
1
2
3
V_A
5

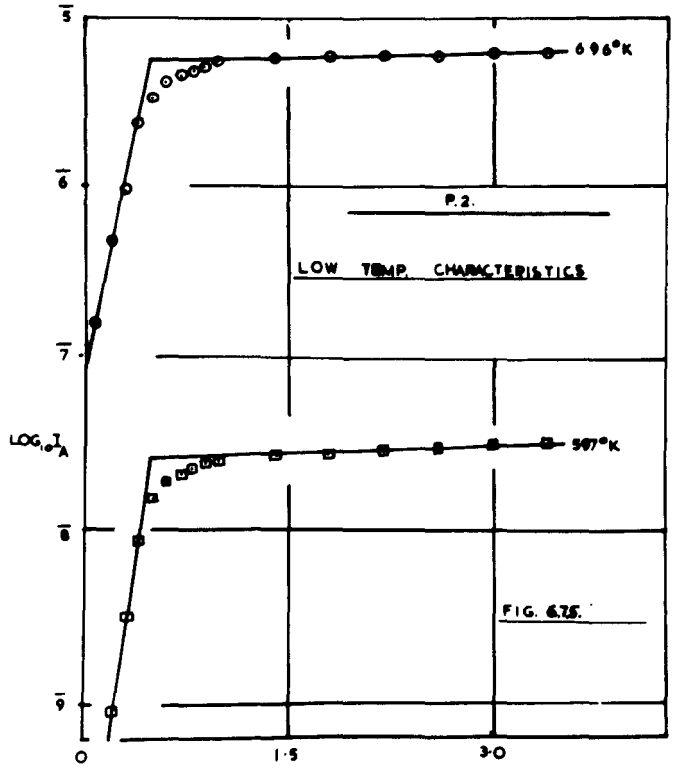
$\bar{5}$
$\bar{6}$
$\bar{7}$
$\bar{8}$
$\bar{9}$
$LOG_{10} I_A$
696°K
507°K
P.2.
LOW TEMP. CHARACTERISTICS
FIG. 6.7.5.
0
1·5
3·0

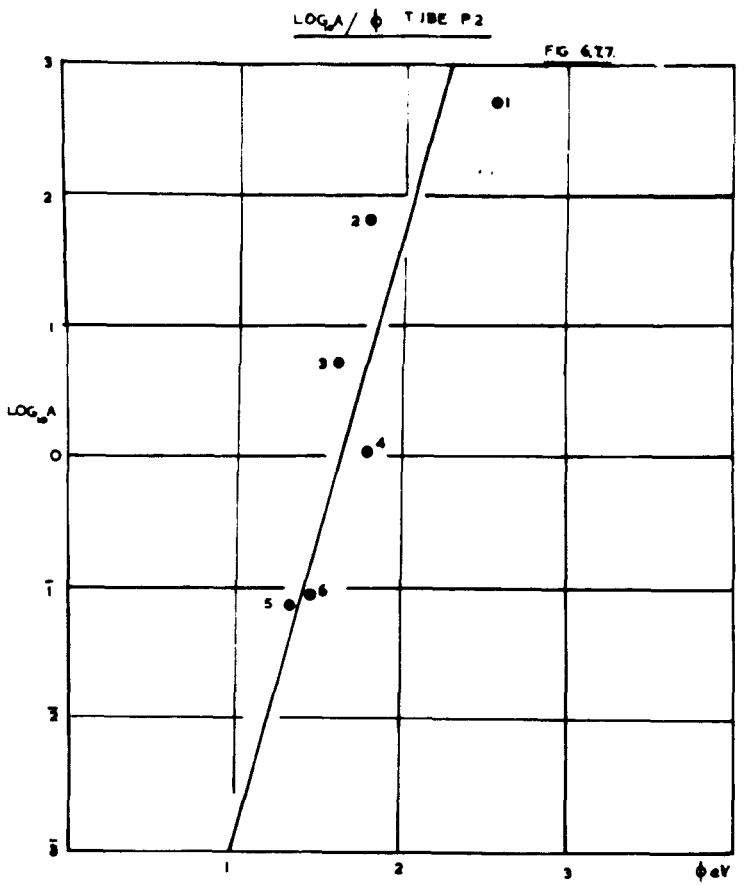
LOG$_{10}$A/ ϕ TUBE P2
FG 6.7.7.
LOG$_{10}$A
ϕ eV
1
2
3
$\bar{1}$
$\bar{2}$
$\bar{3}$
0
1
2
3
4
5
6

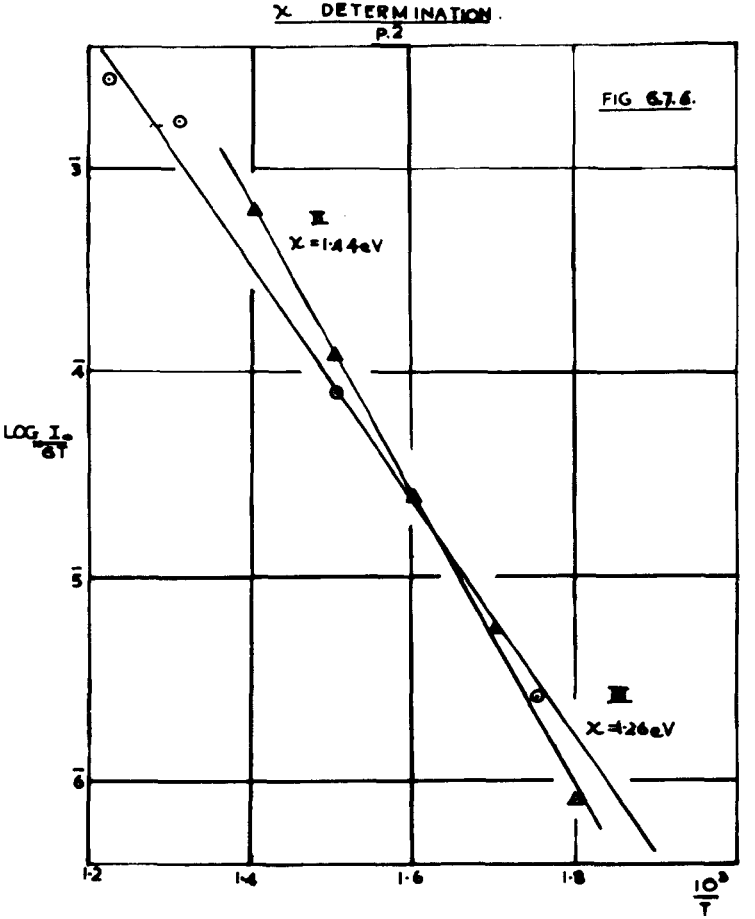
X DETERMINATION
P.2
FIG 6.7.6.
LOG $\frac{I_s}{aT^2}$
$\frac{10^3}{T}$
I
X = 1.44eV
II
X = 4.26eV
$\bar{3}$
$\bar{4}$
$\bar{5}$
$\bar{6}$
1·2
1·4
1·6
1·8

at high temperatures are examined(fig. 6.7.4.) Examples of the anode characteristics at lower temperatures are given in fig. 6.7.5.

Values of the surface work function were determined by the two methods outlined in Chapter 2. Examples of X two graphs of $\frac{\log_{10} i_0}{\sqrt{T}}$ against $\frac{10^3}{T}$, for which the values of were determined are given in fig. 6.7.6.

The values of $\frac{\Delta E}{2}$, and ϕ obtained from the three activation states were:-

	Activation State		
	I	II	III
$\frac{\Delta E}{2}$ (eV)	0.58	0.53	0.44
χ (eV)	2.0	1.44	1.26
$\chi + \frac{\Delta E}{2}$ (eV)	2.58	1.97	1.70
ϕ (eV)	2.56	1.8	1.63

It can be seen that both χ and $\frac{\Delta E}{2}$ decreased during activation while the sum of these two quantities agrees reasonably well with the value of the Richardson work function.

Emission measurements were continued after the probe had short circuited. The values of Richardson work function and the intercept values are given below for six states of activation:-

	State of Activation					
	I	II	III	IV	V	VI
ϕ(eV)	2.56	1.8	1.63	1.79	1.33	1.45
$\log_{10} A$,	2.7	1.81	0.72	0.3	$\bar{2}.85$	$\bar{2}.94$

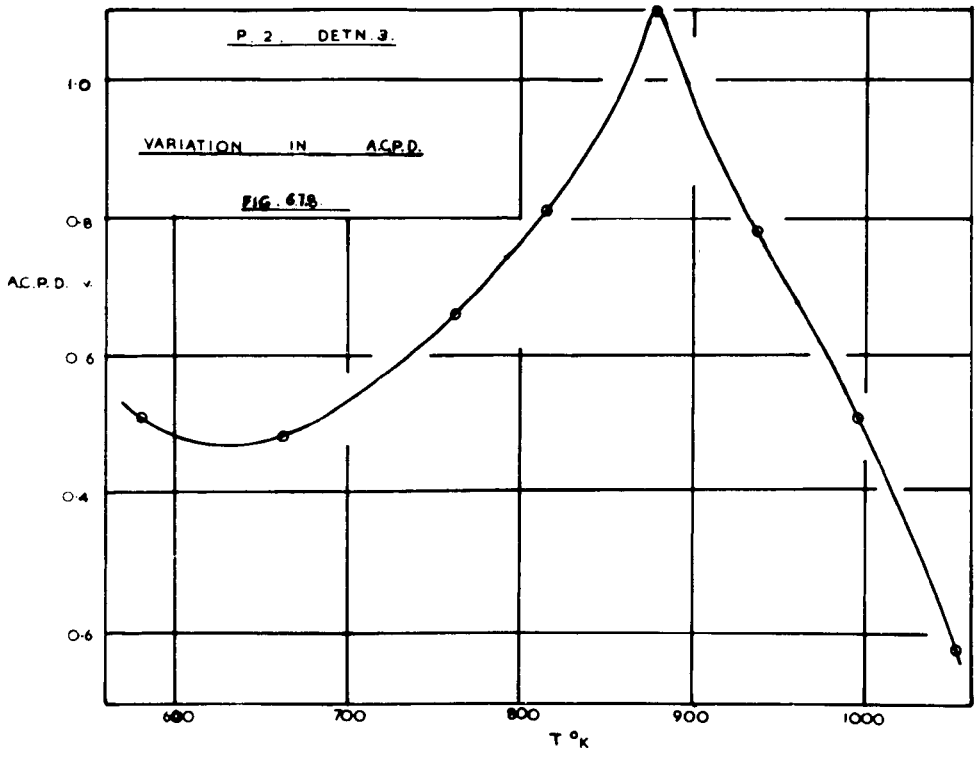

Poisoning of Emission

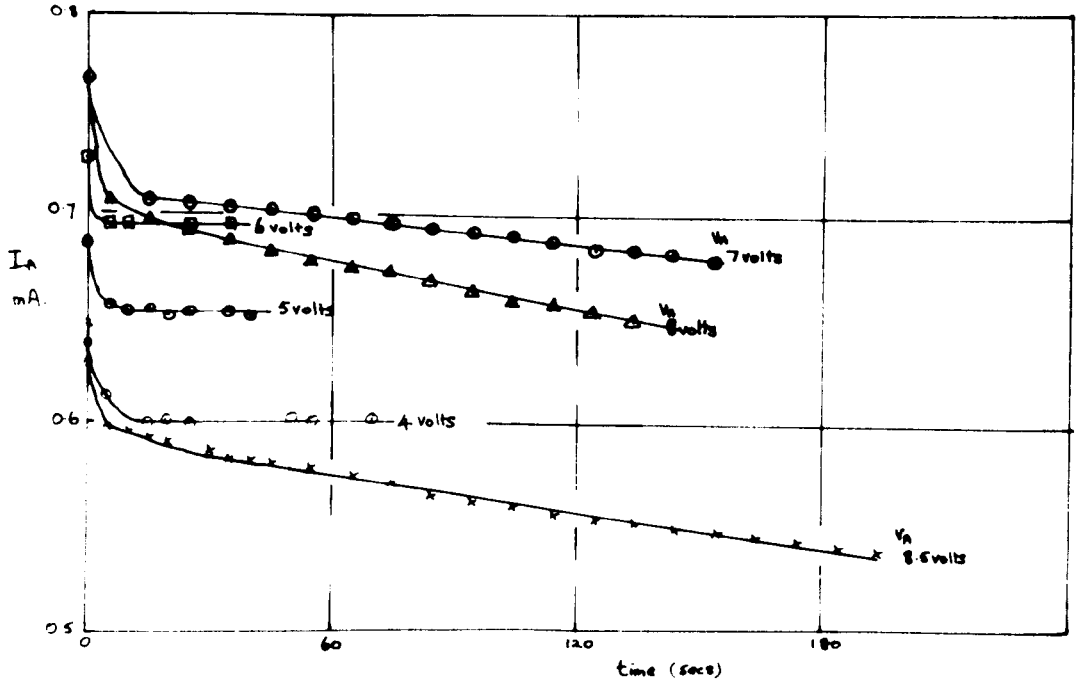

FIG 6.7.9.

A good linear $\log_{10} i/\phi$ relationship was not observed, but there appears to be a trend towards a straight line, fig. 6.7.7. This lack of linearity was to be expected as the Richardson lines did not intersect at a common point.

The activation energies from the high temperature region of the conductivity plots may be compared with the first three values of Richardson work function:-

	Activation State		
	I	II	III
ϕ eV	2.56	1.8	1.63
E(act)eV	2.22	1.23	1.20

It will be noted that the values of the activation energies are considerably smaller than the corresponding values of the Richardson work function.

If the conductivity lines intersect in a common point, a linear relationship should exist between the activation energy of the conductivity plot and the intercept on the log axis. As only three sets of results were obtained from this tube and these did not intersect in a common point, this type of relationship was not observed.

Values of the apparent contact potential difference have been obtained from the anode characteristics. A graph of the results obtained from the third activation state is given as being typical of these results, fig. 6.7.8. In all the determinations, a rise in the apparent contact potential difference was observed up to temperatures of about 900°K. For higher temperatures a decrease in the apparent contact potential difference was observed. The actual values obtained

for other activation states were slightly different from those of determination III, and not all of these results lay on a smooth curve. If the change in apparent contact potential difference is taken as being entirely due to a change in the cathode work function, it is possible to calculate the temperature coefficient of the cathode work function. Below 900°K, this was found to be approximately -3×10^{-3} eV/degree, while above 900°K it was approximately 6×10^{-3} eV/degree. These results, calculated on the basis of the assumption made above, are comparable with those obtained by Gysae(see page 53).

It will be remembered that in section 6.3 the effect of the voltage drop across the cathode material and the current measuring instrument was considered. The first of these is inherent in the contact potential differences as calculated from the anode characteristics. It may well be that the reversal of slope of the apparent contact potential difference curve at 900°K is determined by the reduction in cathode resistance due to the increasing preponderance of the pore conduction process at temperatures in excess of about 900°K.

In an attempt to learn something further about the anode poisoning effect, the highest anode voltage applied for cathode states I, II and III was 4 volts, while the maximum anode voltage applied during determination IV was 8 volts. It was hoped that the 4 volts anode voltage would cause no poisoning of emission, while the application of

8 volts would cause cathode poisoning due to the removal of the electronegative substance which was thought to be present on the anode. No activation by drawing emission was carried out between determinations III and IV. When the 8 volts anode voltage was applied, an immediate change in the anode current was observed. The initial increase, due to the increase in the applied voltage, ceased almost immediately and was followed by a decrease which was attributed to the poisoning effect. The Richardson work function was found to increase from 1.63eV to 1.79eV. Measurements of the apparent contact potential difference indicated that the apparent anode work function had decreased from approximately 2.5 eV to 1.9 eV, consistent with the removal of an electronegative substance from the anode. It will be noted that the anode work function, as derived from the apparent contact potential difference and the Richardson work function of the cathode, has an indicated value smaller , than the accepted value for pure nickel of 4.96 eV. The values of anode work function given by this method were generally consistently lower than the accepted value, which indicates that the surface is probably modified by barium and barium oxide evaporated from the cathode, while an electronegative substance (probably oxygen) is adsorbed onto the resultant surface, and can be removed by electrons having energies greater than about 4 eV.

The poisoning effect was further investigated at a constant cathode temperature of 912°K by application of various values of anode voltage. The results obtained are

given in fig. 6.7.9. Two interesting facts emerge from these results. Firstly, for all the values of anode voltage applied there is a very rapid initial decrease in anode current. Secondly, for applied anode voltages in excess of 6 volts there is a long term decrease in anode current, the rate of decrease being higher for the higher values of V_A.

The short term decrease in anode current could possibly be attributed to physical changes occuring within the cathode (possibly donor depletion), but it is likely that the long term effect is due to an increase in cathode work function, caused by the removal, and redeposition on the cathode, of an electronegative substance adsorbed on the anode. An attempt was made to determine the anode work function by use of the values of emission current in the retarding potential region, but marked scatter of the points prevented any accurate value of ϕ_A from being obtained. The method used will be described for the next tube, for which a satisfactory straight line was obtained for one state of activation.

8. Tube P3.

This probe tube was built to the same specification as the previous tubes and the method of processing was similar to that used for P2 except that an anode voltage of 4 volts was used during activation, which was carried out at a temperature of 1134^{o}K. This low value of anode voltage was used in order that poisoning effects could be kept at a minimum.

After sealing off, the emission and conductivity characteristics were obtained for three activation states,

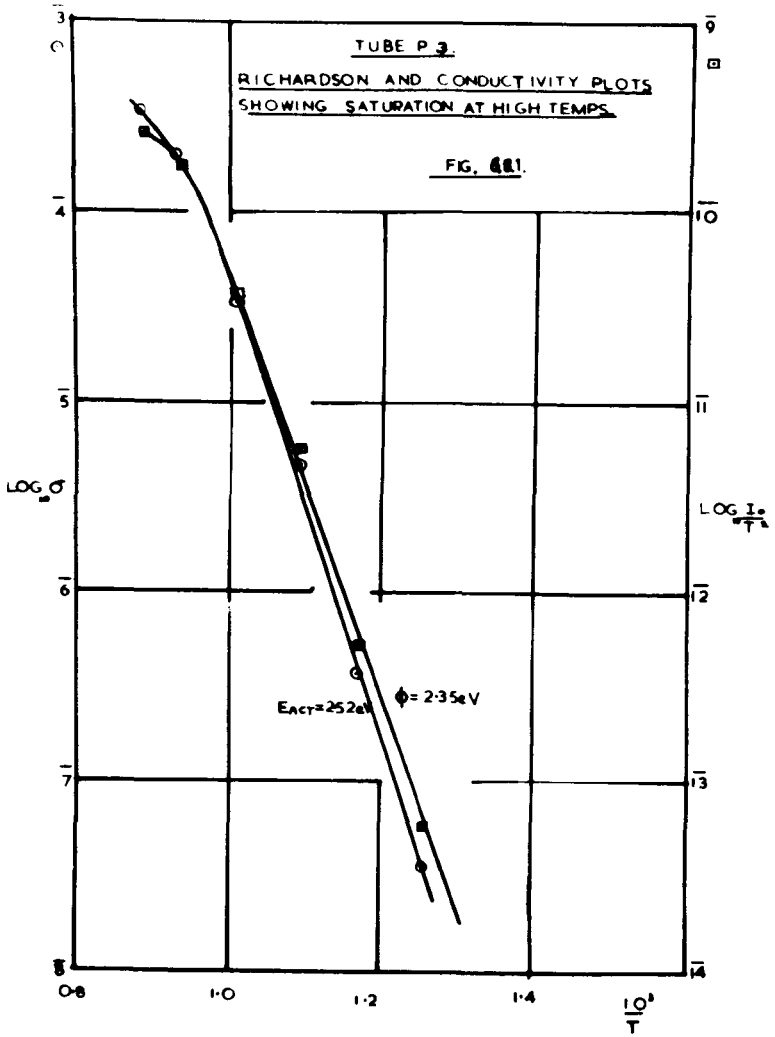
TUBE P 3.
RICHARDSON AND CONDUCTIVITY PLOTS
SHOWING SATURATION AT HIGH TEMPS.
FIG. 681.
Log σ
LOG I₀/T²
Eact=2·52eV
φ= 2·35eV
0·8
1·0
1·2
1·4
10³/T

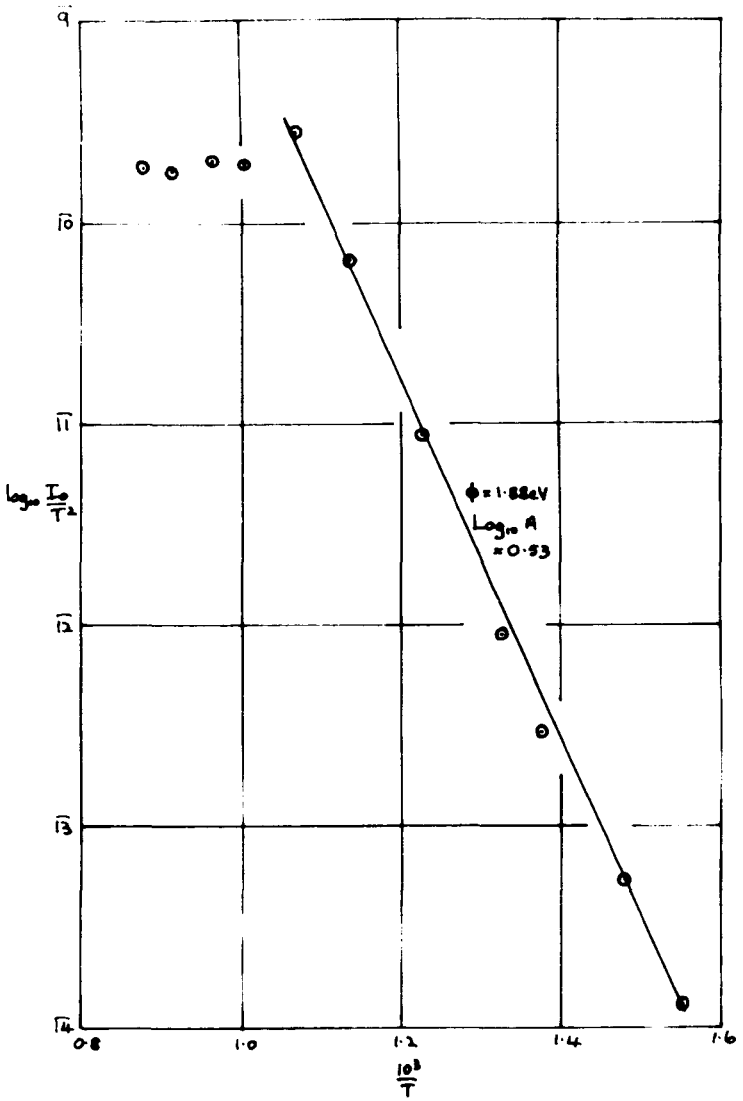
Log₁₀ I₀/T²
φ = 1·88eV
Log₁₀ A
= 0·53
0·8
1·0
1·2
1·4
1·6
10³/T

FIG 6.8.2.

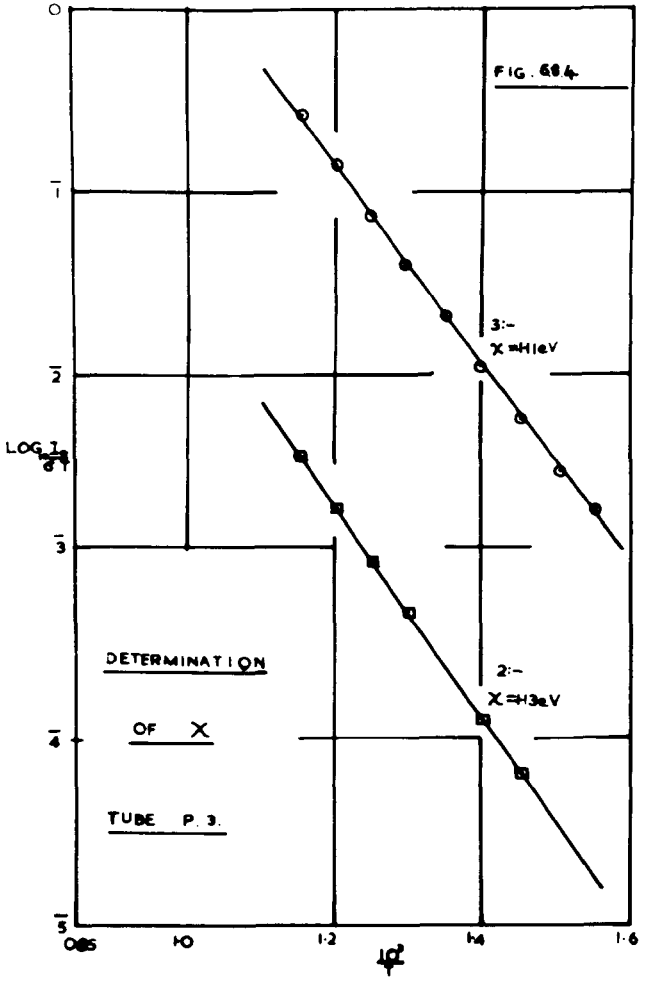
FIG. 6.8.4
3:-
X=H1eV
2:-
X=H3eV
DETERMINATION
OF X
TUBE P. 3.
0·8
1·0
1·2
1·4
1·6

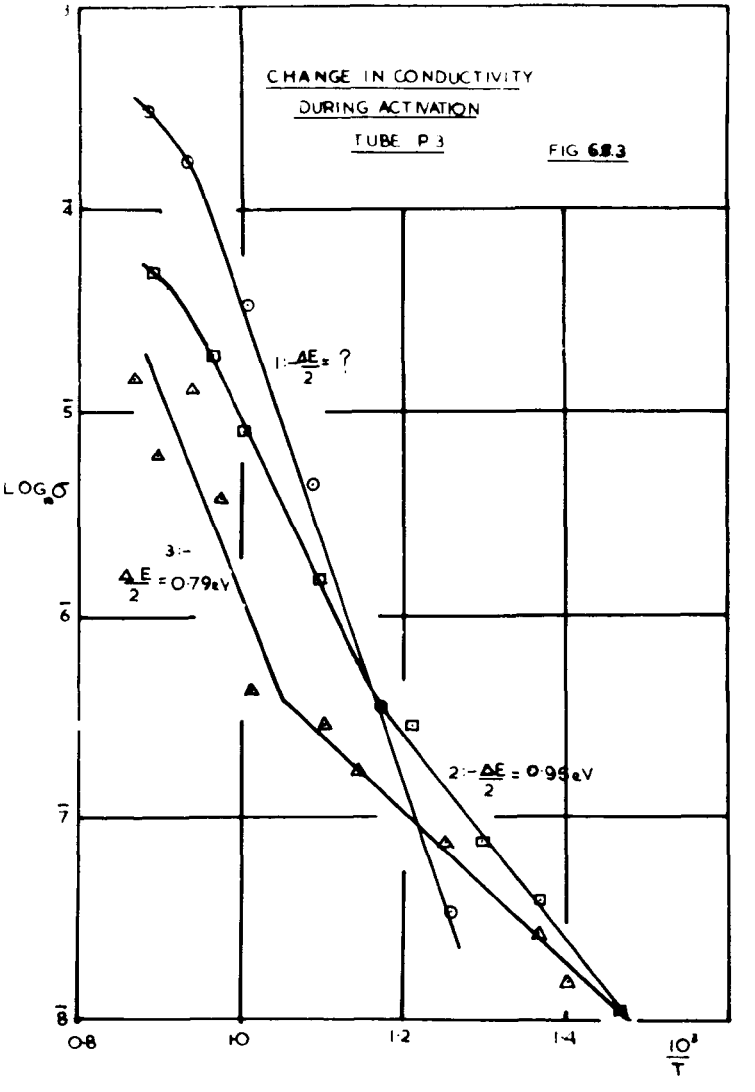
CHANGE IN CONDUCTIVITY
DURING ACTIVATION
TUBE P 3
FIG 6.8.3
1:-ΔE/2 = ?
3:-
ΔE/2 = 0·79eV
2:-ΔE/2 = 0·95eV
0·8
1·0
1·2
1·4

but the probe wire failed after the third activation state and no more conductivity measurements were possible. Both the Richardson plots and the graphs of the logarithm of the conductivity against $\frac{10^3}{T}$ exhibited marked curvature at high temperatures, similar in form to those found for P2. The probe characteristics were fairly linear, thus indicating that rectification effects were very small.

Fig. 6.8.1., shows the Richardson plot and conductivity plot obtained during the first activation state. Fig. 6.8.2 shows the very marked curvature observed in the Richardson plot for the third state of activation, while examination of the conductivity plot for the third activation state shown in fig. 6.8.3, also indicates a scatter of points at high temperatures. This behaviour at high temperatures indicates that the conductivity and emission from the oxide cathode at high temperatures are probably governed by the same mechanism as suggested by the Loosjes-Vink hypothesis. In all probability, this effect can be attributed to a space charge effect in the pores of the cathode, which becomes quite marked when the current density reaches a critical value. This critical value of current density will depend on the mean pore size. If the Richardson plots are examined, it will be noted that this effect becomes noticeable at $\log_{10} \frac{I_o}{T^2} \simeq \overline{10}$ and $\frac{10^3}{T} \simeq 1.0$. This was also observed for the Richardson plot for the second state of activation.

The saturation of emission would therefore indicate that the emission does not come from the outer surface of the

cathode, but must originate at the surfaces of the crystals within the pore structure of the cathode. Saturation of emission could also be attributed to a change in the cathode work function as the temperature is increased. Such effects are the case for caesium on tungsten cathodes when the adsorbed layer of caesium is being rapidly removed at high temperatures. A similar explanation might be invoked if the work function of the oxide cathode was strongly dependent upon an adsorbed layer of barium on the surfaces. The temperature at which a marked change in surface conditions became responsible for a reduction of slope would depend on the heat of adsorption of barium on barium oxide. This heat of adsorption is not given in the literature and hence the temperature range in which such a change in slope would become noticeable cannot be calculated.

The three Richardson plots gave the following values of Richardson work function and intercept:-

	Activation State		
	I	II	III
ϕ(eV)	2.35	2.1	1.88
$\log_{10}A$	1.43	0.37	0.53

No $\log_{10}A/\phi$ relationship was observed, but this is to be expected as only the three experimental results were available.

The results obtained from the emission measurements are summarised below:-

	Activation State		
	I	II	III
$\frac{\Delta E}{2}$ eV	-	0.95	0.79
Log intercept (low temp.)	-	$\bar{1}.09$	$\bar{3}.81$
E (act.) eV	2.52	2.02	2.2
Log intercept (high temp.)	8.32	4.84	4.38

The conductivity given by the first activation state did exhibit a break at low temperatures, which indicated that the pore conduction mechanism predominated over the temperature range investigated. This indicated that the activation energy of the bulk conductivity process was large and probably of the same order as the value indicated by the slope of the conductivity plot. The values of the surface work function were obtained for the second and third activation states by plotting $\log_{10} I_o/6T$ against $10^3/T$. The experimental lines obtained are shown in fig. 6.8.4. The values of χ were also calculated from the corresponding values of $\frac{\Delta E}{2}$ and ϕ.

	Activation State		
	I	II	III
$\frac{\Delta E}{2}$ eV	-	0.95	0.79
χ eV	-	1.11	1.13
$\chi + \frac{\Delta E}{2}$ eV	-	2.06	1.92
ϕ eV	2.35	2.1	1.88

The values of χ are seen to be comparable (experimental error $\sim 15\%$) and indicate that the activation which caused a change in Richardson work function from 2.1 to 1.88 was due to the production of impurity levels near the conduction

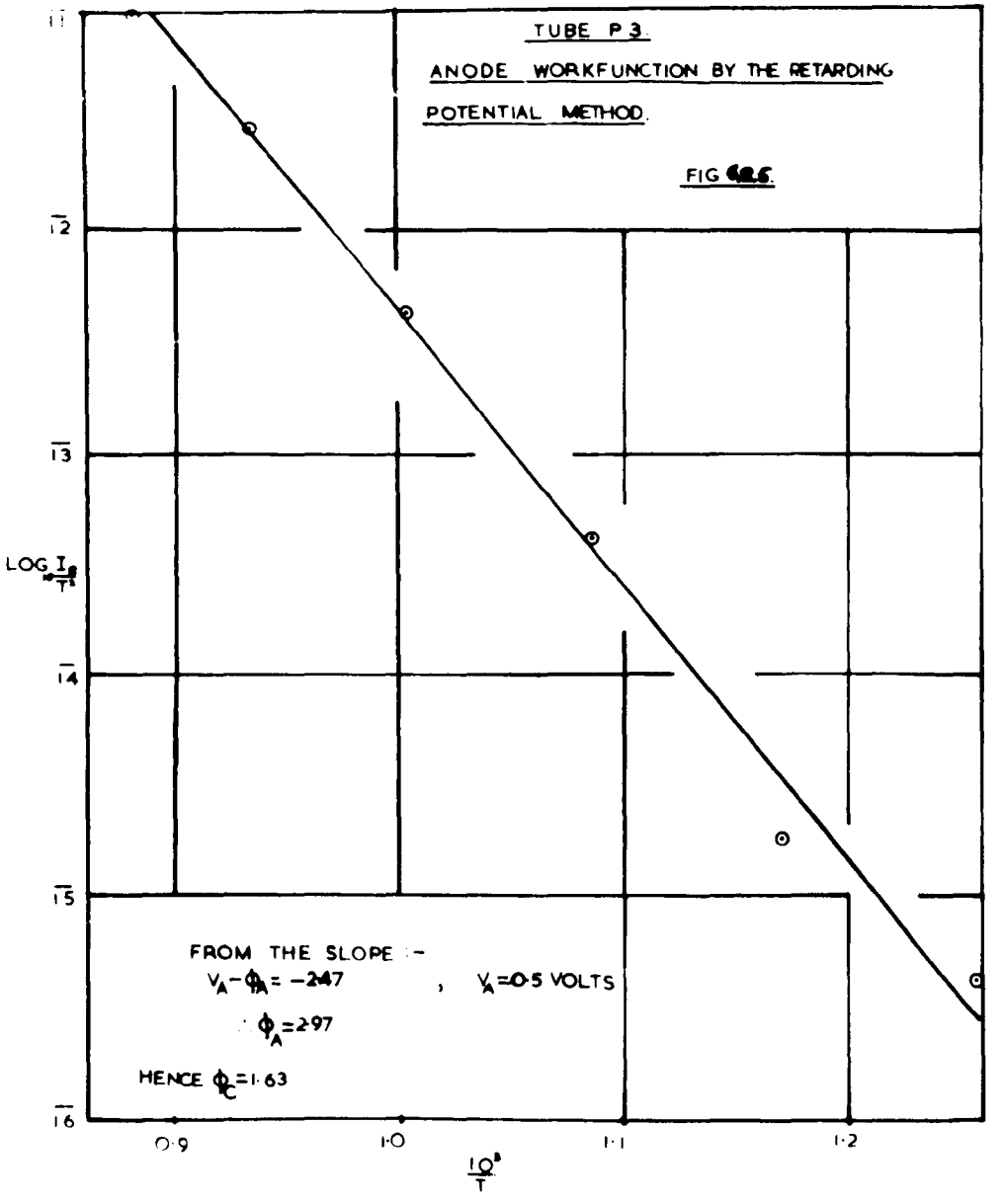
TUBE P 3.
ANODE WORKFUNCTION BY THE RETARDING POTENTIAL METHOD.
FIG 12.6.
$\bar{1}1$
$\bar{1}2$
$\bar{1}3$
$\bar{1}4$
$\bar{1}5$
$\bar{1}6$
LOG $\frac{I_s}{T^2}$
FROM THE SLOPE :-
$V_A - \phi_A = -2.47$, $V_A = 0.5$ VOLTS
$\therefore \phi_A = 2.97$
HENCE $\phi_C = 1.63$
0·9
1·0
1·1
1·2
$\frac{10^3}{T}$

band and not to a modification of the surface work function.

Values of the apparent contact potential difference, as given by the break of the anode characteristics, showed little variation with changing temperature. The average value for the third state of activation was 1.3 eV, from which the apparent anode work function can be calculated as having a value of approximately 3.2 eV. The anode work function was also determined from the values of the emission current in the retarding potential region.

If the voltage drop across the cathode material is ignored, the emission current in the retarding potential region is given by equation 6.3.2. Thus, if the values of $\mathrm{Log}_{10} I_o/T^2$ are plotted against $1/T$ for a constant value of V_A, smaller than the value of the apparent contact potential difference, the slope of the resulting line should have a value $e(V_A - \phi_A)/k$. Hence, ϕ_A can be calculated from the slope of the experimental line. This method was used for tube P2, but a marked scatter of the experimental points was obtained. A similar scatter of points was obtained for all but one of the three determinations on P3. The straight line obtained for P3 III is given in fig. 6.8.5. The anode work function, as calculated from the slope of this line, was 2.97 eV. This may be compared with the value obtained from the apparent contact potential difference which was 3.2 eV. Three values of anode work function, as calculated from the apparent contact potential difference, were:-

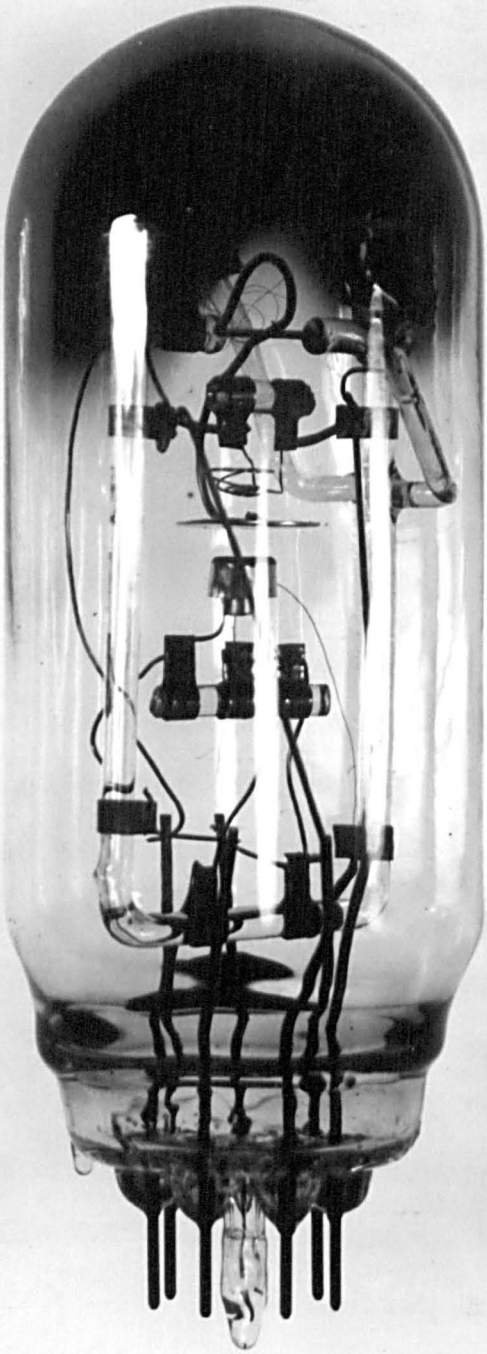

Tube HNW1.

FIG. 6.9.1.

Activation State	I	II	III
Anode work function (eV)	3.75	3.5	3.18

If the effect of the resistance of the cathode material is considered, the decrease in conductivity with increasing activation will cause a decrease in the 'lost volts' developed across the coating. Thus, V_A should approximate more closely to the value of V^+ as the cathode activates. Hence, the value of the anode work function will be relatively constant, regardless of the activation state. This could possibly be attributed to the low value of the anode voltage used in these determinations, which was low enough to prevent removal of the electronegative layer present as an adsorbed layer on the anode.

In view of the interesting effects produced by the change in anode work function, it was decided that a number of experimental tubes should be built in order that the anode work function, and the effects of adsorbed layers, could be examined more easily. The first of these tubes is described below.

9. Tube HNW1.

A photograph of this tube is shown in fig. 6.9.1. The cathode was of the same type as used in the retarding potential tubes. Two anodes were built into the tube. The first anode consisted of a small nickel disc which could be interposed between the cathode and the second anode. A magnetic slug was attached to the mounting of the first

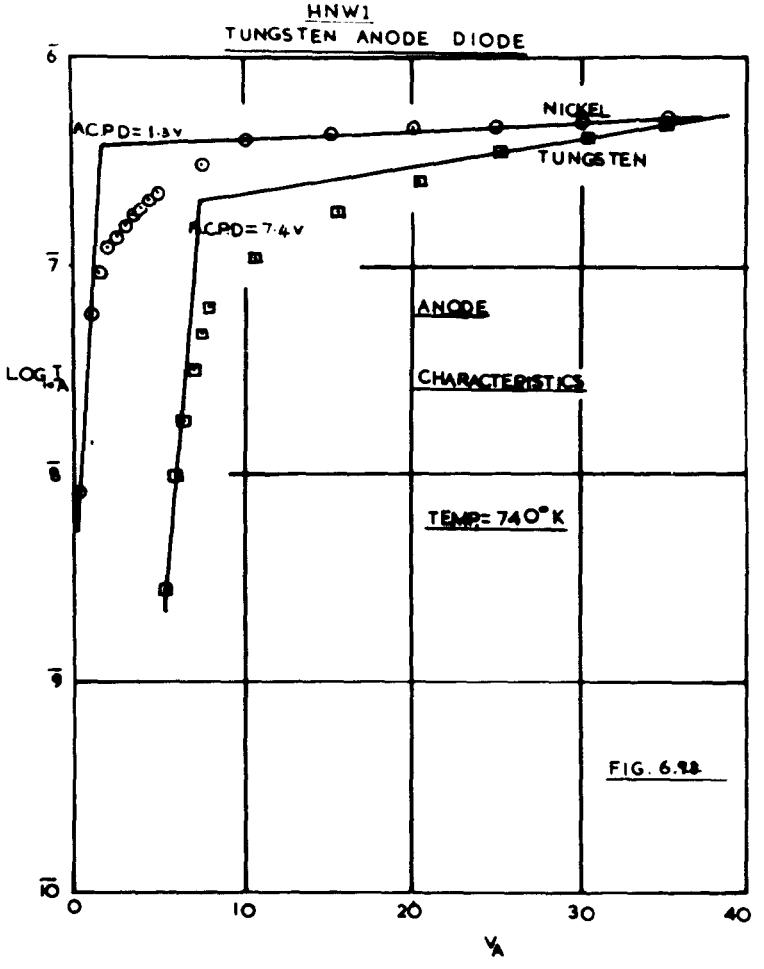

FIG. 6.9a

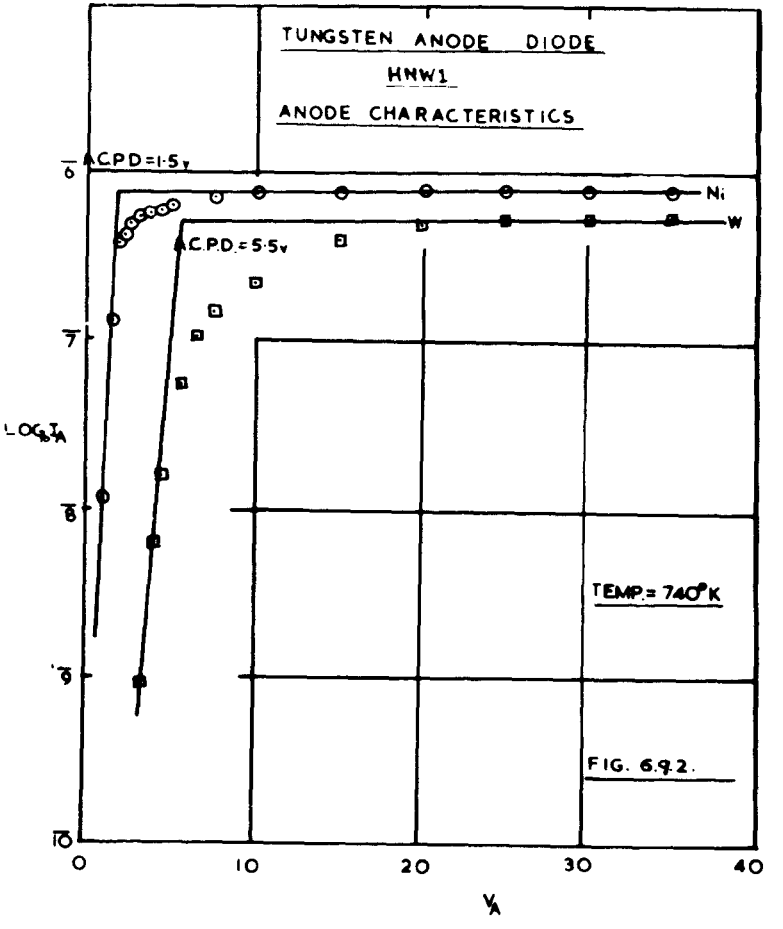

FIG. 6.9.2.

anode so that it could be pivoted away when the second anode was used. The nickel anode was kept in position so as to screen the second anode while the valve was processed. In this way, barium and barium oxide(evaporated from the cathode)were prevented from contaminating the second anode. The second anode was a flat spiral of tungsten wire which could be heated to high temperatures by means of an auxiliary heater supply. The cathode was shielded during this heat treatment by means of the nickel anode disc. It was hoped that when the second anode was heated the adsorbed layers would be removed, so that the work function of the anode would be that of pure tungsten (4.52eV). Values of the contact potential differences obtained by use of both the tungsten and nickel anodes during emission measurements would then give a value of the arithmetic mean work function of both the nickel anode and the cathode. A series of determinations of the anode characteristics were made and examples are given in figs. 6.9.2. and 6.9.3. These are typical of the results obtained. The values of apparent contact potential difference, obtained by use of the tungsten anode, were of the order of 5eV greater than those obtained by use of the nickel anode. These values indicated that the work function of the nickel anode was greatly reduced by an evaporated film of barium or barium oxide and that the work function of the tungsten anode was greatly increased by the presence of an adsorbed layer of strongly electronegative substance (probably oxygen).

The nickel anode could not be heated so that a study of desorption, produced by an increase in temperature, could not be made. The values of apparent contact potential difference existing between the cathode and nickel anode for a particular activation state were found to be relatively constant at a fixed cathode temperature. A decrease from 1.8eV to 1.2eV was observed as the cathode was activated by drawing emission current. The effects observed when the tungsten anode was flashed were very pronounced. It was found that the apparent contact potential differences existing between the tungsten anode and the cathode were strongly dependent upon the heat treatment of the anode and the delay involved before emission measurements were made. A series of values which were determined in rapid succession are given below:-

5.2eV, 4.6eV, 6.2eV, 8.3eV, 6.7eV, 4.8eV.

Thus the rate of adsorption of contaminants onto the tungsten anode was very rapid even though the pressure in the experimental tube must have been less than 10^{-7} mm.Hg. This illustrates the strong dependence of the work functions of the surfaces within the experimental tube on the presence of very small quantities of contaminants. Only two successive determinations of apparent contact potential difference gave a constant value (3.4eV). A cathode work function of 1.2eV was calculated from this value, while the work function of the nickel anode was found to be 2.3eV. The Richardson work function of the cathode, as obtained from emission measurements to each of the two anodes in turn, gave constant

results. Saturation of emission was observed at high temperatures, of the type already described.

The value obtained during the last set of determinations was 1.6eV, and the corresponding value of the intercept was 0.01.

Attempts were made to obtain values of the apparent contact potential difference with the tungsten anode heated to a temperature of about 1200°K and a cathode temperature of 719°K. Under these conditions it was hoped that the effect of the adsorbed layers on the tungsten surface would be reduced. The values of contact potential difference were found to be between 6.7eV and 4.2eV, with an average value of 5.8eV. The variation in the values indicated that the effects of an adsorbed layer on the tungsten surface were very marked, even at this comparatively high temperature. The tungsten anode was also heated to much higher temperatures (about 2500°K) but the electron emission from the tungsten prevented satisfactory measurements of the contact potential difference. The space charge effect was very pronounced when the tungsten anode was employed and this can be attributed to the bad geometry of this type of experimental arrangement.

The results obtained from this experimental tube indicated that adsorbed layers have a considerable effect on the work function of the surfaces within the experimental tube. The effects were very marked in the case of the tungsten anode, but it is likely that adsorbed layers

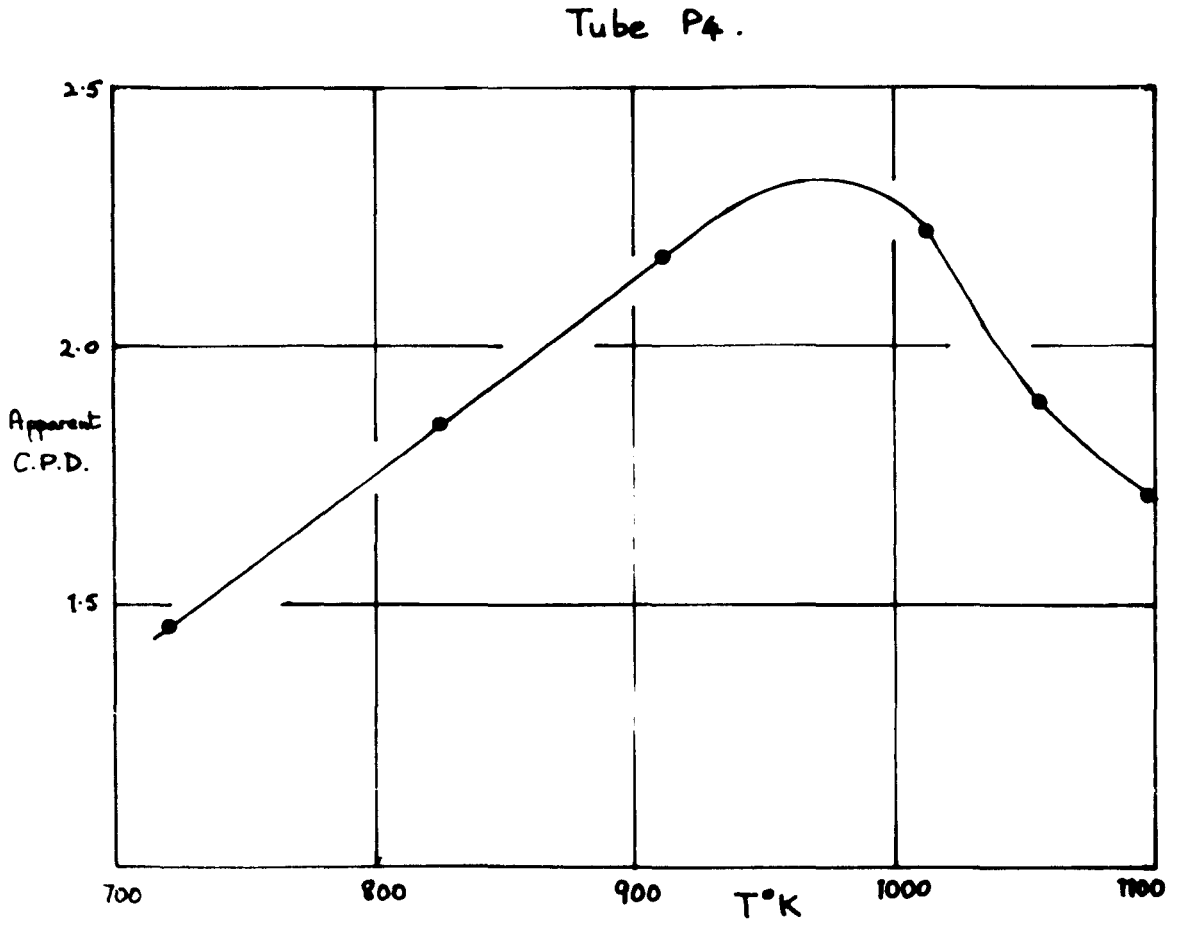

FIG. 6.10.1.

present on the surfaces of the crystals which constitute the oxide cathode, will produce a significant change in work function. It was plain that this method of obtaining information as to the apparent contact potential difference existing between anode and cathode, and of the work function of the cathode, was of little value. For this reason no more tubes of this type were built.

10. Tube P4.

The fourth probe tube built was constructed to the same specification as the previous three probe tubes. The cathode was processed in exactly the same manner as tube P3. The emission current was measured for various values of applied anode voltage, at a number of different temperatures. The Richardson work function had a value of 1.2eV, while the intercept had a value of 3.36. Marked saturation of emission was noted at high temperatures. The value of the anode work function, determined for values of the emission current under retarding field conditions, was 1.9eV. A graph of the apparent contact potential differences obtained are shown in fig. 6.10.1. Failure of the tube prohibited further measurements.

11. Tube MM$_1$.

This tube was built so that more information as to the anode work function could be obtained. The cathode was identical to those used in the retarding potential tubes, while the anode was identical to the cathode except that no sprayed coating of barium was applied. A photograph

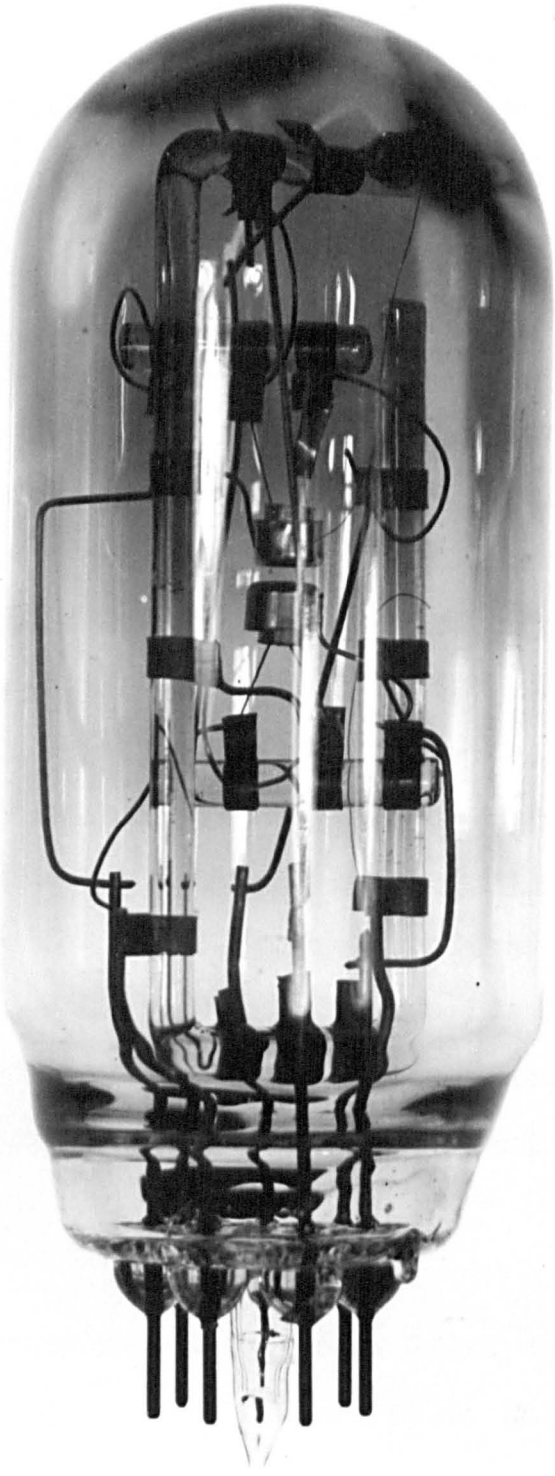

Tube HNN1

FIG. 6.11.1.

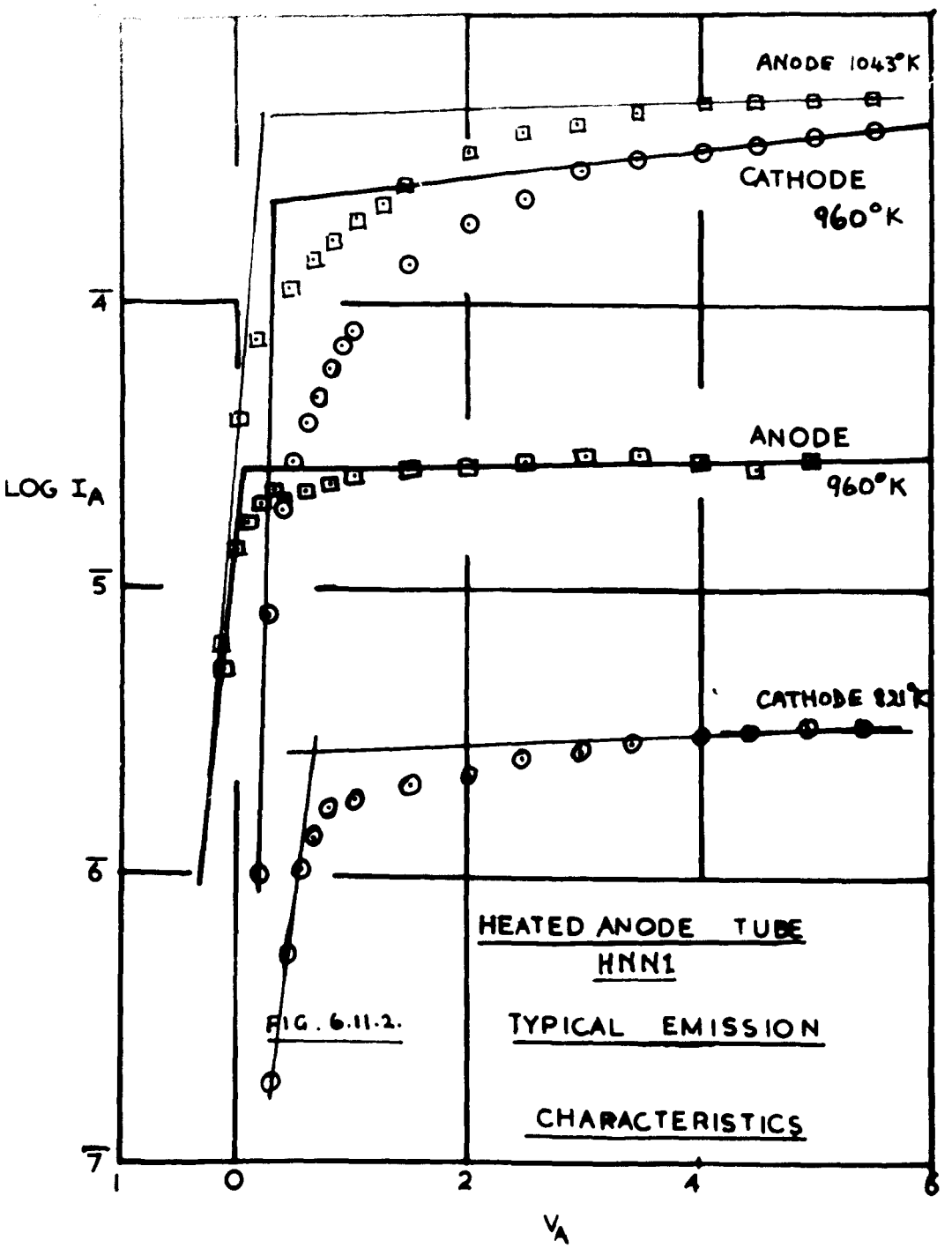

HEATED ANODE TUBE
HNN1

TYPICAL EMISSION

CHARACTERISTICS

FIG. 6.11.2.

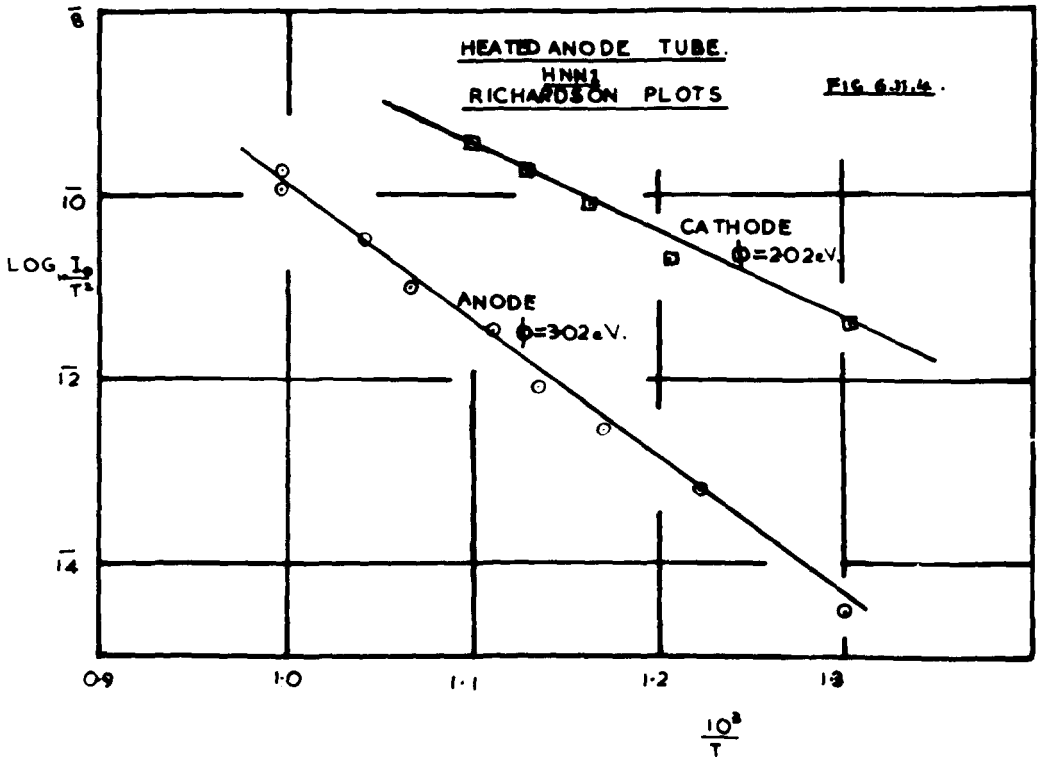
HEATED ANODE TUBE.
HNN1
RICHARDSON PLOTS
FIG. 6.11.4.
CATHODE
ϕ=2·02eV.
ANODE
ϕ=3·02eV.
LOG I/T²
0·9
1·0
1·1
1·2
1·3
10³/T

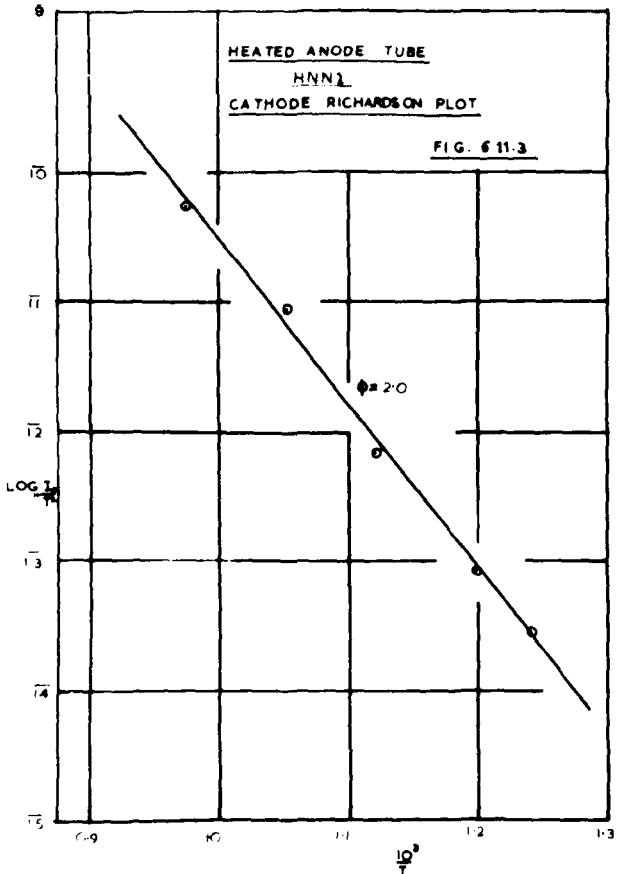
HEATED ANODE TUBE
HNN1
CATHODE RICHARDSON PLOT
FIG. 6 11.3
ϕ= 2·0
LOG I/T²
0·9
1·0
1·1
1·2
1·3
10³/T

of the tube is given in fig. 6.11.1. Processing and breakdown were accomplished by using the same method as for tube P3. Activation was achieved by drawing emission with an applied anode voltage of 4 volts and activation was discontinued when the anode current had attained a value of 0.46mA at 1150°K. Emission measurements were then carried out, firstly using the oxide coated electrode, and secondly the nickel electrode, as the source of electrons. Typical emission characteristics are shown in fig. 6.11.2. The curvature of the emission characteristics, due to space charge effect, was slightly more marked when the emission was drawn from the oxide. This effect could possibly be attributed to a space charge existing in the pores of the oxide. Fig. 6.11.2. indicates that the characteristic of the nickel electrode at 1045°K exhibits curvature over a smaller voltage range than that of the oxide coated electrode at a temperature of 960°K. This would not be expected if the space charge only existed between the electrode surfaces.

The first value of the Richardson work function obtained for the oxide was 2.0eV, while the intercept had a value of 7.86 (fig. 6.11.3.). The values of the apparent contact potential differences did not vary markedly with temperature and had an average value of 0.2eV. The corresponding value of the Richardson work function for the nickel electrode was 4.0eV with an intercept value of 8.98. The apparent contact potential difference was relatively constant with temperature and had a value of 1.2eV. Thus, the values of apparent contact

potential difference were not consistent with the values of Richardson work function. This could be partially explained if it was considered that heating the nickel electrode caused the film of barium, or barium oxide, which is probably evaporated onto it during processing, to be evaporated off the surface. The effect of the voltage drop across the coating and the discrepancy to be expected between the contact potential difference and the Richardson work functions must also be considered.

A further determination of the work function of the oxide by the Richardson method, after activation by drawing emission, indicated that both the electrodes had a work function of 3eV. In this case, the apparent contact potential difference during both determinations was approximately zero and practically independent of temperature. The values of the intercepts of the Richardson plots were 0.8 in the case of the oxide and 1.55 for the nickel.

The third determination of the Richardson work function is shown in fig. 6.11.4. The value for the oxide was 2.02eV with an intercept value of 1.6. The nickel had a work function of 3.02eV and intercept value of 5.1. The mean values of the apparent contact potential differences were -0.2eV for the nickel and 0.5eV for the oxide.

Further determinations were attempted with the automatic equipment described in Chapter 5, but the results,

Tube PAuNA1. Diagramatic.

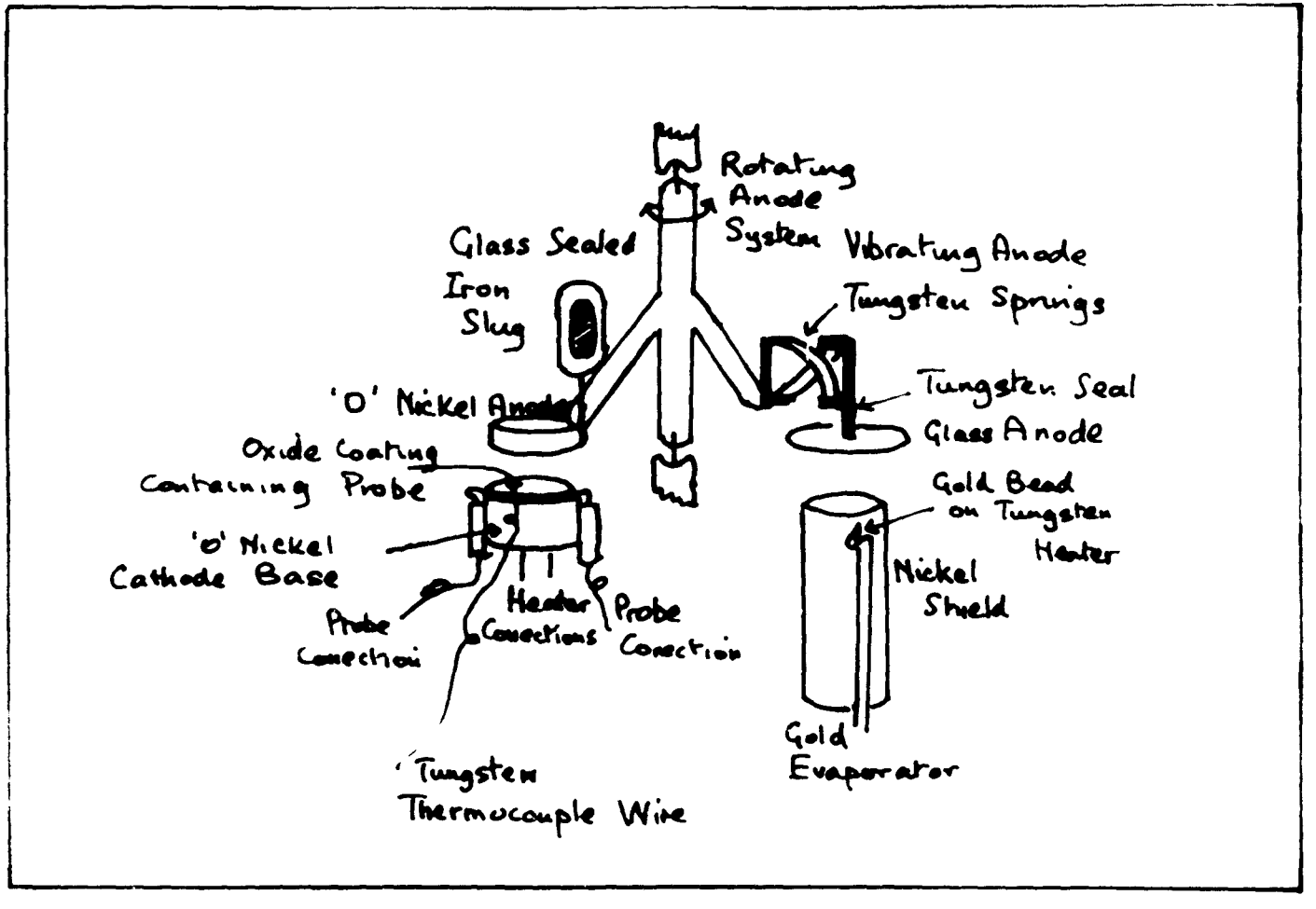

FIG 6.12.1.

which could only be obtained for a limited temperature range, are of little value and will not be quoted here. Further work on this experimental tube was discontinued and another special type of tube was built.

12. Tube PAuNAl

This tube consisted of a button cathode with an embedded probe and two anodes. The first of the two anodes was nickel and the second was a glass electrode onto which a film of gold was to be deposited, by the evaporation of a gold bead fused onto a tungsten heater wire. Both the anodes could be rotated into the correct positions for measurements by means of a iron slug sealed in glass. An Alpert gauge was attached to the envelope of the experimental tube by means of a side arm. The arrangement of the electrodes is shown in the diagram (fig. 6.12.1). It was hoped that the vibrating gold electrode would provide measurements of the contact potential difference by the Kelvin method (see ref 101). But flaking of the cathode and a fracture of the gold evaporator filament prevented any interesting results from being obtained. Preliminary ~~results of~~ results conductivity at a temperature of 890°K indicated an apparent conductivity of 4.5×10^{-8} mhos. Pressure measurements, by the use of the attached Alpert gauge, indicated that the pressure attained by the vacuum system was of the order of 1.0×10^{-6} mm.Hg., which was in agreement with the pressure indicated by the Penning gauge. It was clear that the Alpert gauge was a far more sensitive

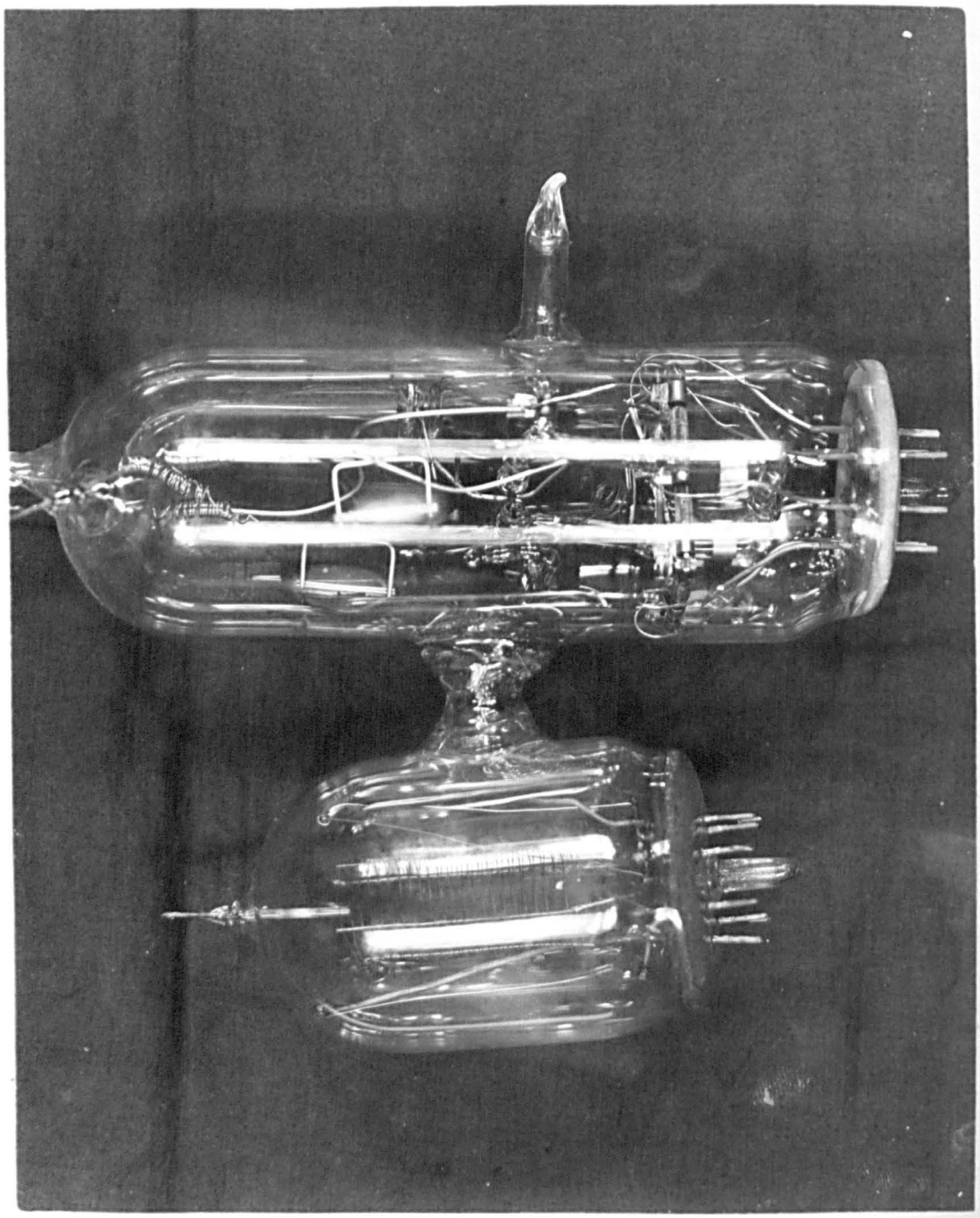

Tube DAuNA1.

FIG. 6.13.1.

pressure gauge than the Penning gauge and so this type of gauge was built into all subsequent experimental tubes. It was decided that a great deal of development work was necessary before satisfactory tubes of this type could be used successfully and hence, further work with this type of tube was suspended and more conventional tubes were built during the closing stages of the research programme. The main reason for attempting to use a gold anode was that this metal is very inactive and therefore provides a surface which, unless contaminated by the deposition of evaporated films, can be assumed to have a constant work function. Two further attempts were made to use a gold anode, and these are described in the next sections.

13. Tube DAuNA1

A photograph of this tube is given in fig. 6.13.1. The cathode consisted of two box electrodes, both of which were fitted with thermocouples. The carbonate suspension was applied by spraying, so that a layer of the carbonate was present between two faces of the box electrodes to form a 'sandwich.' A further layer of the carbonate was sprayed on the top surfaces of the two electrodes so that emission measurements could be made. Two anodes were incorporated. The first anode was of nickel and could be introduced between the cathode and the second anode. The second anode was of gold wire coiled in the form of a flat spiral. It was hoped that emission measurements to the gold spiral would enable the work functions of the nickel anode and the cathode

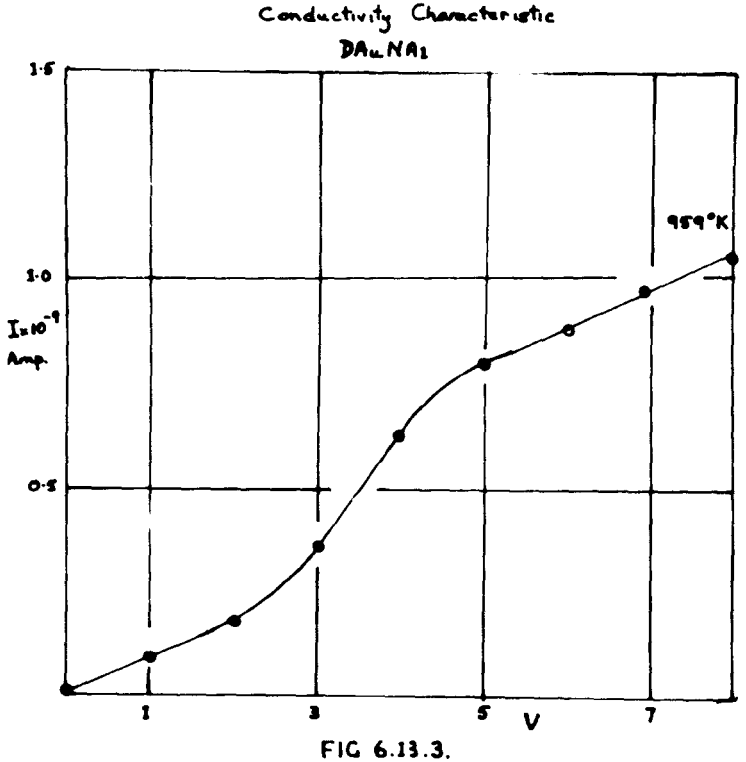

FIG 6.13.3.

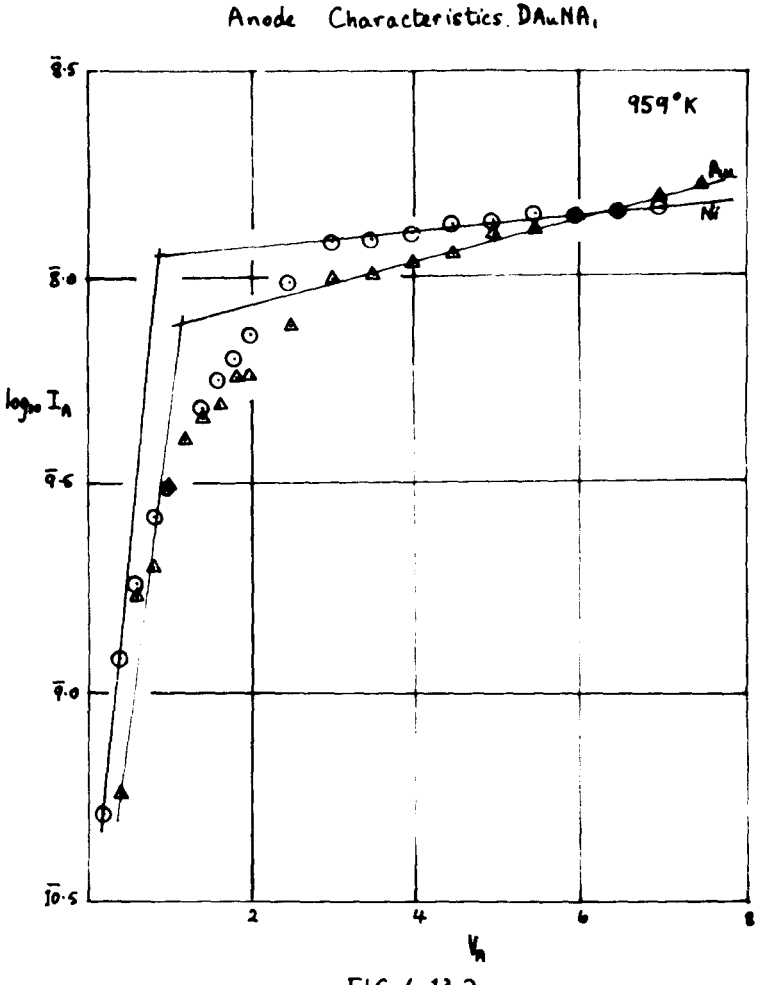

FIG 6.13.2

to be determined by the contact potential difference method. The cathode was broken down over a period of seven hours by means of the motor driven Variac. The usual baking and eddy current heating treatments were carried out and the Alpert gauge was rigorously out-gassed. The pressure in the experimental tube, before it was sealed off, was measured by the Alpert gauge and was found to be of the order of 10^{-6}mm.Hg. One getter was fired before the tube was sealed off and the second was fired after the tube was sealed from the vacuum system. The pressure in the experimental tube after sealing off was measured by the Alpert gauge as being 2.7×10^{-5}mm.Hg.

After activation by drawing emission, measurements of the conductivity of the cathode were attempted. The heater currents through both box electrodes were adjusted so that both were at the same temperature. The two box electrodes were connected together externally when emission measurements were made.

Typical anode characteristics are shown in fig. 6.13.2. A marked space charge effect was noted, particularly in the case of the gold spiral anode. This can be attributed to the large spacing of the electrodes and the fact that the gold anode was in the form of a spiral of wire. Conductivity measurements, also at a temperature of 959°K, showed marked curvature (fig. 6.13.3), and the mean value of conductance, as calculated from the slope of the characteristics, was 1.5×10^{-10} mhos. Further determinations of the emission

current were carried out, but the results obtained also showed very marked space charge effects. For this reason, the results were of little value and will not be quoted here. The determinations of the cathode conductivity necessitated the application of quite large potentials between the two box electrodes, while in addition, the cathode material between the electrodes was not the source of the emission current. Hence, it is unlikely that the conductivity results are representative of a normal oxide cathode. It was decided that conductivity measurements obtained by means of a probe embedded in a cylindrical cathode, provided the most reliable results and the last of the two experimental tubes built during the present investigation were built to the same specifications as the earlier probe tubes. The only conclusion, of any value, which could be drawn from this experimental tube was that the work function of the nickel anode was lower that the accepted value of 4.96eV (the average for the first set of determinations was 4.64eV). This, as suggested previously, was thought to be partially due to a film of barium and barium oxide evaporated from the cathode.

14. Tube PA1

The tube consisted of a normal probe tube attached to an Alpert gauge by means of a side-arm. A photograph of this type of system will be given in section 15. The tube and Alpert gauge were not sealed directly onto the vacuum system, but a manifold of the type illustrated in

fig. 5.4.1., was used. A gold spiral anode was also built into the tube, but was not used because it became contaminated. No side arm, containing barium getters, was used in the case of this tube. Breakdown and processing were carried out in the usual manner, the glass was baked by means of the oven and the metal parts were heated by eddy currents. The metal parts of the Alpert gauge were outgassed by flashing, electron bombardment, and eddy current heating. The pressure was then found to be 2.5×10^{-5} mm.Hg. Measurements of the emission current were carried out on the system after the breakdown process was complete. The pressure indicated by the Alpert gauge was 2.7×10^{-3} mm.Hg. The high pressure was attributed to the presence of carbon dioxide in the system. No activation of the cathode was attempted at this stage because the thermal activation which occured during the breakdown process enabled measurements of the emission to be made. Several emission characteristics were made at constant temperature, with the Alpert gauge switched on and acting as a pump. A marked increase in the emission current was noted, which could be explained in two ways. Firstly, it could have been due to activation caused by the passage of emission current and secondly, the pumping action of the Alpert gauge, which reduced the pressure in the experimental tube, could have partially removed the adsorbed layers of an electronegative substance on the cathode to give an increase in work function. The cathode temperature was then reduced by means of a

motor-driven Variac. The liquid nitrogen trap was then out-gassed and further emission measurements were taken, when a work function of 3.36 eV was obtained together with an intercept value of 3.92. The pressure during these determinations was 6.4×10^{-5}mm.Hg. The experimental tube was then isolated from the vacuum system by sealing a constriction with a hand torch. Emission and conductivity measurements were then attempted, after activation by drawing emission, when a work function of 2.11eV was obtained, together with an intercept value of 2.67. The logarithm of the conductivity plotted against $10^3/T$ showed a marked scatter of the points and a satisfactory straight line could not be drawn. The apparent contact potential difference decreased with increasing temperature from a value of 3.67 eV at 860°K, to 2.83 eV at 1034°K. A measurement of the pressure in the experimental tube indicated a marked increase in pressure to 8.6×10^{-3}mm.Hg, though the pressure was relatively constant during the determinations described above. The high value of the apparent contact potential difference is indicative of an adsorbed layer of an electronegative substance on the anode, which is to be expected from the high pressure present in the experimental tube. This high pressure was attributed to the porosity of a tungsten seal present in the experimental tube. The pressure gradually increased to 1.2×10^{-2}mm.Hg., but the emission current from the cathode was still quite large (1.3×10^{-4}amps at 920°K and an applied anode voltage of 7.3 volts). Further measurements of the conductivity of

the cathode gave a value almost independent of temperature and it was assumed that the probe wire was making contact with the base metal. The value of the Richardson work function, under these conditions, was 2.1 eV, while the intercept value was $\bar{2}.33$. Values of the apparent contact potential difference were approximately constant and had a mean value of 2.64 eV, which again indicated that an adsorbed layer of an electronegative substance was present on the anode. A further determination of the anode characteristic was attempted after operating the Alpert pump for about 10 days. The pressure in the experimental tube was reduced to 7×10^{-3} mm.Hg, but exposure of the cathode to the high pressure of the gas in the experimental tube seemed to have produced deactivation of the cathode, for the Richardson work function after this treatment was found to have a value of 2.6 eV and the intercept value was 3.22. Values of the apparent contact potential difference were still high and had an average value of 2.8 eV. One further determination of the emission characteristics was carried out after activation at a pressure of 4.2×10^{-3} mm.Hg. The Richardson work function had a value of 2.3eV, while the value of the intercept was 0.82.

The values of the Richardson work function and the intercept values are tabulated below:-

	Activation State				
	I	II	III	IV	V
ϕ eV.	3.36	2.11	2.1	2.6	2.3
$\text{Log}_{10}A$	3.92	$\bar{2}.67$	$\bar{2}.33$	3.22	0.82

Tube PA2

FIG. 6.15.1.

No linear $\log_{10} A/\emptyset$ relationship was observed.

It would appear that large values of the intercept were produced by the pressure of gas in the experimental tube. In addition, activation of the tube under these conditions failed to produce a work function of less than 2.1eV. It was decided that another probe tube of similar design should be built so that the effects of gas present in the experimental tube could be studied further.

15. Tube PA2.

This probe diode was built to the same specification as the previous tube PA1, but no gold spiral anode was provided. The tube, together with an Alpert gauge attached by a side arm, was built into the manifold illustrated diagramatically in fig. 6.15.1. The breakdown and processing were carried out in the same manner as for tube PA1. After baking and eddy current heating, the tube and Alpert gauge were isolated from the vacuum system by sealing a constriction. Three getters in the side tube were then fired and the tube cooled with liquid nitrogen. One hour after sealing-off, the pressure, as indicated by the Alpert gauge, was 4×10^{-5}mm. Hg. The experimental tube was then shielded and measurements of probe current and emission current were attempted. These currents were quite appreciable and indicated that thermal activation had occurred. The emission current at this stage was 0.65mA for an applied anode voltage of 6 volts. The pressure in the experimental tube was 3.5×10^{-5}mm.Hg. The liquid nitrogen was then removed from the getter side arm, in order to see what the pressure increase would be, when

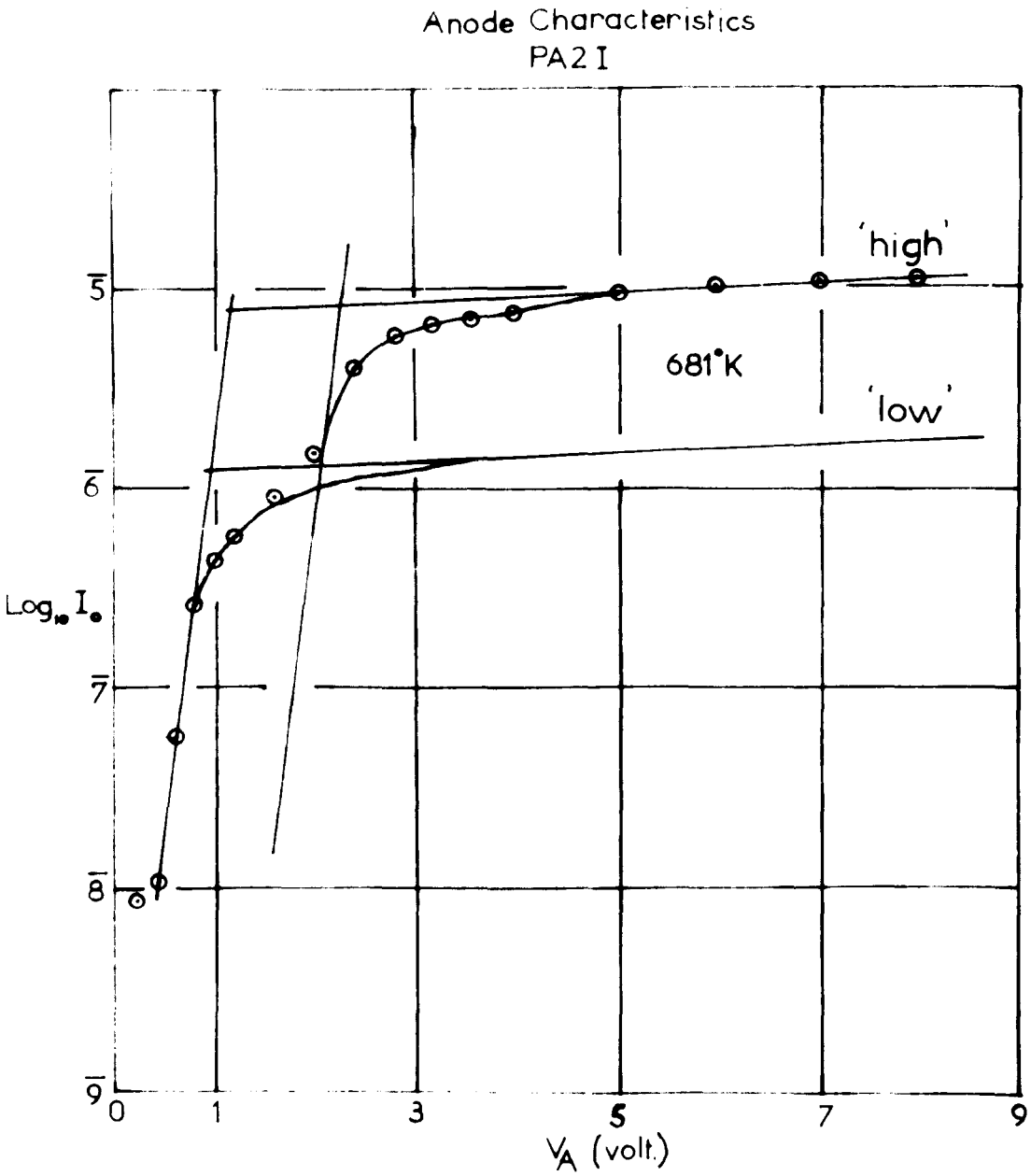
Anode Characteristics
PA2 I
'high'
681°K
'low'
$\bar{5}$
$\bar{6}$
$\bar{7}$
$\bar{8}$
$\bar{9}$
$\text{Log}_{10} I_a$
0
1
3
5
7
9
V_A (volt.)

FIG. 6.15.2.

Richardson Plots

PA2I.

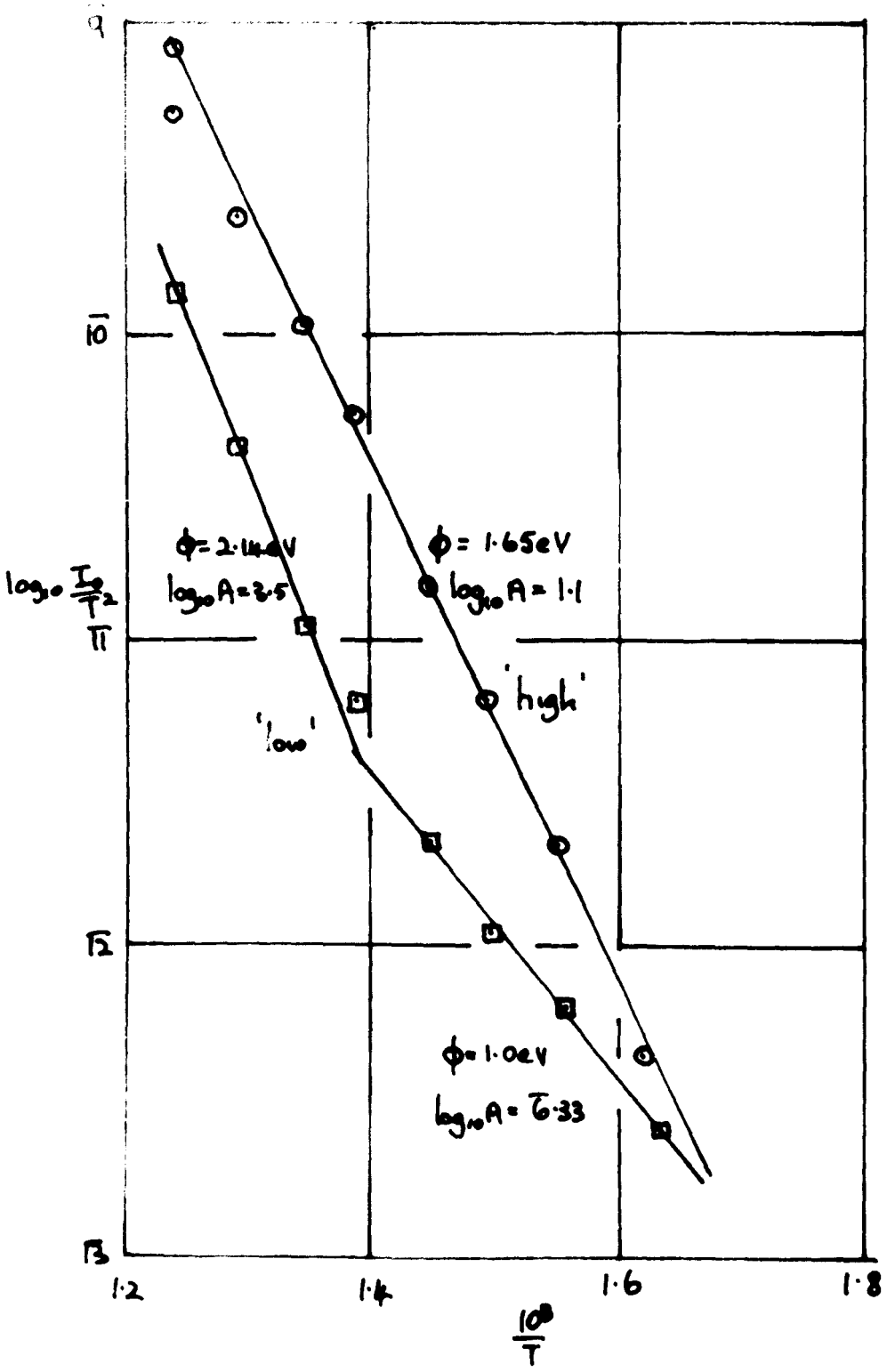

FIG. 6.15.3.

PA2I.

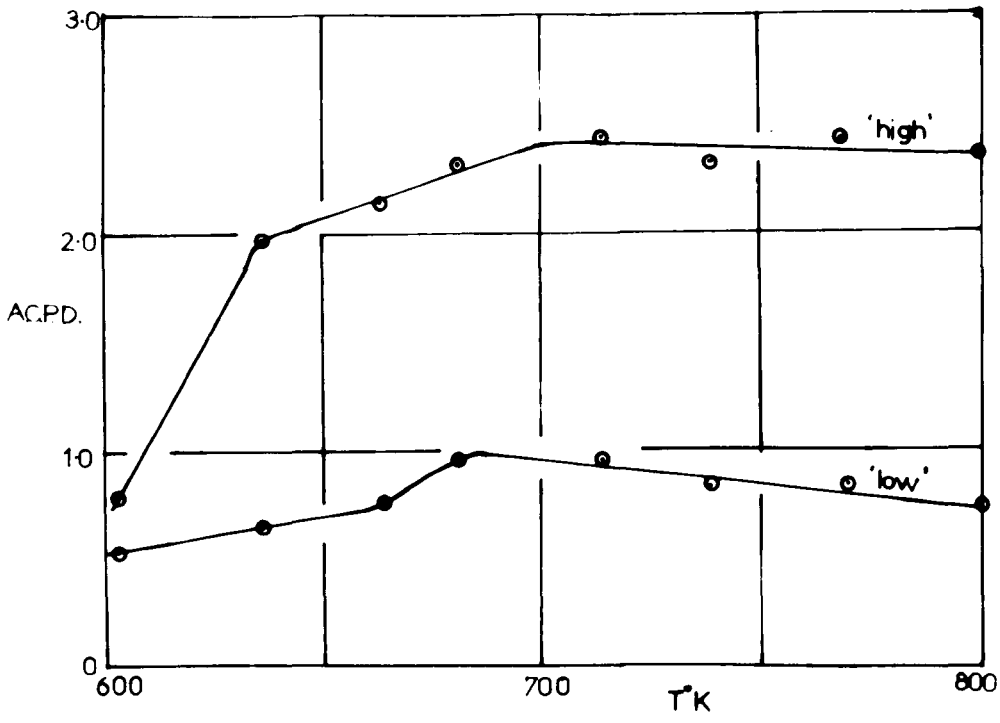

FIG. 6.15.4.

Conductivity Plot PA2I.

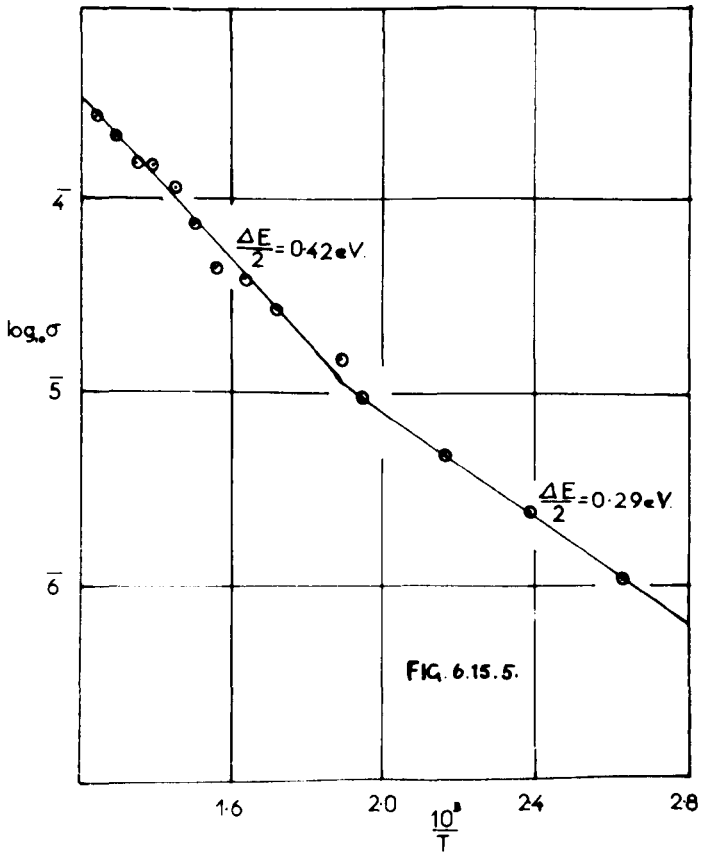

FIG. 6.15.5.

the pressure in the system rose to 3.96×10^{-4}mm.Hg. Emission and conductivity measurements were then made without cooling the side arm with liquid nitrogen. The anode characteristics appeared to exhibit a marked space charge effect, but it was later realized that the marked curvature at the 'knee' of the characteristic was probably due to a change in cathode work function and apparent contact potential difference as emission current was drawn. This was attributed to an anode poisoning effect. An example of this type of anode characteristics, obtained with this tube during all the earlier determinations, is given in fig. 6.15.2. ~~were all of this type.~~ Two Richardson plots were drawn for the two values of I_o obtained from the characteristics and these are shown in fig. 6.15.3. It would appear that the emission current removed an electronegative substance adsorbed on the anode. At high temperatures, adsorption of this substance onto the cathode gave an increase in work function, but it appears that the cathode work function is reduced at low temperatures. The corresponding conductivity curve is given in fig. 6.15.5. Conductivity measurements were obtainable at lower temperatures than emission measurements and it will be noted that two regions were obtained, the first giving a value of activation energy ($\Delta E/2$) of 0.42eV and the second, an activation energy of 0.29eV. This second slope corresponds to conductivity results obtained without emission being taken from the cathode. It would seem from these two values that the act of drawing emission modified the position of the energy levels. The results could also be

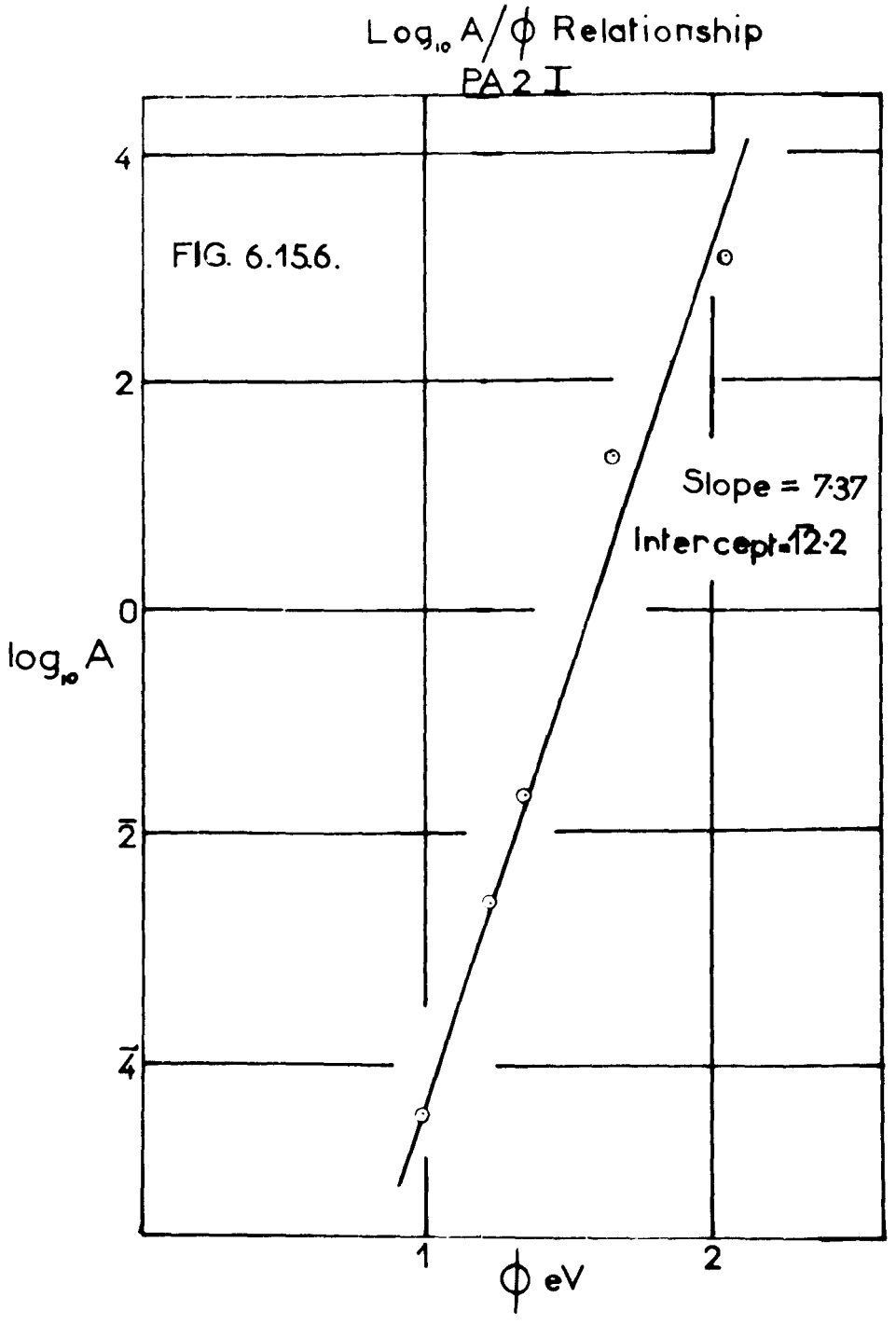
Log10 A/φ Relationship
PA2 I
FIG. 6.15.6.
Slope = 7·37
Intercept = 12·2
log10 A
4
2
0
2̄
4̄
1
2
φ eV

explained in terms of a different mechanism of conductivity at the lower temperatures. The activation of the higher temperature slope should correspond to the Richardson plot marked 'high', because the emission had time to recover from short term poisoning effects before the conductivity measurements were made. Thus the surface work function for this activation state had a value of 1.23eV. The average values of the apparent anode work function were therefore 4.0eV with the adsorbed layer and 2.25eV with the adsorbed layer partly removed.

When tangents were drawn to the smooth curves drawn through the points on the Richardson plot, a linear $\log_{10}A/\phi$ relationship was obtained, fig. 6.15.6. It will be noted that this conforms with the hypothesis outlined in Chapter 4 because all these tangents can be regarded, to a first approximation, as passing through a common point. The slope of the $\log_{10}A/\phi$ plot indicates that the numerical value of $10^3/T$ for the intersection of the tangents is approximately 1.4, while the value of $\log_{10}I_o/T^2$ is approximately $\overline{12}.2$.

A second determination (II) was made after four getters were fired in the side arm in an attempt to reduce the pressure in the experimental tube. It was found that, instead of a decrease in pressure, the pressure increased from 6.6×10^{-4} mm.Hg., to 2.4×10^{-3} mm.Hg and it was assumed that this increase in pressure was produced by the getters outgassing. A Dewar of liquid nitrogen was applied to the getter arm and the average pressure during the determination

Richardson Plots

PA 2 II

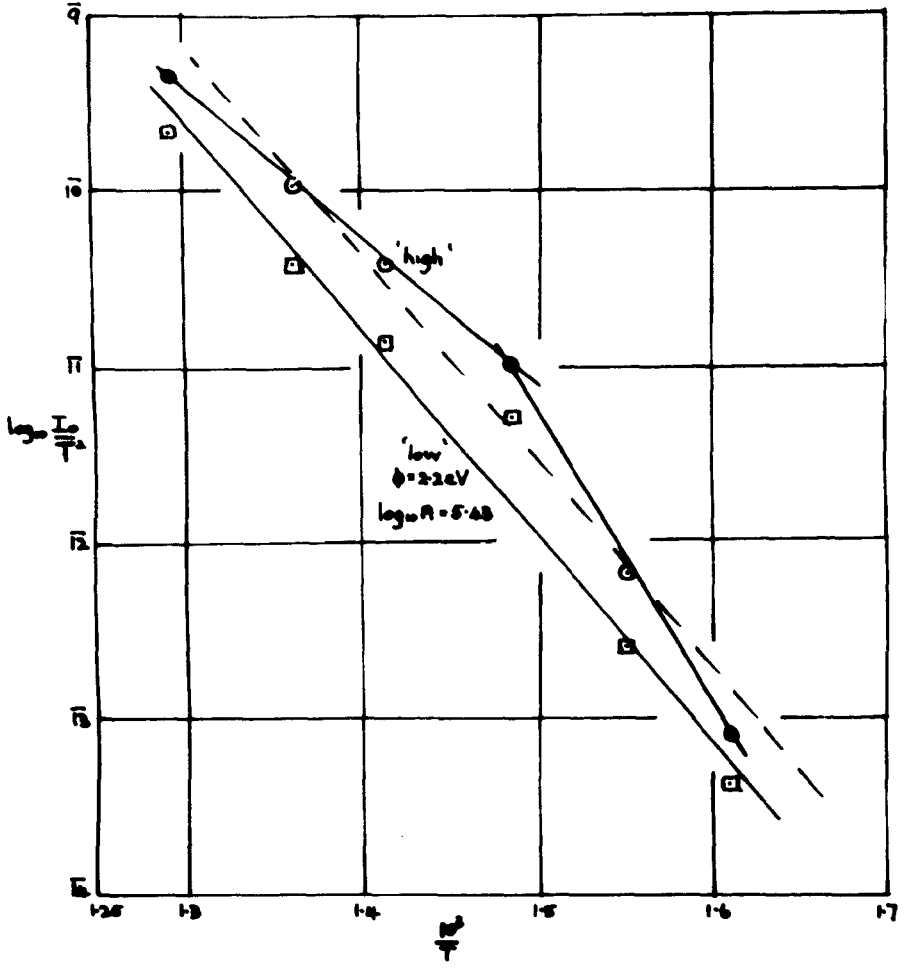

FIG. 6.15.7.

Conductivity Plot

PA 2 II

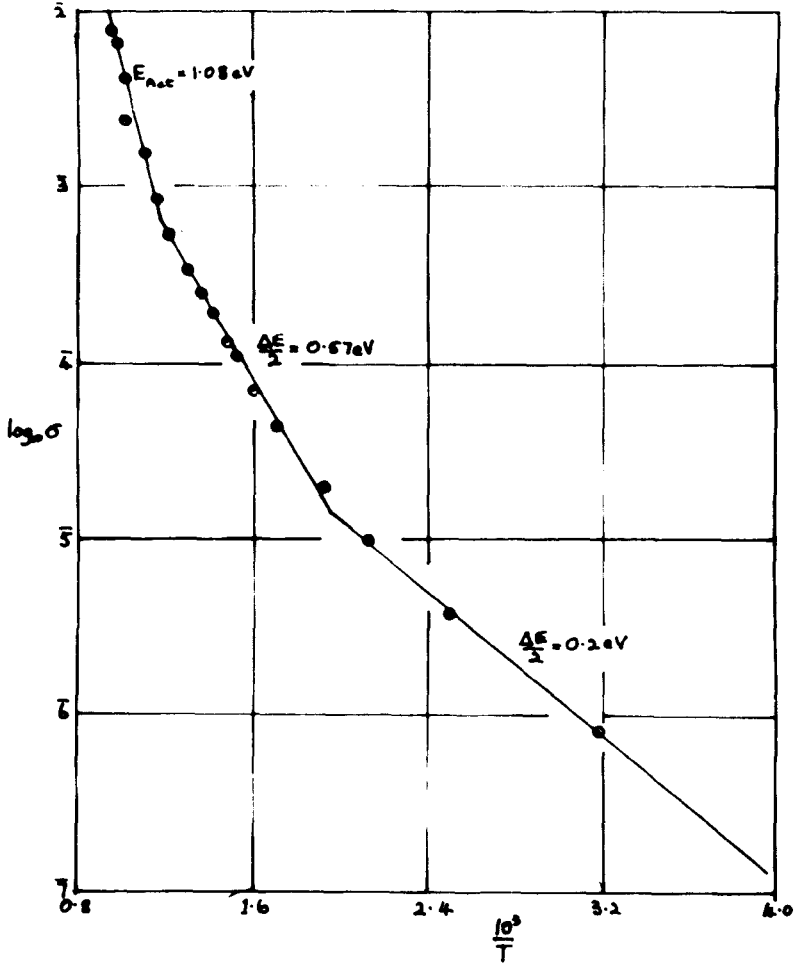

FIG 6.15.8.

Seebeck e.m.f. PA2II

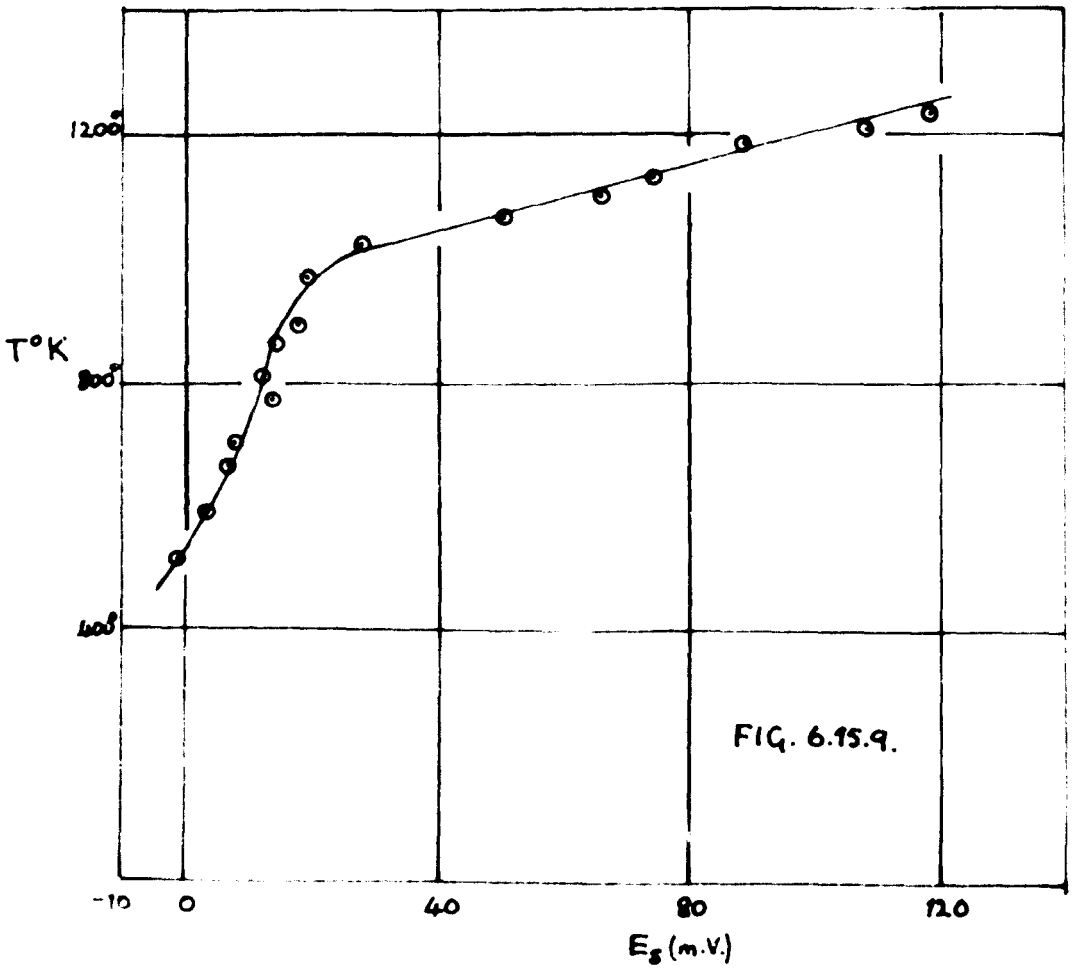

FIG. 6.15.9.

was 3.1×10^{-3}mm. Hg. The form of the emission characteristic was as before. Two Richardson plots were obtained (fig. 6.15.7.) Curvature of the 'high' plot was obtained and the average value of the work function was recorded as being 2.2eV. The conductivity plot obtained is shown in fig. 6.15.8. In this case the uncorrected activation energy from the high temperature slope was 1.08eV. Two low temperature slopes were again noted, a reduction in value was observed when emission measurements were terminated, in exactly the same manner as for PA2.

The value of the surface work function was calculated as being 1.45eV. The values of the Seebeck e.m.fs. as given by the conductivity determinations are shown in fig. 6.15.9. It will be noted that a change in sign occurs at low temperatures, which would indicate an n to p transition as the temperature was reduced. This effect was also observed for other determinations made with this tube. A marked change in the slope of this curve was noted in the high temperature range.

After a period of a few days, the pressure in the experimental tube was reduced by cooling the getters with liquid nitrogen and running the Alpert gauge. A pressure of 4×10^{-5}mm.Hg was indicated by the Alpert gauge. The two values of the Richardson work function were determined as before. The 'high' value of the Richardson work function was 2.8eV with an intercept of 6.4, while the 'low' value of Richardson work function was also 2.8eV, but the intercept had a value of 5.9. The internal work

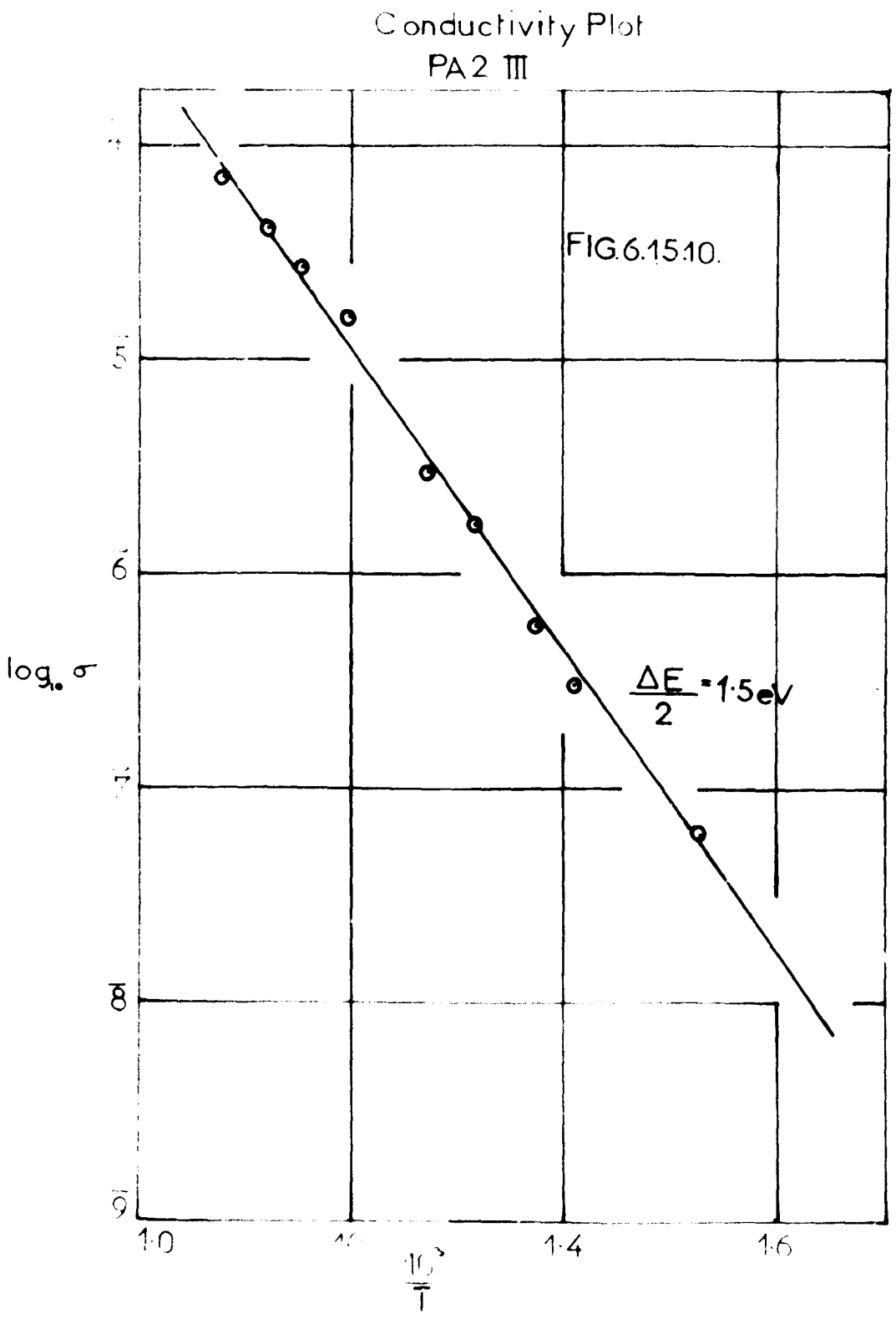
Conductivity Plot
PA2 III
FIG.6.15.10.
$\log_{10}\sigma$
$\frac{\Delta E}{2}$ = 1·5eV
1·0
1·4
1·6
$\frac{10^3}{T}$

function, $\Delta E/2$, was found to have the rather high value of 1.5eV (fig. 6.15.10), from which the surface work function was calculated as being 1.3eV. It was likely that exposure of the cathode to the gases at the higher pressures ($\sim 10^{-3}$ mm.Hg.) had caused an increase in the internal work function without a marked change in the surface work function. It is to be expected that any change in the surface work function would occur rapidly. The values of apparent contact potential difference were fairly independent of temperature and indicated little change in the apparent anode work function from the last determination. Values of conductivity were not determined at temperatures lower than those at which emission measurements were made because the high value of $\Delta E/2$ made the determination of the conductivity difficult.

The next determination was made without liquid nitrogen applied to the getter tube, when the Alpert gauge indicated a pressure of 3.5×10^{-4} mm.Hg. The form of the anode characteristics was as before. The 'high' value of the Richardson work function was 3.6eV with an intercept value of 9.11, while the 'low' values were 3.2eV and 5.3 respectively. The value of $\Delta E/2$ was 1.7eV, which gave the value of χ as 1.8 eV. The values of the apparent contact potential difference were of the same order as those of the previous determination.

It was decided that the tube should be reattached to the vacuum system and consequently a pigstail was broken

by means of a magnet, with both pumps working. The heater of the diffusion pump burnt out over night so that the pressure in the experimental tube was found to have the high value of 4.8×10^{-3} mm.Hg. On cooling, the cathode was found to have a green colouration. The diffusion pump was repaired, then the cathode temperature was increased and emission and conductivity measurements were commenced. Curvature of the anode characteristics at the 'knee' was very much less noticeable than that observed for the previous determinations and it was thought that the poisoning effects, thought to be responsible for the curvature, had been greatly reduced by continuously pumping the experimental tube. Only one Richardson plot could be drawn for this determination. The value of the Richardson work function was 3.3eV and the intercept had a value of 4.0. The emission measurements were carried out at high temperatures, but the current density was so small that the slope of the conductivity plot corresponded to the low temperature conductivity mechanism (2.0eV). The average of the values of the apparent contact potential difference was 1.2eV.

The average pressure during the next determination was approximately 2×10^{-5} mm.Hg. In this case also, the curvature of the anode characteristics was much reduced, indicating the absence of poisoning effects. The Richardson work function had the high value of 4.0eV and the intercept value was 9.73. The low temperature slope of the conductivity plot gave a value for E/2 of 1.5 eV.

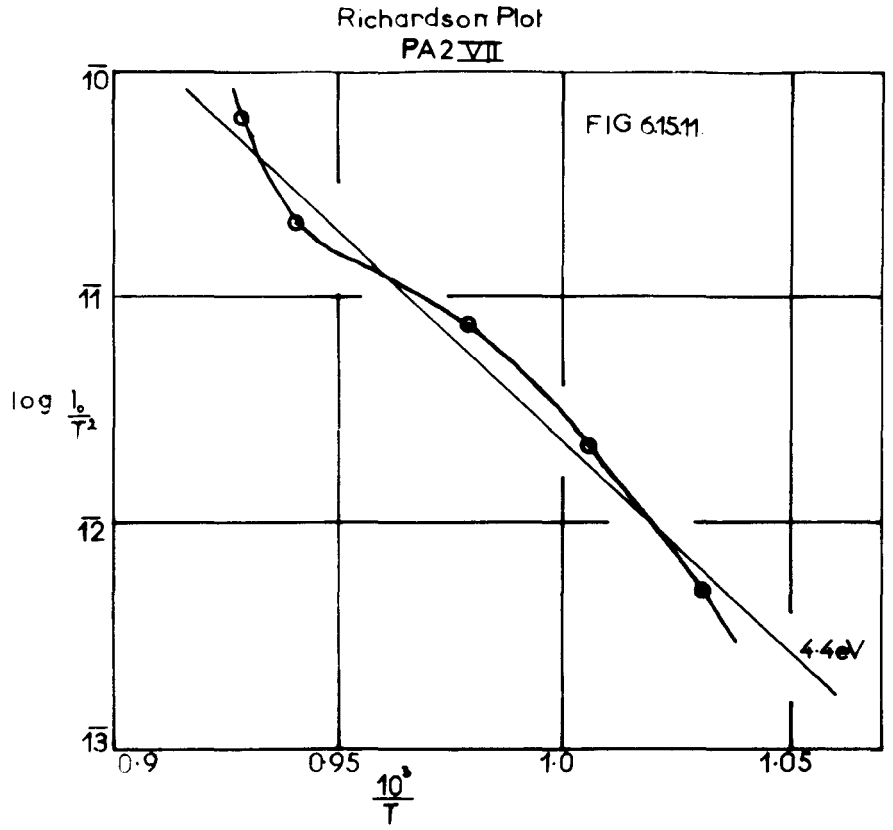
Richardson Plot
PA 2 VII
FIG 6.15.11
$\bar{10}$
$\bar{11}$
$\bar{12}$
$\bar{13}$
log $\frac{I_0}{T^2}$
4·4eV
0·9
0·95
1·0
1·05
$\frac{10^3}{T}$

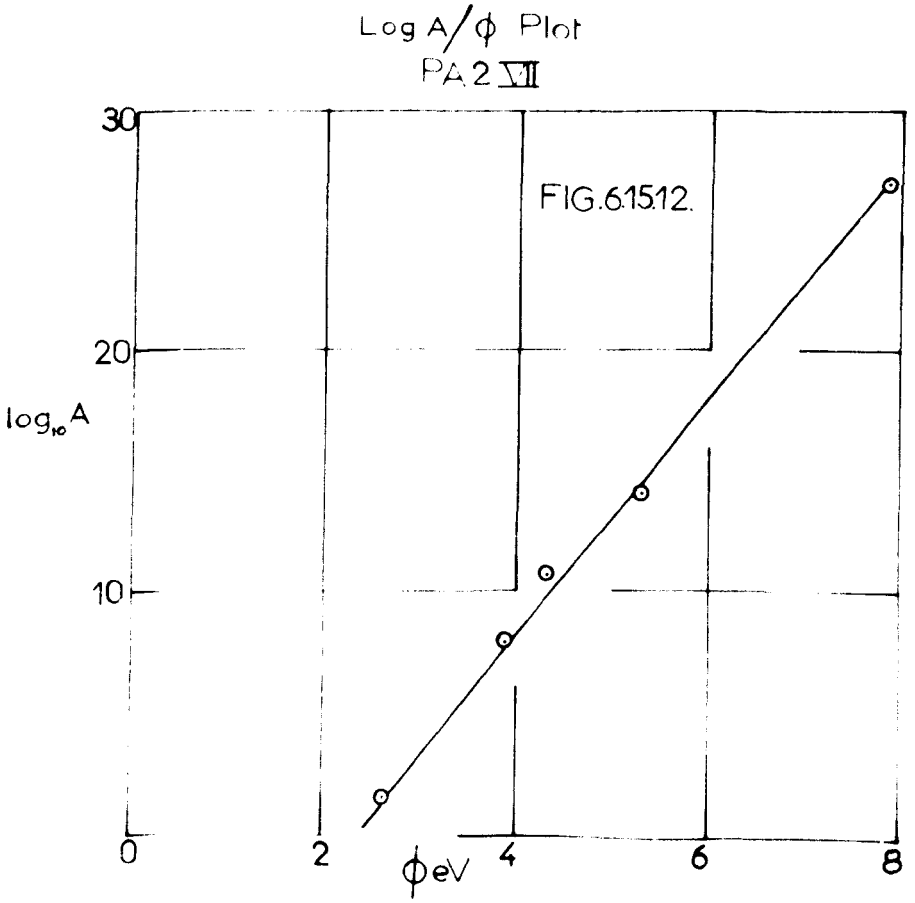
Log A/ϕ Plot
PA 2 VII
FIG.6.15.12.
30
20
10
0
$\log_{10} A$
2
4
6
8
ϕ eV

A change in the sign of the Seebeck e.m.f. was also observed, indicating an n to p transition. The apparent contact potential difference was relatively independent of temperature and had an average value of 2.08eV.

The penultimate set of results obtained with this tube also did not exhibit marked curvature of the anode characteristics. The average pressure was 2×10^{-5}mm.Hg. Both the Richardson plot (fig. 6.15.11) and the conductivity plot showed marked curvature. The best straight line gave a Richardson work function of 4.4eV. The slope and corresponding intercept values of tangents drawn to this curve gave a linear $\text{Log}_{10}A/\phi$ relationship, (fig. 6.15.12) in conformity with the explanation given in Chapter 4. The average value of $\Delta E/2$, though not very reliable, was approximately 2.0eV.

The final values obtained from the tube, at an average pressure of 2×10^{-5}mm.Hg were:-

ϕeV = 4.4; $\log_{10}A$ = 8.9; $\Delta E/2$ = 2.0eV; χ = 2.4eV; Average contact potential difference = 1.29eV. These high values of cathode work function can be attributed to the removal of donor levels as the gas in the experimental tube diffused into the body of the cathode. The values of the surface work function were also fairly high and can be attributed to an adsorbed layer of an electronegative substance on the cathode surface. The getters used in this experimental tube appeared to provide little reduction in the pressure within the experimental

tube and instead out-gassing produced a marked increase in pressure.

The results obtained from the experimental tube are summarised as follows:-

Activation State

	I	II	III	IV
	'High'	'High'	'High'	'High'
ϕ eV.	1.65	2.2	2.8	3.6
$\log_{10} A$	1.1	-	6.4	9.11
$\frac{\Delta E}{2}$ eV	0.42	0.57	1.5	1.7
χ eV.	1.23	1.45	1.3	1.8
P mm. Hg.	3.96×10^{-4}	3.1×10^{-3}	4.0×10^{-5}	3.5×10^{-3}

	V	VI	VII	VIII
ϕ eV.	3.3	4.0	4.4	4.4
$\log_{10} A$	4.0	9.73	-	8.9
$\frac{\Delta E}{2}$ eV	2.0	1.5	2.0	2.0
χ eV.	1.3	2.5	2.4	2.4
P mm. Hg.	2×10^{-5}	2×10^{-5}	2×10^{-5}	2×10^{-5}

CHAPTER 7

Discussion of the Experimental Results and Suggestions for Further Work.

The experimental results obtained from each of the various types of experimental tube have been described and discussed in the previous chapter. Hence, only the general conclusions which can be drawn from these results will be given in this chapter.

1. The work Function Determinations.

Richardson plots have been obtained for both comparatively high and low gas and vapour pressures. The values of the slopes of the plots obtained under low pressure conditions, were, in general, smaller than those obtained at higher pressures. The actual values were, of course, dependent on the state of activation and also appeared to be strongly dependent on the previous history of the cathode (especially the pressure of the gas in the experimental tube). This effect was particularly pronounced in the case of tube PA2 when, although the pressure was reduced, the large values of the apparent Richardson work functions and the large values of the internal work function obtained appeared to be the result of the previous exposure of the cathode to gases at high pressures.

Negative values of the intercept were normally found to be associated with the lower values of the Richardson work function and vica versa. An explanation of this fact, in terms of an adsorbed layer of an electronegative substance,

has been given for a simple model in Chapter 4. It is not suggested that this simple model provides a complete explanation of the behaviour of the oxide cathode. The treatment outlined in Chapter 4 was given to indicate that the slope of the Richardson plot was not representative solely of the energy required to remove an electron from the cathode at absolute zero. The treatment does, however, give some indication of the other factors involved.

Values of the surface work function, calculated from the emission and conductivity results obtained from the experimental tubes P2, P3 and PA2, show that surface work function cannot be regarded as constant and independent of the state of activation of the cathode.

It appears that the value of the surface work function is very dependent on the pressure in the experimental tube and that the surface work function changes more rapidly with pressure than the internal work function.

The importance of the presence of the gases and the effects of the formation of adsorbed layers was demonstrated in a particularly marked manner by the changes in the apparent contact potential difference, as measured with the tungsten anode in tube HNW1. Values of apparent contact potential difference obtained by a method involving current flow have been shown to include the voltage drop across the cathode material and the current measuring instrument, so the anode work function cannot be obtained directly. However, the values of apparent contact potential difference did

indicate that the work function of the nickel anodes was normally lower than that of the pure metal, and this was confirmed by the emission measurements made on the anode of tube HNN1. It appeared that the anode work function was modified in two ways. Firstly the decrease in work function was attributed to a film of barium or barium oxide evaporated from the cathode and deposited on the anode. Secondly, the anode surface appeared to be further modified by an adsorbed layer of an electronegative substance. Experiments, in which the anode was bombarded with electrons of various energies, indicated that this electronegative adsorbed layer could be removed by electrons of fairly low energy (~ 4 eV). These experiments also indicated that 'poisoning' of emission was caused by two mechanisms. At low values of anode voltage the emission current, at constant temperature, decreased rapidly to give a value independent of time, but the higher values of anode voltage also produced a long term decay of emission, attributed to an anode poisoning effect which probably results in a change in the surface work function of the cathode. The short term decay can be attributed to changes occuring in the body of the cathode as emission was drawn (possibly donor depletion).

The effects obtained when the anode was heated were also interesting (Tube HNN1). When the anode was heated, an anode work function was observed which could be attributed to the removal of an adsorbed layer of an electronegative substance. Prolonged heating appeared to give

an increase in the work function which was thought to be caused by the removal of the layer of barium or barium oxide previously evaporated from the cathode. The decrease in the anode work function on heating was reflected in an increase in the cathode work function and vica versa. In the first case, it would appear that the electonegative substance removed from the anode gives rise to an increase in the surface work function of the cathode, while in the case of prolonged heating, the active layers present on the anode were deposited on the cathode, which was thereby activated, probably by the reduction of the surface work function.

It was unfortunate that the experimental tube containing the vibrating gold electrode did not function satisfactorily. It would be interesting to compare values of the apparent contact potential difference obtained from emission measurements and those obtained by the Kelvin method. It is likely that the values obtained by the two methods would not be in agreement. Any difference in the values obtained could, in part, be attributed to the voltage drop occurring across the cathode and the current measuring instrument, but the possibility of poisoning effects must also be considered. If the poisoning effects were limited, these measurements might well provide a satisfactory method for the determination of the cathode conductivity. It would also be interesting to compare values of the cathode work function, obtained by means of the Kelvin method,

with the values of the work function calculated from the Richardson plots. Further work on these lines seems justified.

2. The Pressure of the Gas Present in the Experimental Tube.

A number of the experimental tubes were attached, by a side-arm, to an Alpert gauge. The pressures, as indicated by the Alpert gauge, were in general quite high. These high pressures were originally attributed to the porosity of the tungsten seals, used in the construction of the experimental tubes, because the methods of leak detection, outlined in Chapter 5, failed to indicate the presence of 'pin-holes' in the glass envelopes. A large quantity of gas was found to be evolved when the getters (though previously out-gassed at the highest possible temperatures) were fired. In fact the quantity of gas liberated when the getters of tube PA2 were fired was considerable and this was not removed by the gettering action of the barium film. The getter film was not noticeably discoloured and this might suggest that the gettering action of the barium getter is not a satisfactory as might be hoped.

There is a distinct possibility that the pressures indicated by the Alpert gauge do not accurately represent the pressure in the experimental tube. At low pressures the pumping action of the gauge is quite marked and thus the pressure present in the experimental tube might be somewhat higher than that indicated by the gauge. At the higher pressures observed during this investigation out-gassing of the gauge during operation could result in

an increase of pressure in the experimental tube. When investigations were commenced with experimental tubes incorporating the Alpert pump, it was hoped that determinations could be carried out at low pressures, but this was not possible in the time available.

3. The Significance of the Values of the Richardson Work Function.

From the experimental results obtained, it appears that the presence of even small quantities of gas and vapour considerably influence the work functions of the experimental surfaces. The values of work function, as calculated from the slope of the Richardson plot, cannot be regarded as being representative of the work function of a clean surface. The fact that the sprayed coating of the oxide cathode is made up of a large number of crystals, probably differing in work function (due, in part, to the dependence of the rate of activation on the crystal size and the areas of contact with other crystals), also indicates that the slope of the Richardson plot cannot represent a simple work function. If this is the case, the values of the intercept of the Richardson plot cannot be regarded as being representative of the temperature coefficient of the work function as assumed by some workers. These factors have been discussed in greater detail in Chapters 3 and 4.

No information, as to the variation of the work function over the cathode surface, has been obtained during this investigation. For this reason, no further comment as to the significance of the experimental values obtained

can be made. A further investigation of the values of the slope of the Richardson plot, the values of the intercept and the manner in which they are influenced by variations of the work function over the emitting surface should prove to be very rewarding. It is hoped that it may be possible to extend the work to simpler systems than the oxide cathode. An investigation of the electron emitting properties of single crystals of metals and semi-conductors, under ultra-high vacuum conditions, together with the effects produced the admission of controlled quantities of contaminents, would be of great interest. If possible, an investigation of the properties of individual crystal faces will be attempted.

4. The Linear $\text{Log}_{10} A/\phi$ relationship.

I has been shown (Chapter 4) that the linear $\log_{10} A/\phi$ relationship should be observed when a number of Richardson plots intersect at particular values of $\frac{10^3}{T}$ and $\log_{10}\frac{I_a}{T^2}$. This has been confirmed by the results obtained from a number of the experimental tubes. It seems unlikely that such behaviour should be fortuitous. The present investigation has not suggested a reason for this behaviour, but the work done does indicate that the theories outlined in Chapter 3 (the interference density theory and the theory of G Haas) cannot individually provide a complete explanation of this relationship.

It is possible that a further investigation, with the simper system suggested in the previous section, might

provide information which would enable this relationship to be explained.

5. The Temperature Coefficient of the Work Function and the Saturation of Emission and Conductivity at High Temperatures.

It has been suggested that intercept values from the Richardson plot cannot be taken as representing the temperature coefficient as suggested by some workers. Another method used for the determination of this temperature coefficient involves the measurement of contact potential differences. Most of the measurements of the apparent contact potential difference, obtained from the various experimental tubes, indicated that the temperature coefficient had a negative value at low temperatures. Other results from a number of experimental tubes have indicated a positive value in the higher temperature range. The values obtained from tube P2, though uncorrected for the voltage drop across the cathode and current measuring instrument, indicated a value of approximately -3×10^{-3}eV/degree at temperatures below 900°K, and approximately 6×10^{-3}eV/degree for higher temperatures. These values are comparable with the results obtained by Gysae, who used a similar method.

The decrease in the values of the apparent contact potential difference with increasing temperature responsible for the positive value of the temperature coefficient at high temperatures is found to occur at

those temperatures where the pore-conduction mechanism becomes dominant. If these values are representative of the changes in anode and cathode work functions, this would signify either that the cathode work function increases at higher temperatures, or that the anode work function decreases, or both. This could be interpreted in two ways. Firstly, the high temperatures might cause the removal of an electropositive substance adsorbed on the cathode, or secondly, the high cathode temperature might result in an increase of the temperature of the anode, which in turn might cause electronegative adsorbed layers to be removed, possibly to be deposited on the cathode. The exact behaviour would depend on the heats of adsorption of the substance for the anode and cathode materials, but it must be noted that no "bending" of theRichardson plot was observed in this temperature range. An alternative explanation could involve the voltage dropped across the cathode coating. It is possible that, as the pore conduction mechanism becomes dominant and the resistance of the coating decreases more rapidly with increasing temperature, the voltage dropped across the cathode material is reduced. Under these circumstances the relative decrease of the resistance of the cathode material with increasing temperature would be greater than the increase of anode current with increasing temperature so that the product RI_A decreases with increasing temperature. The fact that both the emission and the conductivity saturate at high temperatures, provides additional evidence

in favour of the Loosjes-Vink hypothesis. The saturation of emission and conductivity at high temperatures could be attributed to a space-charge effect in the pores or to the changes of the adsorbed layers postulated above. It cannot be readily decided whether adsorption effects or space-charge effects are responsible for the saturation, because the marked curvature of the anode characteristics in the space-charge limited region at high temperatures prevents an accurate value of the apparent contact potential difference from being obtained, but a space-charge limitation in the pores would be consistent with other evidence.

6. The Form of The Anode Characteristics.

The form of the anode characteristics obtained from the earlier measurements of tube PA2 are of interest. A marked curvature was observed at small values of applied field. This curvature was attributed to a change in the apparent contact potential difference and cathode work function as electrons, emitted from the cathode, removed an electronegative adsorbed layer from the anode. This behaviour would cause the anode work function to decrease. It was assumed that some of the liberated substance was redeposited on the surface of the cathode. This would result in an increase in the cathode work function, a decrease in emission and a decrease in apparent contact potential difference, as observed.

It is likely that the large space charge effects observed for other tubes, and attributed to bad geometry,

might, in part, be due to the same type of behaviour. The apparent deficiency of low energy electrons, which can be inferred from the shape of some of the anode characteristics at small values of applied field, can probably be attributed, in part, to another factor. The applied voltage, as plotted on the characteristic, is larger than the actual potential difference which exists between the anode and cathode because of voltage drop across the cathode coating and the current measuring instrument. This was mentioned in Section 7.5 and is further explained in Chapter 6. The apparent deficiency of low energy electrons observed by some workers has been attributed to a 'thin penetrable potential barrier', but it is likely that the explanation given above is partially responsible for the observed behaviour. The voltage drop might also be partially responsible for the fact that the temperature calculated from the slope of the retarding potential region of the emission characteristics does not always correspond to the measured temperature.

7. The Conductivity Measurements.

Results obtained with the three types of experimental tube showed that the probe diode provided the most satisfactory method for the measurement of cathode conductivity. Some of the probe characteristics indicated a small rectification effect, which can be associated with the base metal oxide interface. The effect was most pronounced for tube P1, but was also observed for other probe tubes.

The graphs of $\log_{10} \sigma$ against $\frac{10^3}{T}$, obtained by the author, were found to be representative of four main types of behaviour. The four regions of the graph were not obtained for all the experimental determinations because it was not always possible to make measurements over a wide range of temperatures. At the highest temperatures a saturation effect caused a 'flattening' of the conductivity curve. This behaviour has already been discussed above. At slightly lower temperatures the slope of the lines (after correction for the effects of the low temperature mechanism) were found to be representative of the pore - emission conductivity process, first suggested by Loosjes and Vink. The activation energies, calculated from the corrected values of the slope in this region, were generally slightly smaller than the corresponding values of the Richardson work function. It is likely that this effect is due to the absence of anode poisoning effects, which occur when the anode is heated or bombarded with electrons.

The activation energies, calculated from the third region of the conductivity curve, were interpreted as being mainly representative of the bulk conduction process, so that the calculated activation energy was taken as giving a value for $\Delta E/2$.

Values of the surface work function were obtained from the Richardson work function and those conductivity measurements representative of the third region of the curve by the two methods outlined in Chapter 2. The values

were in agreement to within experimental error (~ 15%).

A fourth region of the conductivity plot was observed for the earlier activation states of tube PA2. This reduction of the slope of the conductivity curve was observed at low temperatures where no attempt was made to measure the emission current. Because of this, it was thought that the act of drawing emission current might be responsible for the change of slope. This reduction in slope could be interpreted in terms of a donor depletion hypothesis, but could also be interpreted in terms of a conduction process involving the surfaces of the crystals. The charge carriers involved in a surface conduction mechanism could be positive or negative ions, but electrons moving from one surface state to another could also be responsible. If the surface conduction hypothesis is invoked, the decrease in the slope after emission measurements were finished might be due to a termination of the deposition of an adsorbed electronegative substance on the cathode. This electronegative substance could be liberated from the anode by bombardment with electrons. The effect could also be interpreted in terms of the accumulation of an electropositive layer on the cathode when emission is not being drawn, or at low temperatures. The presence of an electronegative adsorbed layer might provide an additional potential barrier, so that the activation energy of the conductivity process, during emission measurements, is increased. A similar effect could be caused by the removal of an electropositive layer as the cathode

temperature increased but this is less likely because the presence of adsorbed electronegative layers have been indicated by the experimental work. If the hypothesis, involving the adsorbed layers, is accepted, the activation energy of the third region of the conductivity plot would probably represent the activation energy of the surface conduction mechanism. (The fourth region being a modification of this due to the creation of emission measurements). The experimental results obtained do not indicate whether the bulk mechanism or the surface mechanism is responsible for the low temperature conductivity process, but evidence as to the formation of an electronegative adsorbed layer or the cathode, during emission measurements, has been obtained.

8. Values of the Seebeck E.M.F. obtained from the Conductivity Measurements.

As the temperature difference existing between the probe and the base metal of the probe diode could not be determined, the value of the internal work function could not be calculated from the observed values of the Seebeck e.m.f.

The sign of the Seebeck e.m.f. normally indicated that the oxide was behaving as an n-type semiconductor. A transition from n-type to p-type conduction, as the temperature was reduced, was indicated during a number of the determinations on tube PA2. The high gas pressure in the experimental tube may well have been responsible for this effect. These results are in agreement with those obtained by Ishikawa, Sato and Sasakai[60] and Wright[46].

9. The Source of Emission.

The experiment with tube R1, in which the top layers of the cathode coating were detached and gave a marked increase in Richardson work function, indicated that the emitting surface is the oxide rather than a layer of active material on the base metal. The experiments in which saturation of emission was observed at high temperatures, can be interpreted as indicating that the major part of the emission comes from surfaces within the pores of the cathode. This was also indicated for tube HNN1, by the greater space charge effect observed when emission was drawn from the oxide cathode.

10. The Cathode Colouration.

A green/blue colouration was observed for a number of experimental tubes when the cathode was at room temperature. This kind of colouration has also been observed by Hopkins[101] and Mee[131] for calcium oxide cathodes. The colouration was found to disappear when the cathode was heated. Hopkins has suggested that the colouration may be due to the formation of F-centres such as those invoked by Pohl to explain the colouration of alkali halides treated with an excess of the alkali metal. Hensley[132] has also suggested that colour centres may exist in the alkaline earth oxides and he proposed that they should be designated by the terms F^1-centre and F^2-centre. The number refers to the number of electrons present in the anion vacancy. Metson[133] has suggested

that the colouration might be caused by sodium liberated from impurities in the ceramic insulators. No evidence as to the cause of this colouration has been provided by this investigation.

11. Suggestions for Further Work

If the linear $\log_{10} A/\emptyset$ relationship is to be explained, it is clear that experimental work should be carried out on a much simpler system than the oxide cathode. It is hoped that the work on single crystals, mentioned earlier, will provide more information as to the significance of this relationship. Techniques for the production of single crystals of barium oxide have been described, but the production of such crystals is very difficult. The information which could be obtained from such crystals and single metal crystals, with, and without adsorbed layers would be of considerable value.

Further work on the oxide cathode, using a gold vibrating electrode, should also provide useful information. The value of the contact potential difference obtained by means of this Kelvin method should be compared with the values obtained from the 'knee' of the emission characteristics. Comparison of the value of the cathode work function obtained by this method and the value obtained from the Richardson work function should give some indication of the variation of the work function over the cathode surface. This method might also provide values of cathode conductivity as described earlier. Such

methods would also provide more information as to the value of the anode work function and the manner in which it is modified by the evaporation of active materials from the anode and the formation of adsorbed layers of the gases and vapours present in the experimental tube.

REFERENCES

1. Wehnelt, A., S-B physik-med soz. Erlangen 95, 115, (1903)
2. Wehnelt, A., Verh Dtsch physik Ges. 5, 346, (1903)
3. Wehnelt, A., Ann Physik 14, 425, (1904)
4. Metson, J.I.E.E. B 102, 1, (1955)
5. Liebold, R., Thesis Univ. Berlin (1941)
6. Fineman and Eisenstein, J.App Phys. 17, 663, (1946)
7. Eisenstein A.S., J. App Phys. 20, 776, (1949)
8. Eisenstein A.S., J. App Phys. 22, 138, (1951)
9. Hermann and Wagener, 'The Oxide Cathode' Chapman and Hall (1951)
10. Spanner H.J., Ann Physik 75, 609, (1924)
11. Simon H., Z techn Physik 8, 434, (1927)
12. Benjamin M. and Rooksby H.P., Phil. Mag. 15, 810, (1933)
13. Burgers, W.G., Z Physik 80, 352, (1933)
14. Huber H. and Wagener S., Z techn. Physik 23, 1, (1942)
15. Eisenstien A., J. App Phys., 17, 434, 654, (1946)
16. Violet and Rothmuller, J. Ann Radioelectricite 4, 184, (1949)
17. Moore Wooten and Morrison, J. App Phys. 26, 943, (1955)
18. Benjamin Cosgrove and Warren, J. Instn. Elctr. Engr. 80, 401, (1937)
19. Prescot and Morrison, J. Amer. Chem. Soc. 60, 3047, (1938)
20. Eisenstien A., J. App Phys. 20, 776, (1949)
21. Forman, Phys. Rev. 96, 6, 1479, (1954)
22. ~~Wagener, Proc. Phys. Soc. B66, 400, (1953)~~ Huber, Thesis, University of Berlin (1941)
23. Kawamura H., J. Phys. Soc. Japan 3, 126, (1948)
24. Nergaard L., R.C.A. Rev. 13, [illegible]4, (1952)

25. Wright, D.A., Phys. Rev. 82, 574, (1951)

26. Becker, J.A., Phys. Rev. 34, 1323, (1929)

27. Metson, G.H., Vacuum 1, 283, (1951)

28. Herrmann and Krieg, Ann Phys. 4, 441, (1949)

29. Metson, G.H., Nature 164, 540, (1949)

30. Higginson G.S., Thesis Univ. Birmingham (1957)

31. Herrmann, G., Z physik. chem. Abt. B35, 288, (1937)

32. Liebold W., Thesis Univ. Berlin (1941)

33. Eisenstein, A., { J. Appl. Phys 11 654 (1946) Phys. Rev., 71, 473, (1947)

34. Becker and Sears, Phys. Rev., 38, 2193, (1931)

35. Gehrts, A., Z techn. physik 11, 246, (1930)

36. Berdennikowa, T.P., Physik Z Sow-Union 2, 77, (1932)

37. Clausing See Ref. 9 Vol. 2, Page 158.

38. Jenkins and Newton, Nature 163, 572, (1949)

39. Barton, H.A., Phys. Rev. 26, 360, (1925)

40. Shepherd, A.A., Brit. J. Appl. Phys. 4, 70, (1953)

41. Isenee, H., Z physik. Chem. Abt. B35, 309, (1937)

42. Becker and Sears, Phys. Rev. 38, 2193, (1931)

43. Schottky, W., Z physik. Chem. B 29, 335, (1938)

44. Jost and Nehlep, Z physik. Chem. B 32, 1, (1936)

45. Shriel, M., Z amorg. allg. Chem. 231, 313, (1937)

46. Wright, Nature 164, 714, (1949), Brit. Journ. App Phys. 1, 150, (1950)

47. Langmuir, J. Amer.Chem.Soc. 54, 2798, (1932)
Nobel Lecture Angam Chem. 46, 728, (1933)
Chem. Rev. 13, 147, (1933)

48. Johnson and Vick, Proc. Roy. Soc. A 158, 55, (1937)

49. Lowry, Phys. Rev. 35, 1367, (1930)

50. Riemann and Murgoci, Phil.Mag. 9, 440, (1930)

51. Becker, Phys. Rev. 34, 1323, (1929)

52. Becker and Sears, Phys. Rev. 38, 2193, (1931)

53. Espe, Wiss. Ver. Siemens - Konz 5, 3es Heft 29, (1927)

54. Gehrts, Naturwissenschaften 20, 732, (1932)

55. Jones, "Thermionic Emission" p 82 Methuen London (1936)

56. Darbyshire, J.A., Proc. Phys. Soc. Lond. 50, [redacted] 635 (1938)

57. Metson, G.H., I.E.E. Monograph No. 269 R (1957)

58. Wilson, M.A., Proc. Roy. Soc. A 134, 277, (1931)

59. Fowler, R.H., Statistical Mechanics C.U.P. p 399 (1956)

60. Ishikawa, Sato, Okumra, and Sasaki, Phys. Rev. 84, 371, (1951)

61. Seitz, Modern Theory of Solids, McGraw-Hill.

62. Blewett, J. App Phys. 10, 668-679 (1939)
J. App Phys. 10, 831-848 (1939)

63. Nishibori, E. and Kawamura H., Proc. Phys. Math. Soc. Japan III 22, 378, (1940)

64. Young, J.R., Phys. Rev. 85, 388, (1952)

65. Schottky, Ann der Physik 44, 1011 (1914)

66. Mott N. and Gurney R., Electronic Processes in Ionic Crystals C.U.P. (1940)

67. Wright, D.A.., Proc. Roy. Soc. A190, 394, (1947)

68. Fan, H.Y., Phys. Rev. 74, 1505, (1948)

69. Wright, D.A., Proc. Roy. Soc. A 190, 394, (1947)

70. Young, J.R., J. Appl. Phys. 23, 1129, (1952)

71. Loosjes and Vink, Phil. Tech. Res. Reps. 4, 449, (1949)

72. Tomlinson, J.App. Phys., 25, 720, (1954)

73. Sparks and Phillips, J.App. Phys. 24, 4, (1953)

74. Blewett, J.P., J.App. Phys. 10, 668, (1939)

75. Hensley, E.B., J. App. Phys. 23, 1122, (1952)

76. Forman, R., Phys. Rev. 96, 1479, (1954)

77. Nakai, Inuishi, and Tsung-Che, J. Phys. Soc. Japan 10, 437, (1955)

78. Young, J.R., J.App. Phys., 23, 1129, (1952)

79. Tomlinson, T.B., J. App. Phys. 25, 710, (1952)

80. Higginson, Brit. J. App. Phys. 9, 257, (1958)

81. Metson, G.H., Inst. Elec. Eng. Monograph

82. Prescott and Morrison, J. Amer. Chem. Soc. 60, 3047, (1938)

83. Wooten, L.A., Phys. Rev. 69, 248, (1946)

84. Sproull, R.L., Phys. Rev. 67, 166, (1945)

85. Coomes, E.A., J. App. Phys. 17, 647, (1946)

86. Wright, D.A., Proc. Phys. Soc. 62B, 398, (1949)

87. Metson, G.H., Nature 164, 540 (1949)

88. Nergaard, R.C.A. Rev. 13, 464, (1952)

89. Spanner, H.J., Ann der Physik, 75, 609, (1924)

90. Heinz, W., and Hass, W., Z techn. phys. 19, 166, (1938)

91. Fan, H.Y., J. App. Phys. 14, 552, (1943)

92. Eisenstein, 'Advances in Electronics' Vol. 1. P. 38.

93. Nottingham, W.B., 'Handbuch der Physik' Vol XXI P.129.

94. Schottky, Ann der Physik 44, 1011 (1914)

95. Rose, A., Phys. Rev. 49, 838 (1936)

96. Hung, C.S., J.App.Phys. 21, 37 (1950).

97. Morgulis, N., J.Phys. USSR 11, 67, (1947)

98. Wright & Woods, Proc. Phys. Soc. B 65, 134, (1952)

99. Chapieux, R., Ann. Radioelectricite 1, 208, (1946)

100. Heinz & Wagener, Z f. Physik 110, 164, (1938)

101. Hopkins, B.J., Thesis Univ. Birmingham (1958).

102. Nishibori & Kawamura, Proc. Phys.Math. Soc. Japan 22, 378, (1940)

103. Hannay, McNair & White, J. App. Phys., 20, 669, (1949)

104. Sommerfeld, Z. Physik 47, 27, (1928)

105. Nordheim, Proc.Roy.Soc., 121, 626 (1928)

106. MacColl, Phys.Rev. 56, 699,(1939)

107. Herring & Nichols, Rev.Mod.Phys. 21, 185 (1949)

108. Schottky, Handb.d.Experimental physik XIII/2 45 (1928)

109. Becker, N.H., & Brattain, J.A., Phys. Rev. 43, 428 (1933)

110. Wigner, Phys. Rev. 49, 696, (1936)

111. Gysae B. & Wagener, S., Z Physik 115, 296, (1940)

112. Gysae B., Thesis Technical Univ. Berlin (1938)

113. Huber, H., Thesis Univ. Berlin (1941)

114. Detels, F., Jb.d.Drahlt.Telegru.u.Teleph. 30, 10, 52 (1927)

115. Huxford, W.S., Phys.Rev., 38, 379, (1931)

116. Patai & Frank, Z.Techn.Physik. 16, 254 (1935)

117. Espe, W., Wiss Veröff Siemens-Werken 5, 29, 46,(1927)

118. Kniepkanp & Nebel, Wiss Veröff Siemens-Werken 11(II) 75, (1932)

119. Veenemans, C.F., Nederl Tijdsch Naturkunde, 10, 1 (1943)

120. Jacobs, Mees & Crossley, Proc. IRE. 36, 1109 (1948)

121 Hermann & Wagener, Vol. 2"The Oxide Coated Cathode" (1951)

and Neldel
122. Meyer, Z.Techn.Physik, 18, 588 (1937)

123. Mott & Gurney, Electronic Processes in Ionic Crystals C.U.P. (1940)

124. Haas, G., American Navy Dept., Publication (1955)

125. Richardson, O.W., Proc.Roy.Soc. A91, 524 (1915)

126. de Boer, 'Electron Emission and Adsorption Phenomena' C.U.P. (1935)

127. Veenemans, Physica 2 (1935)

128. Zwicker, Phy.Z. 30, 578 (1929)

129. de Boer, J.H., Dynamical Character of Adsorption O.U.P. (1953)

130. Bayard, R.I. & Alpert, D., Rev. Sci.Inst. 21, 571,(1950)

131. Mee, C.H.B., Ph.D. Thesis Univ. Birmingham (1960)

132. Hensley, J.App.Phys. 32, No.2, 301, (1961)

133. Metson, G.H., Private Communication.

Appendix :- Photographs of the Apparatus.

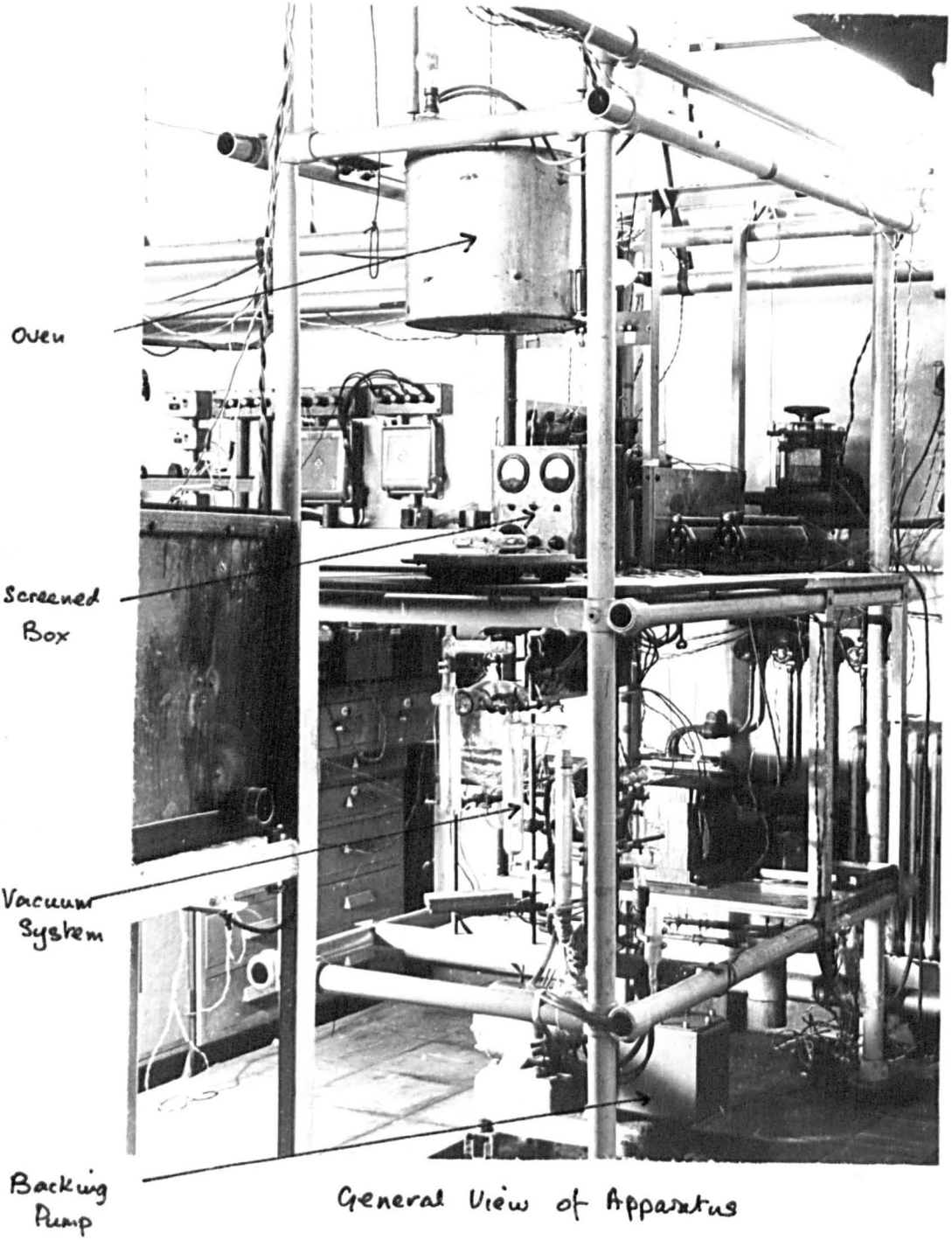

General View of Apparatus

FIG. A1.

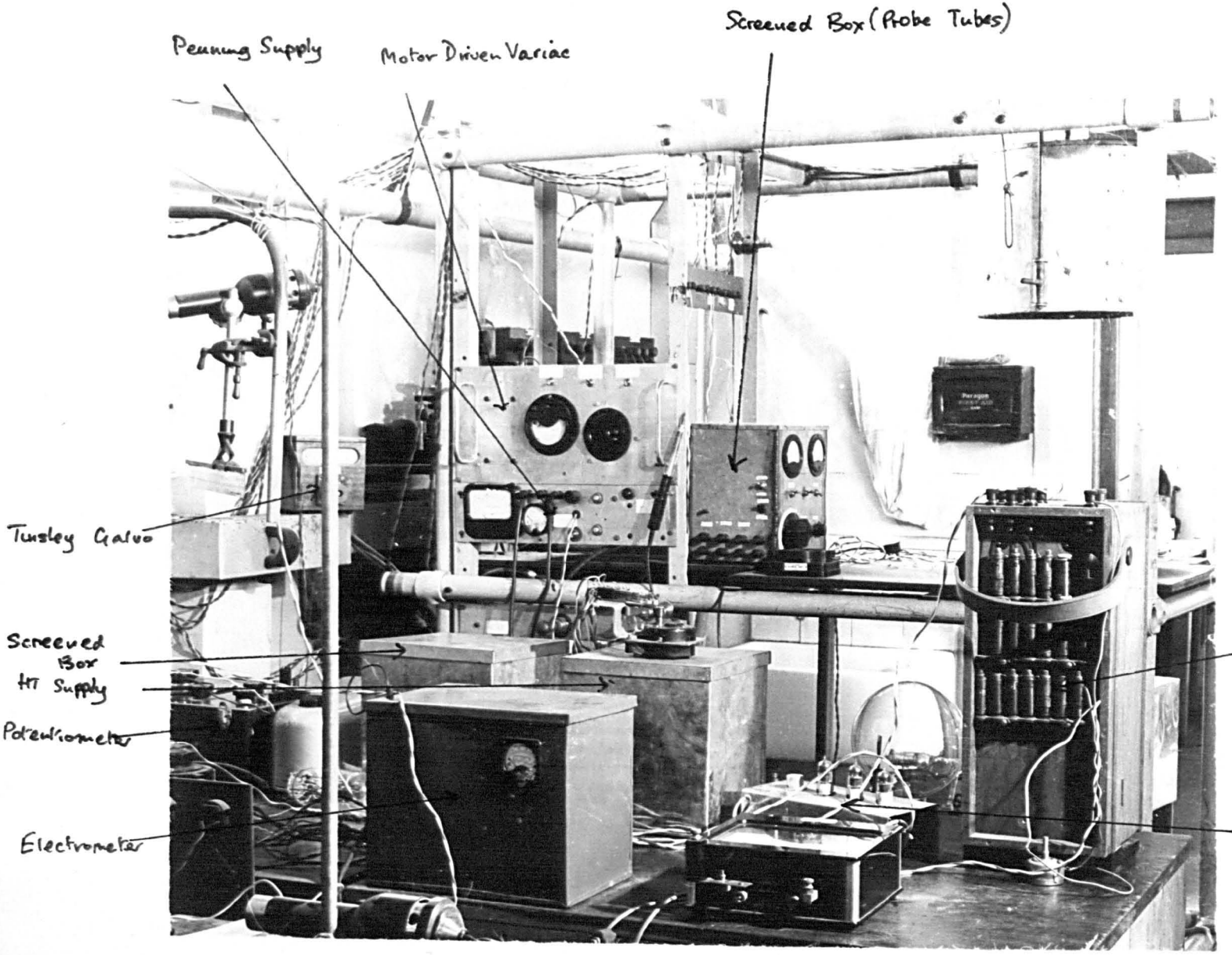

Apparatus
Fig. A2.

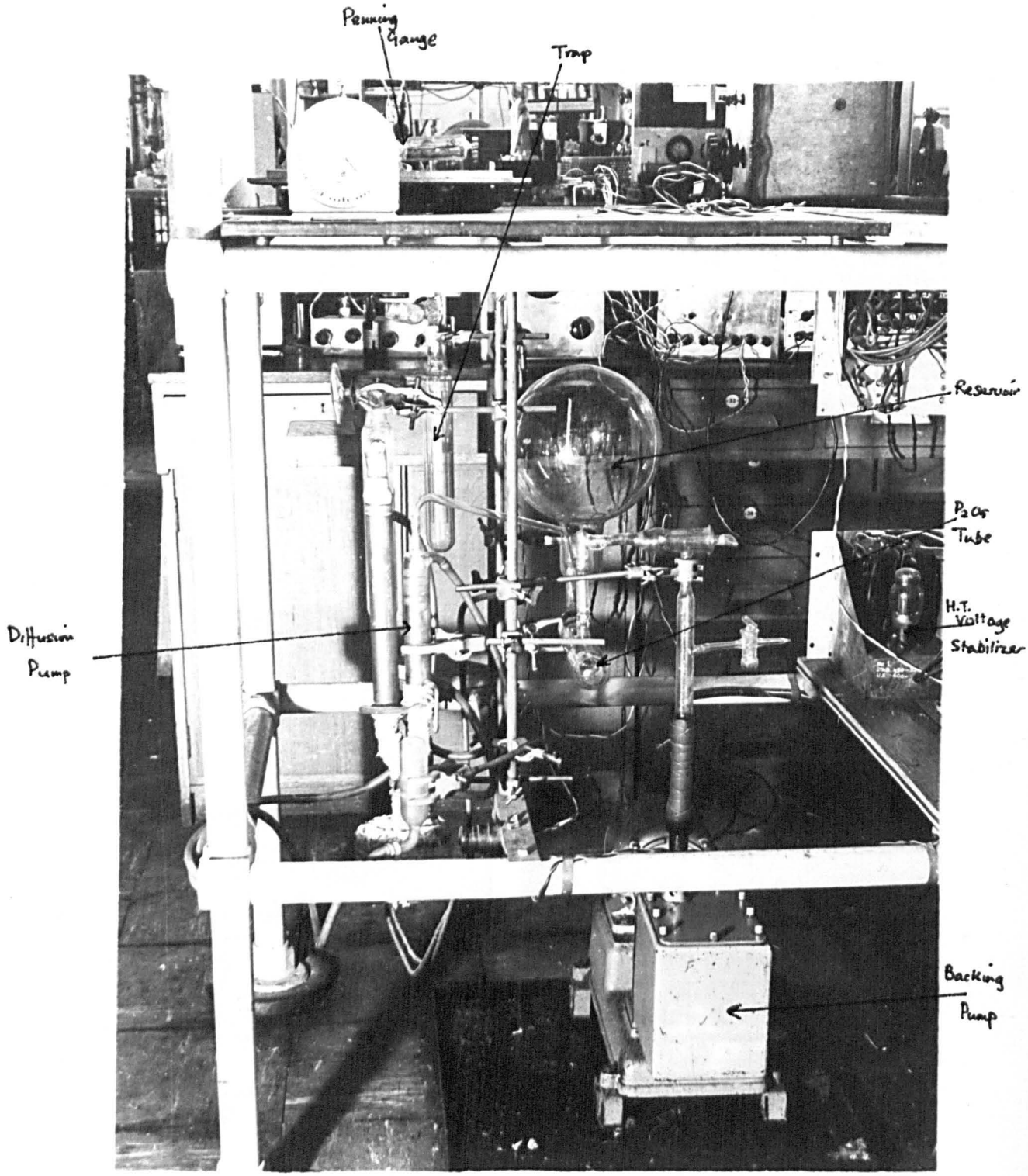

THE VACUUM SYSTEM

FIG. A3.

Acknowledgements.

The Author wishes to express his appreciation to the following:-

D.S.I.R. for financial assistance.

Professor F.A. Vick, now Director of the Atomic Energy Research Establishment at Harwell, for guidance received during the work.

Professor D.J.E. Ingram for the use of the facilities of his department.

My wife for help and encouragement.

My colleagues of the Physics Department for useful discussion.

Mr. F. Rowerth and the Technical Staff for assistance given during the work.

Miss S. Greatbatch for the typing.